

## Response to reviewer 1 (response in red).

We thank Reviewer 1 for taking the time to review the paper. We agree that additional validation, of  $p\text{CO}_2$  would improve the paper, as well as some additional analysis of the causes for the discrepancy between our estimates of riverine  $\text{FCO}_2$  vs those of Borges et al (2019), such as gas transfer velocity and stream surface area. We respond in more detail (point by point) below (excerpts from the text are in quotation marks-in some longer experts we have highlighted particularly important sentences in bold).

The model validation step is very slim, as authors compare the model outputs of dissolved organic carbon (DOC) to a sub-set of published field data. DOC in tropical rivers is extremely refractory and provides little grasp on aquatic carbon cycling as the most labile DOC fraction is very rapidly mineralized (both in soils and in water). So DOC provides a poor validation of the carbon cycling in the river, and might be considered almost as a passive tracer and provide a rough validation of the hydrological connectivity between soils and rivers. Conversely, a convincing validation of the model would be to compare the model outputs of the dissolved  $\text{CO}_2$  concentration (or the corresponding partial pressure of  $\text{CO}_2$ ) with the extensive field data collected by Borges et al. (2019) that are publically available (Borges and Bouillon 2019). While a point by point comparison would not make sense, it could be useful to check if the model captures the overall range of spatial variations along the river and among the different stream sizes. Such validation would be extremely convincing because the  $\text{CO}_2$  evasion from the river to the atmosphere (the core topic of the paper) is computed from the dissolved  $\text{CO}_2$  concentration (the atmospheric  $\text{CO}_2$  is comparatively invariant) and the gas transfer velocity. So if the model does not represent correctly the dissolved  $\text{CO}_2$  concentration then this implies that the  $\text{CO}_2$  evasion rates are incorrect (as well as any conclusion based on past reconstruction and future projection from the model outputs).

Thank you for these suggestions. We have conducted some analysis (in line with your suggestions-including against observed  $p\text{CO}_2$ ) and added additional text.

Please see lines 387-414:

“In Figure 5, we compare simulated DOC concentrations at six locations (Fig. 1) along the Congo River and Oubangui tributary, against the observations of Borges et al. (2015<sup>b</sup>). We show that we can recreate the spatial variation in DOC concentration within the Congo basin relatively closely with an  $R^2$  of 0.74 and an RMSE of 23% (Fig. 5). We are also able to simulate the broad spatial pattern of  $p\text{CO}_2$  measured in Borges et al. (2019). During high flow season (mean of 6 consecutive months of highest flow, 2009-2019) we simulate a mean  $p\text{CO}_2$  of 3,373 ppm and 5,095 ppm at Kisangani and Kinshasa (Brazzaville) respectively, compared to the observed values of 2,424 ppm and 5,343 ppm during high water (measured in December 2013, Borges et al., 2019) (Table 3). Similarly, during low flow season (mean of 6 consecutive months of lowest flow, 2009-2019) we simulate a mean  $p\text{CO}_2$  of 1,563 ppm and 2,782 ppm at Kisangani and Kinshasa respectively, compared to the observed values of 1,670 ppm and 2,896 ppm during falling water (June 2014, Borges et al., 2019) (Table 3).

While we are able to recreate observed spatial differences in DOC and  $p\text{CO}_2$ , as well as broad seasonal variations, we are not able to correctly predict the exact timing of the simulated highs and lows, a reflection of not fully capturing the hydrological seasonality. For example, our mean June  $p\text{CO}_2$  at Kinshasa (Brazzaville) is 4,470 ppm, while Borges et al measured a mean of 2,896 ppm (Table

3). However, our value for July of 2,621 ppm is much closer, and moreover our mean value for December of 5,154 ppm is relatively close to the observed value of 5,343 ppm. Similarly, we fail to predict the timing of the June falling water at Kisangani (Table 3).

In Figure 6, we compare simulated  $pCO_2$  against the observed monthly time series at Bangui on the Oubangui River (Bouillon et al., 2012 & 2014), as far as we are aware the most complete time series of  $pCO_2$  published from the Congo basin, spanning March 2010 to March 2012 (with only the single month of June 2010 missing). Again, while the model fails to correctly predict the precise timing of the peak as with the Kinshasa and Kisangani datasets the broad seasonal variation in  $pCO_2$  is captured, with the observed and modelled times series ranging from 227- 4040 ppm and 415- 2928 ppm, respectively (Fig. 6).”

We have also added an additional Table (Table 3, see below) and Figure (Fig. 6, see below)

421



**Table 3: Observed (Borges et al., 2019) and modelled  $pCO_2$  (in ppm) at Kinshasa (Brazzaville) and Kisangani on the Congo river at various water levels.**

Location	Observed $pCO_2$ highwater (December 2013)	Modelled $pCO_2$ highwater (December 2019)	Modelled $pCO_2$ high flow season (mean of 6 consecutive months of highest flow 2009-2019)	Observed $pCO_2$ falling water (June 2014)	Modelled $pCO_2$ falling water (June 2009-2019)	Modelled $pCO_2$ low flow season (mean of 6 consecutive months of lowest flow 2009-2019)
Kinshasa (Brazzaville)	5,343	5,154	5,095	2,896	4,470	2,782
Kisangani	2,424	2,166	3,373	1,670	3,126	1,563

23

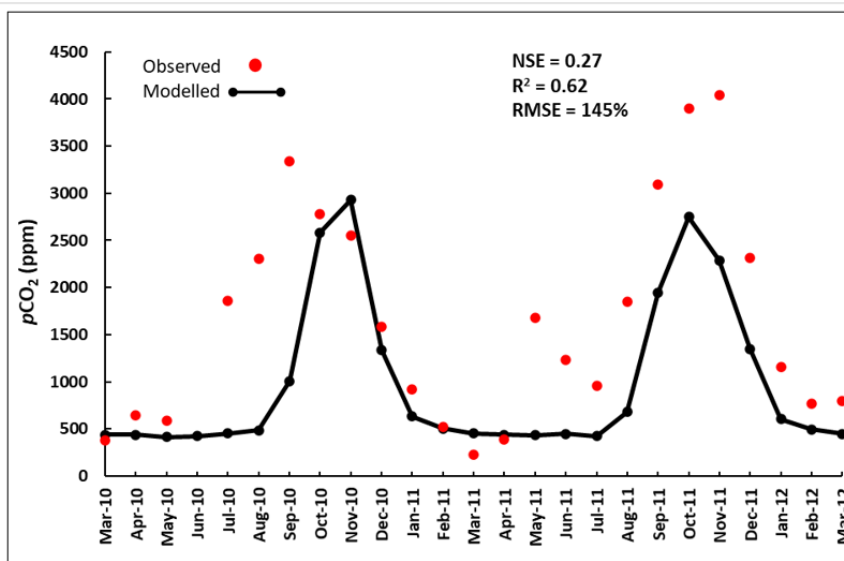


**Figure 6: Time series of observed versus simulated pCO<sub>2</sub> at Bangui on the River Oubangui. Observed data is from Bouillon et al., 2012 and Bouillon et al., 2014.**

The overall emission of CO<sub>2</sub> from the fluvial component of the Congo Basin (TgC/yr) is based on the product of a CO<sub>2</sub> flux density (mol/m<sup>2</sup>/yr) and a stream surface area; the areal CO<sub>2</sub> flux is itself computed from the air-water CO<sub>2</sub> concentration gradient, and the gas transfer velocity; the air-water CO<sub>2</sub> concentration gradient in turn is mainly function of the dissolved CO<sub>2</sub> concentration. So there are three quantities that could explain the difference between the 4 estimates of integrated CO<sub>2</sub> emissions discussed in section L-513-517: the CO<sub>2</sub> dissolved concentration, the gas transfer velocity and the stream surface area. The evaluation of the model performance would be much more convincing if each of these three quantities was compared to available estimates.

In response to these comments we have added additional discussion (now lines 572-641):

“Our estimate of the integrated present-day aquatic CO<sub>2</sub> evasion from the river surface of the Congo basin (32 Tg C yr<sup>-1</sup>) is the same as that estimated by Raymond et al. (2013) (also 32 Tg C yr<sup>-1</sup>), downscaled over the same basin area, but smaller than the 59.7 Tg C yr<sup>-1</sup> calculated by Lauerwald et al. (2015) and far smaller than that of Borges et al. (2015<sup>a</sup>), 133-177 Tg C yr<sup>-1</sup> or Borges et al. (2019), 251±46 Tg C yr<sup>-1</sup>. **The recent study of Borges et al. (2019) is based on by far and away the most extensive dataset of Congo basin pCO<sub>2</sub> measurements to date and thus suggests that we substantially underestimate total riverine CO<sub>2</sub> evasion.** As previously discussed, we simulate the broad spatial and temporal variation in observed DOC and pCO<sub>2</sub> (2015<sup>a,b</sup>, Fig. 5, Table 3) relatively well. It is therefore somewhat surprising that our basin-wide estimate of riverine CO<sub>2</sub> evasion is so different. Below we discuss some possible explanations for this discrepancy related to methodological differences and limitations.

One potential cause for the differences could be the river gas exchange velocity  $k$ . However, we applied a mean riverine gas exchange velocity  $k$  of  $3.5 \text{ m d}^{-1}$  which is similar to the  $2.9 \text{ m d}^{-1}$  used by Borges et al. (2015<sup>a</sup>). Moreover, a sensitivity analysis was performed in Lauerwald et al. (2017) which showed that in the physical approach of ORCHILEAK,  $\text{CO}_2$  evasion is not very sensitive to the  $k$  value, unlike data-driven models. Namely, Lauerwald et al (2017) showed that an increase or decrease of  $k$  by 600 for rivers and swamps of 50% only led to 1% and -4% change in total  $\text{CO}_2$  evasion, respectively. Therefore, we can discount  $k$  as a major source of the discrepancy.

Another potential reason for our smaller riverine  $\text{CO}_2$  evasion could be river surface area. We simulate a mean present day (1980-2010) total river surface area of  $25,900 \text{ km}^2$ , compared to the value of  $23,670 \text{ km}^2$  used in Borges et al (2019, supplementary information) and so similarly we think that this can be discounted as a major source of discrepancy.”

The difference in our simulated riverine  $\text{CO}_2$  evasion compared to the empirically derived estimate of Borges et al. (2019), could be caused by the lack of representation of aquatic plants in the ORCHILEAK model. Borges et al. (2019) used the stable isotope composition of  $\delta^{13}\text{C-DIC}$  to determine the origin of dissolved  $\text{CO}_2$  in the Congo River system and found that the values were consistent with a DIC input from the degradation of organic matter, in particular from  $\text{C}_4$  plants. Crucially, they further found that the  $\delta^{13}\text{C-DIC}$  values were unrelated to the contribution of *terra-firme*  $\text{C}_4$  plants, rather that they were more consistent with the degradation of aquatic  $\text{C}_4$  plants, namely macrophytes. ORCHILEAK does not represent aquatic plants, and the wider LSM ORCHIDEE does not have an aquatic macrophyte PFT either (though root respiration of floodplain plants for the PFTs represented, is accounted for as a C source). This could at the very least partly explain our conservative estimate of river  $\text{CO}_2$  evasion, given that tropical macrophytes have relatively elevated NPPs. Rates as high as  $3,500 \text{ g C m}^{-2} \text{ yr}^{-1}$  have been measured on floodplains in the Amazon (Silva et al., 2009). While this value is higher than the values simulated in the Cuvette Centrale by ORCHILEAK (Figure 8), they are of the same order of magnitude and so this alone cannot fully explain the discrepancy compared to the results of Borges et al. (2019). In the Amazon basin it has been shown that wetlands export approximately half of their gross primary production (GPP) to the river network compared to upland (*terra-firme*) ecosystems which only export a few percent (Abril et al. 2013). More importantly, Abril et al. (2013) found that tropical aquatic macrophytes export 80% of their GPP compared to just 36% for flooded forest. Therefore, the lack of a bespoke macrophyte PFT is indeed likely to be one reason for the discrepancy between our results and those of Borges, but largely due to their particularly high export efficiency to the river-floodplain network as opposed to differences in NPP. While being a significant limitation, creating and incorporating a macrophyte PFT would be a substantial undertaking given that the authors are unaware of any published dataset which has systematically mapped their distribution and abundance. It is important to note that while ORCHILEAK does not include the export of C from aquatic macrophytes it also neglects their NPP. Moreover, most aquatic macrophytes described in the literature have short (<1 year) life-cycles (Mitchel & Rogers, 1985). As such, while this model limitation is likely one of the causes for our relatively low estimate of riverine  $\text{CO}_2$  evasion, it will only have a limited net effect on our estimate of the overall annual C balance (NBP, NEP) of the Congo basin.

Finally, another cause for the difference in riverine  $\text{CO}_2$  evasion could be that the resolution of ORCHILEAK ( $0.5$  degree river network and  $1^\circ$  for C fluxes) is not sufficient to fully capture the dynamics of the smallest streams of the Congo Basin which have been shown to have the highest DOC and  $\text{CO}_2$  concentrations (Borges et al., 2019). Indeed, ORCHILEAK typically does not simulate the highest observed  $p\text{CO}_2$  measurements of the smallest tributaries (i.e. > 16,000 ppm). This is partly because for the fast reservoir (headwaters) in ORCHILEAK we assume full  $p\text{CO}_2$  equilibrium

with the atmosphere over one full day, which prevents very high  $p\text{CO}_2$  values from building in the water column.

Despite these limitations, it is important to note that in our simulations, the evasion flux from rivers only contributes 15% of total aquatic  $\text{CO}_2$  evasion, and including the flux from wetlands/floodplains, we produce a total of  $235 \text{ Tg C yr}^{-1}$ . Moreover, the majority of this evasion occurs in the Cuvette Centrale (Fig. 8) which suggests that while ORHILEAK fails to attribute a large portion of this flux to small rivers (owing to the coarse resolution of the river network) we nonetheless do capture the source of carbon. In other words, in ORCHILEAK the majority of this carbon evades directly from the floodplain and wetlands of the Cuvette Centrale as opposed to the small rivers.”

Final elements of validation and discussion that are missing are the contribution of  $\text{HCO}_3^-$  to the export of dissolved inorganic carbon (DIC) from the river to the ocean. The export of DIC from rivers to the ocean is mainly in the form of  $\text{HCO}_3^-$  including the Congo river (Wang et al. 2013). So ignoring  $\text{HCO}_3^-$  would lead to a very substantial under-estimation of DIC export to the ocean. This should be fairly easy to implement with a weathering model and GIS of lithology. This is of course of interest for the topic of paper as weathering intensity is a function of temperature and precipitation that are used by the authors to study the long-term (1861-2099) trends of aquatic carbon fluxes. Further, there are substantial data-sets of total alkalinity (that mainly corresponds to  $\text{HCO}_3^-$ ) providing spatial (Borges et al. 2019) and seasonal (Wang et al. 2013; Bouillon et al. 2012; 2013) patterns of  $\text{HCO}_3^-$  variability. Additionally, dissolved  $\text{CO}_2$  is in thermodynamic equilibrium with  $\text{HCO}_3^-$ , so it is required to have some grasp on  $\text{HCO}_3^-$  variability to correctly model dissolved  $\text{CO}_2$  dynamics, hence,  $\text{CO}_2$  emissions to the atmosphere.

We appreciate these comments and suggestions and acknowledge that the lack of accounting for  $\text{HCO}_3^-$  is a limitation of the model. However, we would consider creating and implementing a weathering model outside the scope of our study and therefore as an alternative, we have added estimates from the literature and discuss these limitations.

Please see lines 642-658:

“Our simulated export of C to the coast of  $15 (15.3) \text{ Tg C yr}^{-1}$  is virtually identical to the TOC+DIC export estimated by Borges et al. (2015<sup>a</sup>) of  $15.5 \text{ Tg C yr}^{-1}$ , which is consistent with the fact that we simulate a similar spatial variation of DOC concentrations (Fig. 8 and Fig. 1 for locations). It is also relatively similar to the  $19 \text{ Tg C yr}^{-1}$  (DOC + DIC) estimated by Valentini et al. (2014) in their synthesis of the African carbon budget. Valentini et al. (2014) used the largely empirical based Global Nutrient Export from WaterSheds (NEWS) model framework and they point out that Africa was underrepresented in the training data used to develop the regression relationships which underpin the model, and thus this could explain the small disagreement.

Of the total  $15 \text{ Tg C yr}^{-1}$  exported to the coast, we simulate a  $2.4 \text{ Tg C yr}^{-1}$  component of dissolved  $\text{CO}_2$ , which is relatively similar to the empirically derived estimate of the total DIC export of  $3.3 \text{ Tg C yr}^{-1}$  calculated in Wang et al. (2013). According to Wang et al., dissolved  $\text{CO}_2$  accounts for the majority ( $1.9 \text{ Tg C yr}^{-1}$ ) with the rest being the weathering derived flux of  $\text{HCO}_3^-$ . Thus, the discrepancy between the two estimates is likely to be largely caused by our lack of accounting for the weathering derived flux ( $\text{HCO}_3^-$ ) which they estimate at  $1.4 \text{ Tg C yr}^{-1}$ . In summary, despite this

model limitation the results of Wang et al. (2013) suggest that we still capture the majority of the DIC flux.”

L44 : In this section it’s unclear what is meant by “increase” of “net primary productivity” and “storage in tree biomass”. A recent study shows that African forests are sinks of carbon on yearly basis, and that the carbon sink is constant in time from the mid-1990’s to present (Hubau et al. 2020). So, according to this study, there is no “increase” in NPP as stated but a constant sink. Please clarify.

In response to these comments, we have added additional lines in the introduction (now lines 64-66):

“Moreover, recent field data suggests that the above ground C sink in tropical Africa was relatively stable from 1985 to 2015 (Hubau et al., 2020).”

Please also see additional discussion (now lines 673-698):

“Up to a point, our results also concur with estimates based on the upscaling of biomass observations (Lewis et al., 2009; Hubau et al., 2019). Lewis et al. (2009) up-scaled forest plot measurements to calculate that intact tropical African forests represented a net uptake of approximately 300 Tg C yr<sup>-1</sup> between 1968 and 2007 and this is consistent with our NEP estimate of 275 Tg C yr<sup>-1</sup> over the same period. However, more recently an analysis based on an extension of the same dataset found that the above ground C sink in tropical Africa has been relatively stable from 1985 to 2015 (Hubau et al., 2020).

A major source of the uncertainty associated with future projections of NPP and NEP comes from our limited understanding and representation of the CO<sub>2</sub> fertilization effect. Recent analysis of data from some of the longest-running Free-Air CO<sub>2</sub> Enrichment (FACE) sites, consisting of early-successional temperate ecosystems, found a 29.1 ± 11.7% stimulation of biomass over a decade (Walker et al., 2019). A meta-analysis (Liu et al., 2019) of seven temperate FACE experiments combined with process-based modelling also found substantial sensitivity (0.64 ± 0.28 PgC yr<sup>-1</sup> per hundred ppm) of biomass accumulation to atmospheric CO<sub>2</sub> increase, and the same study showed that ORCHIDEE model simulations were largely consistent with the experiments. However, other FACE experiments on mature temperate forests (Körner et al., 2005), as well as eucalyptus forests bring into question whether the fertilization effects observed in temperate FACE experiments can be extrapolated to other ecosystems. For example, the Swiss FACE study, a deciduous mature forest, found no significant biomass increase with enhanced CO<sub>2</sub> (Körner et al., 2005), while a FACE experiment on a mature eucalyptus forest in Australia found that while CO<sub>2</sub> stimulated an increase in C uptake through GPP, this did not carry to the ecosystem level, largely as a result of a concurrent increase in soil respiration (Jiang et al., 2020). Unfortunately, no results are yet available from any tropical FACE experiments, though the Amazon FACE experiment is underway and the eventual results will be crucial in developing our understanding of the CO<sub>2</sub> fertilization effect beyond the temperate zone.”

L74 : The tropical region is also a hotspot of aquatic C cycling due to wetland productivity and wetland carbon inputs to rivers (Abril & Borges 2019), in addition to “terrestrial NPP”. In the Amazon

river a large fraction of fluvial CO<sub>2</sub> emissions to the atmosphere are sustained by wetland inputs (Abril et al. 2014). L74: The fact that the “tropical region is a hotspot area for inland water C cycling” (as stated) was authoritatively demonstrated by seminal papers such as Richey et al. (2002) and Melack et al. (2004), more than a decade before the recent Lauerwald et al. (2015) work. L 78-80: there are (at least) two additional elements of context that could be relevant for the introduction: 1) the Raymond et al. (2013) and the Lauerwald et al. (2015) estimates are in fact based on the same initial data-base of pCO<sub>2</sub> computed from pH and alkalinity (GLORICH) that was extrapolated globally using two different approaches; this illustrates how uncertain these global estimates are, since the resulting values differ by a factor of 3; 2) While the conclusion of Lauerwald et al. (2015) that the majority of CO<sub>2</sub> emissions from rivers comes from the tropics is probably correct, field data (used in the global extrapolation) is nearly absent in the tropics. For instance for the Congo River there is only one single data entry in the GLORICH data-set. Most of the data used to develop the statistical model of Lauerwald et al. (2015) come from non-tropical areas such as North America and Scandinavia.

We have changed the references to prioritise empirical estimates and also added additional context for the Lauerwald et al. (2015) and Raymond et al. (2013) estimates.

Please see lines 81-94:

“The tropical region is a hotspot area for inland water C cycling (Richey et al., 2002; Melack et al., 2004; Abril et al., 2014; Borges et al., 2015<sup>a</sup>; Lauerwald et al., 2015) due to high terrestrial NPP and precipitation, and a recent study used an upscaling approach based on observations to estimate present day CO<sub>2</sub> evasion from the rivers of the Congo basin at 251±46 Tg C yr<sup>-1</sup> and the lateral C (TOC +DIC) export to the coast at 15.5 (13-18) Tg C yr<sup>-1</sup> (Borges et al., 2015<sup>a</sup>; Borges et al., 2019). To put this into context, their estimate of aquatic CO<sub>2</sub> evasion represents 39% of the global value estimated by Lauerwald et al. (2015, 650 Tg C yr<sup>-1</sup>) or 14% of the global estimate of Raymond et al. (2013, 1,800 Tg C yr<sup>-1</sup>). **Note that while Lauerwald et al. (2015) and Raymond et al. (2013) relied largely on the same database of pCO<sub>2</sub> measurements (GloRiCh, Hartmann et al., 2014) as the basis for their estimates, they took different, albeit both empirically led approaches. Moreover, both approaches were limited by a relative paucity of data from the tropics, which also explains the high degree of uncertainty associated with our understanding of global riverine CO<sub>2</sub> evasion.”**

L 244: Borges et al. (2019) report discharge data from the mainstem Congo at Kisangani. So there are additional data-sets to validate the model hydrology.

We performed the Hydrology validation before this paper was published. Moreover, we were unable to access this dataset.

L513: It could be useful to put into context how these different fluxes were computed. The Raymond et al. (2013) estimate is based on a single pCO<sub>2</sub> value (apparently from pH and alkalinity measurements in Pool Malebo) that was extrapolated to the whole basin. The comparison of this single value of pCO<sub>2</sub> with the extensive data set reported by Borges et al. (2019) shows that it is unrealistically low (refer to Supplemental Figure 18). Lauerwald et al. (2015) et al. estimate of pCO<sub>2</sub> compares better to the Borges et al. (2019) data-set but still fails to represent the influence of the Cuvette Centrale (refer to Supplemental Figure 18). Please also note that the CO<sub>2</sub> estimate for the Congo reported by Borges et al. (2015) was based on exactly the same stream surface area and gas

transfer velocity as those used by Raymond et al. (2013), and also showed that the Raymond et al. (2013) estimate was under-estimated (obviously, since the  $p\text{CO}_2$  value is unrealistically low). So there is some clear convergence that the present estimate of  $\text{CO}_2$  emission based on ORCHILEAK is under-estimated even if it is coincidentally close to the one reported by Raymond et al. (2013). The actual reasons of the under-estimation need to be explored as suggested in the above Major Comments.

We have added some additional explanation (now lines 572-582):

“Our estimate of the integrated present-day aquatic  $\text{CO}_2$  evasion from the river surface of the Congo basin ( $32 \text{ Tg C yr}^{-1}$ ) is the same as that estimated by Raymond et al. (2013) (also  $32 \text{ Tg C yr}^{-1}$ ), downscaled over the same basin area, but smaller than the  $59.7 \text{ Tg C yr}^{-1}$  calculated by Lauerwald et al. (2015) and far smaller than that of Borges et al. (2015<sup>a</sup>),  $133\text{-}177 \text{ Tg C yr}^{-1}$  or Borges et al. (2019),  $251\pm 46 \text{ Tg C yr}^{-1}$ . **The recent study of Borges et al. (2019) is based on by far and away the most extensive dataset of Congo basin  $p\text{CO}_2$  measurements to date and thus suggests that we substantially underestimate total riverine  $\text{CO}_2$  evasion.** As previously discussed, we simulate the broad spatial and temporal variation in observed DOC and  $p\text{CO}_2$  (2015<sup>a, b</sup>, Fig. 5, Table 3) relatively well. It is therefore somewhat surprising that our basin-wide estimate of riverine  $\text{CO}_2$  evasion is so different. Below we discuss some possible explanations for this discrepancy related to methodological differences and limitations.”

Please also see the preceding paragraphs for further discussion of the potential causes for our underestimation of the aquatic  $\text{CO}_2$  evasion from the river surface.

## References

- Bouillon, S., Yambélé, A., Spencer, R. G. M., Gillikin, D. P., Hernes, P. J., Six, J., Merckx, R., and Borges, A. V.: Organic matter sources, fluxes and greenhouse gas exchange in the Oubangui River (Congo River basin), *Biogeosciences*, 9, 2045–2062, <https://doi.org/10.5194/bg-9-2045-2012>, 2012.
- Bouillon, S., Yambélé, A., Gillikin, D. P., Teodoru, C., Darchambeau, F., Lambert, T., & Borges, A. V. (2014). Contrasting biogeochemical characteristics of the Oubangui River and tributaries (Congo River basin). *Scientific Reports*, 4, 5402. Retrieved from <https://doi.org/10.1038/srep05402>
- Borges, A. V, Darchambeau, F., Teodoru, C. R., Marwick, T. R., Tamoo, F., Geeraert, N., Bouillon, S. (2015). Globally significant greenhouse-gas emissions from African inland waters. *Nature Geoscience*, 8, 637. Retrieved from <https://doi.org/10.1038/ngeo2486>
- Borges, A. V., Darchambeau, F., Lambert, T., Morana, C., Allen, G. H., Tambwe, E., Toengaho Sembaito, A., Mambo, T., Nlandu Wabakhangazi, J., Descy, J.-P., Teodoru, C. R., and Bouillon, S. (2019). Variations in dissolved greenhouse gases ( $\text{CO}_2$ ,  $\text{CH}_4$ ,  $\text{N}_2\text{O}$ ) in the Congo River network overwhelmingly driven by fluvial-wetland connectivity, *Biogeosciences*, 16, 3801–3834, <https://doi.org/10.5194/bg-16-3801-2019>.



Cai, W.-J., Guo, X., Chen, C. T. A., Dai, M., Zhang, L., Zhai, W., Lohrenz, S. E., Yin, K., Harrison, P. J., and Wang, Y.: A comparative overview of weathering intensity and HCO<sub>3</sub><sup>-</sup> flux in the world's major rivers with emphasis on the Changjiang, Huanghe, Zhujiang (Pearl) and Mississippi Rivers, *Cont. Shelf Res.*, 28, 1538–1549, 2008.

Korner C, Asshoff R, Bignucolo O (2005) Carbon flux and growth in mature deciduous forest trees exposed to elevated CO<sub>2</sub>. *Science*, 309, 1360–1362.

Lauerwald, R., Regnier, P., Camino-Serrano, M., Guenet, B., Guimberteau, M., Ducharne, A., ... Ciais, P. (2017). ORCHILEAK (revision 3875): a new model branch to simulate carbon transfers along the terrestrial-aquatic continuum of the Amazon basin. *Geoscientific Model Development*, 10(10), 3821–3859. <https://doi.org/10.5194/gmd-10-3821-2017>

Lewis, S. L., Lopez-Gonzalez, G., Sonké, B., Affum-Baffoe, K., Baker, T. R., Ojo, L. O., ... Wöll, H. (2009). Increasing carbon storage in intact African tropical forests. *Nature*, 457, 1003. Retrieved from <https://doi.org/10.1038/nature07771>

Walker AP, De Kauwe MG, Medlyn BE, Zaehle S, Iversen CM, Asao S, Guenet B, Harper A, Hickler T, Hungate BA et al. 2019. Decadal biomass increment in early secondary succession woody ecosystems is increased by CO<sub>2</sub> enrichment. *Nature Communications* 10: 454

Wang, Z. A., Bienvenu, D. J., Mann, P. J., Hoering, K. A., Poulsen, J. R., Spencer, R. G. M., and Holmes, R. M. (2013), Inorganic carbon speciation and fluxes in the Congo River, *Geophys. Res. Lett.*, 40, 511–516, doi:10.1002/grl.50160.

## Response to reviewer 2 (response in red).

We thank Reviewer 2 for taking the time to review the paper. We are confident that the comments and associated changes (outlined below) have helped to substantially improve the paper.

Point by point reply (excerpts from the text are in quotation marks-in some longer excerpts we have highlighted particularly important sentences in bold):

Introduction L44-58: Though based on published papers, the estimates of carbon stocks and fluxes in the forests and soils of the Congo would benefit from a more critical evaluation given the logistic difficulties and paucity of data for the region.

In response to this comment, we have modified the wording of the corresponding lines (now lines 47-51).

“As the world’s second largest area of contiguous tropical rainforest and second largest river, the Congo basin has a significant role to play in the global carbon (C) cycle. Current estimates of its C stocks and fluxes are limited by a sparsity of field data and therefore have substantial uncertainties, both quantified and unquantified (Williams et al., 2007; Lewis et al., 2009; Dargie et al., 2017).”

Further discussion is reserved for section 4.1.

L73-74: To support the statement that ‘The tropical region is a hotspot area for inland water C cycling’ it would be more appropriate to cite results from empirical studies, rather than modelled estimates.

In response to this comment we have modified the corresponding lines to cite empirical studies (now lines 81-86).

“The tropical region is a hotspot area for inland water C cycling (Richey et al., 2002; Melack et al., 2004; Abril et al., 2014; Borges et al., 2015<sup>a</sup>; Lauerwald et al., 2015) due to high terrestrial NPP and precipitation, and a recent study used an upscaling approach based on observations to estimate present day CO<sub>2</sub> evasion from the rivers of the Congo basin at 251±46 Tg C yr<sup>-1</sup> and the lateral C (TOC +DIC) export to the coast at 15.5 (13-18) Tg C yr<sup>-1</sup> (Borges et al., 2015<sup>a</sup>; Borges et al., 2019).”

L81-82: How well are the current fluxes known?

In response to this comment we have modified the corresponding lines.

Lines 48-51- “Current estimates of its C stocks and fluxes are limited by a sparsity of field data and therefore have substantial uncertainties, both quantified and unquantified (Williams et al., 2007; Lewis et al., 2009; Dargie et al., 2017).”

Lines 89-94- “Note that while Lauerwald et al. (2015) and Raymond et al. (2013) relied largely on the same database of *p*CO<sub>2</sub> measurements (GloRiCh, Hartmann et al., 2014) as the basis for their estimates, they took different, albeit both empirically led approaches. Moreover, both approaches were limited by a relative paucity of data from the tropics, which also explains the high degree of uncertainty associated with our understanding of global riverine CO<sub>2</sub> evasion.”

L86-92: These are rather ambitious goals, given the large uncertainties in current conditions and paucity of historical and current data.

We agree that these are ambitious goals given the uncertainties and paucity of data. However, we would argue that it is still better to present the full results, but with the caveats up front (including immediately in abstract). See for example lines 36-45.

Methods ORCHILEAK is a valuable modification to the land surface model, ORCHIDEE, and is well described in Lauerwald et al., 2017. Given that 'All of the processes represented in ORCHILEAK remain identical to those previously represented for the Amazon ORCHILEAK', the veracity of the model for the Amazon would need careful evaluation before accepting its use in the Congo. It is outside the scope of this review to revisit issues, some of which were noted by the authors, with regard the application to the Amazon. However, it is misleading to state that 'ORCHILEAK model . . . is capable of simulating both terrestrial and aquatic C fluxes in a consistent manner for the present day in the Amazon and Lena' without caveats and limitations acknowledged.

In response to this comment we have modified the corresponding lines. (now line 109-117)

"The ORCHILEAK model (Lauerwald et al., 2017), a new version of the land surface model ORCHIDEE (Krinner et al., 2005), is capable of simulating observed terrestrial and aquatic C fluxes in a consistent manner for the present day in the Amazon (Lauerwald et al., 2017) and Lena (Bowring et al., 2019<sup>a</sup>; Bowring et al., 2019<sup>b</sup>) basins, **albeit with limitations including a lack of explicit representation of POC fluxes and in-stream autotrophic production (see Lauerwald et al., 2017; Bowring et al., 2019<sup>a</sup>; Bowring et al., 2019<sup>b</sup> and Hastie et al., 2019 for further discussion)**. Moreover, it was recently demonstrated that this model could recreate observed seasonal and interannual variation in Amazon aquatic and terrestrial C fluxes (Hastie et al., 2019)."

Moreover, the differences between the Congo and Amazon would seem to require thorough consideration before accepting identical application. As described in Borges et al. (2019): The Congo basin has a wide range of tributaries with differing lithology, soils, vegetation and rainfall in their catchments, has extensive peat deposits, and has large areas of year-round inundation. These conditions differ significantly from the Amazon basin.

We accept that the conditions in the Amazon and Congo are very different, though the Amazon also has been shown to contain significant peat deposits-( see for example Draper et al, 2014 and is expected to have larger 'undiscovered peatlands' Gumbricht et al., 2017), and also a wide range of tributaries with differing lithology soils etc, as well as a large east-west precipitation gradient. We would debate the term 'identical application' as we recalibrated the model as fully as we could with the available data, under the current model structure (admittedly with associated limitations and caveats).

L111: Camino Serrano 2015 is not listed in references. In Lauerwald et al., 2017 this reference is listed as - Camino Serrano, M.: Factors controlling dissolved organic carbon in soils: a database analysis and a model development, Universiteit Antwerpen, Belgium, 2015. This is not readily accessible.

Thanks for pointing out. Noted and change accordingly to:

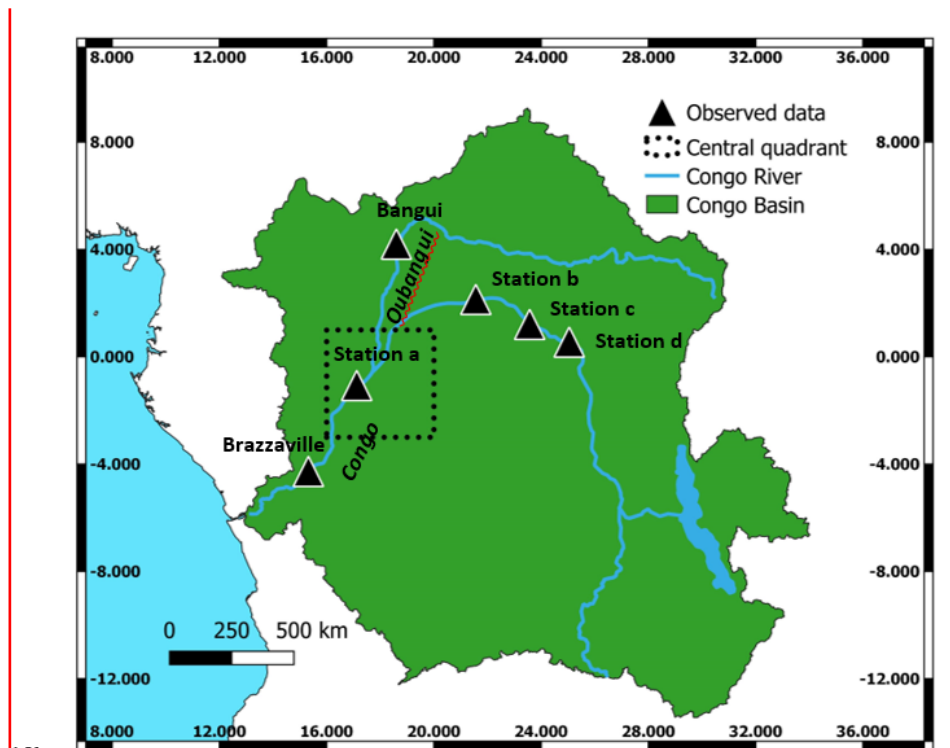
“Camino-Serrano, M., Guenet, B., Luyssaert, S., Ciais, P., Bastrikov, V., De Vos, B., Gielen, B., Gleixner, G., Jornet-Puig, A., Kaiser, K., Kothawala, D., Lauerwald, R., Peñuelas, J., Schrumppf, M., Vicca, S., Vuichard, N., Walmsley, D., and Janssens, I. A.: ORCHIDEE-SOM: modeling soil organic carbon (SOC) and dissolved organic carbon (DOC) dynamics along vertical soil profiles in Europe, *Geosci. Model Dev.*, 11, 937–957, <https://doi.org/10.5194/gmd-11-937-2018>, 2018”

L124: Why is the water surface area varied diurnally?

This is the time step for the routing scheme of ORCHILEAK and the surface area varies with discharge.

Figure 1. The figure needs latitudes and longitudes indicated. Lake Tanganyika is drawn as if a loop of rivers; redraw as a lake.

This figure has been changed accordingly (line 165):



165

166

167

168

Figure 1:Extent of the Congo Basin, central quadrant of the “Cuvette Centrale” and sampling stations (for DOC and discharge) along the Congo and Oubangui Rivers (in italic).

Figure 2 and associated text (L153-168) do not consider the veracity of these data. Though 13 plant functional groups (pft) are prescribed, how well are their ecophysiological characteristics in the conditions of the Congo known? ‘Tropical broadleaved raingreen trees’ is an odd phrase. Section 2.2: Given the importance of the wetlands to the modeling, further discussion of datasets used is warranted.

We take these points. While it is difficult to find directly comparable empirical estimates for the Congo Basin for which to compare the PFTs against, we have added a few sentences detailing a broader comparison (now lines 177-185):

“Most published estimates for land-cover follow national boundaries and so we can make broad comparisons with published estimates for the Democratic Republic of Congo (DRC). For example, our value for total forest cover for the DRC (65%), is close to the 67% and 68% values estimated by the Congo Basin Forest Partnership (CBFP, 2009), and Potapov et al. (2012), respectively. Agriculture covers only a small proportion of the basin according to the LUH dataset that is based on FAO cropland area statistics, with C3 (PFT12, Fig. 2 g) and C4 (PFT13, Fig. 2 h) agriculture making up a maximum basin area of 0.5 and 2% respectively. In reality, a larger fraction of the basin is composed of small scale and rotational agriculture (Tyukavina et al., 2018).”

L177: What is the definition of swamps versus floodplains and how are they distinguished in the Congo?

In terms of determining the maximum extent of swamps and floodplains forcing files, these are taken from the dataset of Gumbricht et al. (2017) and therefore follow his definitions. His definition of swamps can be found in Table 1 of his paper but the main characteristics are as follows: “Usually bound to valleys and plains; planar surfaces. Wet all year around, but not necessarily inundated. Usually tree covered.”

The max floodplain is defined by aggregating all of the wetland categories in the Gumbricht dataset (including swamps).

In terms of the representation in ORCHILEAK, the difference between swamps and floodplains is outlined in section 2.2. See Lauerwald et al. (2017) for further details.

In response to these comments we have also modified the corresponding paragraph (now lines 199-217):

“In grids where swamps exist, a constant proportion of river discharge is fed into the base of the soil column; **ORCHILEAK does not explicitly represent a groundwater reservoir and so this imitates the hydrological coupling of swamps and rivers through the groundwater table.** The maximal proportions of each grid which can be covered by floodplains and swamps are prescribed by the maximal fraction of floodplains (MFF) and the maximal fraction of swamps (MFS) forcing files respectively (Guimberteau et al., 2012). See also Lauerwald et al. (2017) and Hastie et al. (2019) for further details. We created an MFF forcing file for the Congo basin, derived from the Global Wetlands<sup>v3</sup> database; the 232 m resolution tropical wetland map of Gumbricht et al. (2017) (Fig. 3 a and b). We firstly amalgamated all the categories of wetland (which include floodplains and swamps) before aggregating them to a resolution of 0.5° (the resolution at which the floodplain/swamp forcing files are read by ORCHILEAK), assuming that this represents the maximum extent of inundation in the basin. This results in a mean MFF of 10%, i.e. a maximum of 10% of the surface area of the Congo basin can be inundated with water. This is identical to the mean MFF value of 10% produced with the Global Lakes and Wetlands Database, GLWD (Lehner, & Döll, P., 2004; Borges et al., 2015<sup>b</sup>). We also created an MFS forcing file from the same dataset (Fig. 3 c and d), merging the ‘swamps’ and ‘fens’ wetland categories (although note that there are virtually no fens in the Congo basin) from Global Wetlands<sup>v3</sup> database (Gumbricht et al., 2017) and again aggregating them to a 0.5° resolution. Please see Table 1 of Gumbricht et al. (2017) for further details.”

L178: Does inundation of the floodplains require exceedance of 'bank-full discharge'? See comment about section 2.3.

Yes, it does, and bank-full discharge is defined as the median stream flow over the period 1990 to 2005.

In response to these comments we have also modified the corresponding text to make it clearer (now lines- 255-258):

"As in previous studies on the Amazon basin (Lauerwald et al. 2017, Hastie et al., 2019) we defined bank-full discharge, i.e. the threshold discharge at which floodplain inundation starts (i.e. overtopping of banks), as the median discharge (50<sup>th</sup> percentile i.e.  $streamr_{50th}$ ) of the present-day climate forcing period (1990 to 2005)."

L179-180: It is unclear why 'a constant proportion of river discharge is fed into the base of the soil column'.

ORCHILEAK does not yet explicitly represent a groundwater reservoir. This imitates how rivers and swamps are hydrologically coupled through the groundwater table.

In response to these comments we have also modified the corresponding text to make it clearer (now lines- 199-201):

"In grids where swamps exist, a constant proportion of river discharge is fed into the base of the soil column; ORCHILEAK does not explicitly represent a groundwater reservoir and so this imitates the hydrological coupling of swamps and rivers through the groundwater table."

Please see section 2.1.2 and Figure 3 of Lauerwald et al. (2017) for a more detailed explanation.

L188-190: Round the MFF to 10%. Is this value the maximum MFF or the mean maximum?

Done (rounded to 10%)

Mean maximum

L193: How are 'fens' different from swamps in the Congo?

We have merged the swamps and fens categories from Gumbrecht et al. (2017) so effectively they are not different in our study. Irrespectively, according to the Gumbicht dataset there are virtually no fens in the Congo.

See modified lines 213-217:

"We also created an MFS forcing file from the same dataset (Fig. 3 c and d), merging the 'swamps' and 'fens' wetland categories (although note that there are virtually no fens in the Congo basin) from Global Wetlands<sup>v3</sup> database (Gumbrecht et al., 2017) and again aggregating them to a 0.5° resolution. Please see Table 1 of Gumbrecht et al. (2017) for further details."

Section 2.3: Indeed, simulating the hydrology well is critical. The description of the calibration steps is somewhat confusing. For example, line 217 states ‘Without calibration, the majority of the different climate forcing model runs performed poorly .’. However, key hydrological parameters needed calibration. Hence, it would seem issues with both forcings and model parameters are confounded.

Virtually all hydrological models require calibration through the modification of model parameters. Admittedly, the forcing datasets generally do not perform as well for the Congo as for the Amazon for example (likely a result of more climate data being available for the gridded climate forcing fields in the Amazon), which is why we tested several different climate forcing data to estimate uncertainties. The performance without calibration would not have been acceptable/ reasonable, and we feel that we struck the right balance between improving river flow simulation and over-calibration of parameters, keeping in mind the limitations of climate forcing datasets, and that we are calibrating/ validating for 3 quite different situations (the main stem of the Congo, a much smaller tributary, and overall inundation area).

L233-240: The concept of bank-full discharge as a threshold for initiation of inundation of floodplains is questionable as applied to tropical floodplain such as those in the Amazon or Congo. Studies inundation dynamics in the Amazon with detailed measurements or modeling indicate that inundation occurs more or less continuously as the rivers rise and that the water comes from both the rivers and uplands (e.g., Lesack and Melack 1995 *Water Resources Res* 31:329–334; Bonnet et al. 2017 *Hydrol. Processes* 31: 1702–1718; Rudorff et al 2014 *Water Resources Res* 31:329–349; Ji et al. 2019 *Water Resources Res* 54).

While we appreciate this point, we would respectfully debate some of your conclusions. For example, in their paper Bonnet et al. (2017) conclude that “The mainstream was the main input of water to the flooded area, accounting on average for 93% of total water inputs by the end of the water year. Direct precipitation and runoff from uplands contributed less than or equal to 5% and 10%, respectively. The seepage contribution was less than 1%”. They go on to explain that in their model “Diffusive overbank flows occur where the mainstream water level is above levee crests.”

Similarly, Rudorff et al. (2014) conclude that “Diffuse overbank flows represent 93% of total river to floodplain discharge”

It is true that Lesack and Melack (1995) find a much higher percentage of inflow coming from runoff (57%) but this is the results from a single case study of a small lake in the central Amazon basin.

Moreover, the majority of the wetlands which we represent in the Congo in ORCHILEAK are swamps, and so do not rely on overtopping at bank-full discharge.

L248-249: The algorithms used to generate the GIEMS vary in their effectiveness depending the density and extent of the inundated vegetation. Section 2.4.1: How well do the soil processes derived for Europe (Camino Serrano et al. 2018) apply to the Congo, how were the passive, slow and active pools determined and how were the decomposition rates in the flooded and non-flooded soil derived?

One of the main limitations which Camino Serrano et al. (2018) identified with the potential application of ORCHIDEE-SOM to the tropics was the lack of representation of DOC coming from throughfall, which is incorporated into ORCHILEAK (Lauerwald et al., 2017). The other main limitation in applying it to the Congo is the lack of an explicit representation of peatlands which we discuss in detail (see lines 735 to 760).

The active passive and slow pools are explained in detail on page 3832 of Lauerwald et al. (2017) but the main part of the text is as follows “ The soil carbon module distinguishes 3 different pools of DOC depending on the source material: active, slow and passive (Camino Serrano et al, 2018 - GMD). The DOC derived from the active SOC pool and metabolic litter is assigned to the active DOC pool, while the DOC derived from the slow and passive SOC pools are assigned to the slow and passive DOC pools, respectively (Eqs. 43–45). A part of DOC derived from structural plant litter, which is related to the lignin structure of the litter pool (Krinner et al., 2005), is allocated to the slow DOC pool, while the remainder feeds the active DOC pool. The proportion of the decomposed litter and SOC that is transformed into DOC instead of CO<sub>2</sub> depends on the carbon use efficiency (CUE), set here to a value of 0.5 (Manzoni et al., 2012). Taken that the same residence time for the slow and passive DOC pools is used in ORCHIDEE-SOM (Camino Serrano, 2015), we merge these two pools when computing throughfall and lateral transport of DOC. Thus, the labile pool is identical to the active pool of the soil carbon module, while the refractory pool combines the slow and passive pools. The labile (FTF,DOClab ) and refractory (FTF,DOCref ) proportions of throughfall DOC are added to the active and slow DOC pools of the first soil layer, respectively” We acknowledge the fact that these modelled SOC pools are not measurable, as in any land surface model, and there is no sufficient radiocarbon age data in Congo to accurately calibrate SOC turnovers in the model.

Moreover, note that in ORCHILEAK decomposition rates of SOC, DOC and litter in flooded soils are 3x lower than that of those in non- flooded soils. This is based on the findings by Rueda-Delgado et al., (2006) but also supported by additional research such as Dos Santos & Nelson., (2013).

Section 2.4.2: What were the projected land use changes? These would seem rather difficult to prescribe, as noted in the text. The exclusion of shifting cultivation would seem a serious omission.

The main land-use changes are detailed in Figure A2 of the Appendix. We acknowledge the fact that exclusion of shifting cultivation is a major limitation, though one which would be difficult to incorporate in view of the lack of a spatially explicit dataset. The LUH1 reconstruction indicates for instance shifting cultivation affecting all the tropics with a residence time of agriculture of 15 years, whereas the review from Heinan et al. 2017 (Plos one) revised downwards the area of this type of agriculture, with generally low values in Congo, except in the North east and South East, but suggested a shorter turnover of agriculture of two years only. In view of such uncertainties, we did not include shifting agriculture in the model. But added in the discussion the possibility to improve this situation using new remote sensing datasets on high resolution land cover change (Tyukavina et al. 2018, Sci. Adv)

In response to these comments we have also added to the corresponding text.

Lines 304-311:

“In the paper which describes the development of the future land use change scenarios under RCP 6.0 (Hurtt et al., 2011), it is shown that land use change is highly sensitive to land use model assumptions, such as whether or not shifting cultivation is included. The LUH1 reconstruction for



instance indicates shifting cultivation affecting all of the tropics with a residence time of agriculture of 15 years, whereas the review from Heinemann et al. (2017) revised downwards the area of this type of agriculture, with generally low values in Congo, except in the North East and South East, but suggested a shorter turnover of agriculture of two years only. In view of such uncertainties, we did not include shifting agriculture in the model.”

Lines 769-771:

“Finally, the issue of shifting cultivation demands further attention; at least for the present day a shifting cultivation forcing file could be developed based on remote sensing data (Tyukavina et al., 2018).”

Results Section 3.1: In general, simulations of mean monthly discharge for large tropical river systems without large dams at downstream stations has been demonstrated as feasible with several models. Hydrological simulations can become increasingly difficult as the scale decreases, as indicated by the less successful simulations of the Ubangi River. Though the text comparing the GIEMS and simulated inundated areas makes sense, the issue of topography as a factor influencing simulated inundated area deserves mention. L358-362: These judgments should be left to the reader to make.

We accept these points and have removed these sentences accordingly.

Section 3.2: What is the basis for the calculated standard deviations for the fluxes? Figure 5 would be clearer if redrafted larger with simpler graphics. Given all the uncertainties in the modeling and underlying data, Figure 6 would seem quite questionable.

The standard deviation represents the interannual variation across the relevant period (for example 1981-2010. We have made Figure 5 (now Figure 7) larger and simpler (note that a high definition version will be submitted at a later stage). While we note and indeed discuss the uncertainties in detail, we feel that Fig 6 (now Fig. 8) is still interesting and illustrates the fact that the Cuvette Centrale is a hotspot region of exchange between the terrestrial and aquatic realms.

Section 3.3: These results seem premature without a thorough, rigorous evaluation of the model's output under current conditions. Section 3.4: ‘The dramatic increase in the concentration of atmospheric CO<sub>2</sub> (Fig. 8 g) and subsequent fertilization effect on terrestrial NPP has the greatest overall impact on all of the fluxes across the simulation period’ is a critical point and raises a fundamental question about the veracity of the projected changes. As illustrated in a recent paper (Jiang et al. 2020 Nature 580:227-231), the possible CO<sub>2</sub> enrichment effects on mature forests are not well captured by current models and need considerably more work to be understood and properly incorporated into models. Figure 9 would be clearer if redrafted larger with simpler graphics. The colors and simple depictions of habitats are distractions.

In response to these comments we have added substantial additional discussion.

Lines 661-698:

“There is relatively sparse observed data available on the long-term trends of terrestrial C fluxes in the Congo. Yin et al. (2017) used MODIS data to estimate NPP between 2001 and 2013 across central Africa. They found that NPP increased on average by 10 g C m<sup>-2</sup> per year, while we simulate

an average annual increase of  $4 \text{ g C m}^{-2} \text{ yr}^{-1}$  over the same period across the Congo Basin. The two values are not directly comparable as they do not cover precisely the same geographic area but it is encouraging that our simulations exhibit a similar trend to remote sensing data. As previously noted, MODIS derived estimates of NPP do not fully include the effect of  $\text{CO}_2$  fertilization (de Kauwe et al., 2016) whereas ORCHILEAK does. Thus, the MODIS NPP product may underestimate the increasing trend in NPP, which would bring our modeled trend further away from this dataset. On the other hand, forest degradation effects and recent droughts have been associated with a decrease of greenness (Zhou et al., 2014) and above ground biomass loss (Qie et al., 2019) in tropical forests.

Up to a point, our results also concur with estimates based on the upscaling of biomass observations (Lewis et al., 2009; Hubau et al., 2019). Lewis et al. (2009) up-scaled forest plot measurements to calculate that intact tropical African forests represented a net uptake of approximately  $300 \text{ Tg C yr}^{-1}$  between 1968 and 2007 and this is consistent with our NEP estimate of  $275 \text{ Tg C yr}^{-1}$  over the same period. However, more recently an analysis based on an extension of the same dataset found that the above ground C sink in tropical Africa has been relatively stable for the three decades leading to 2015 (Hubau et al., 2020).

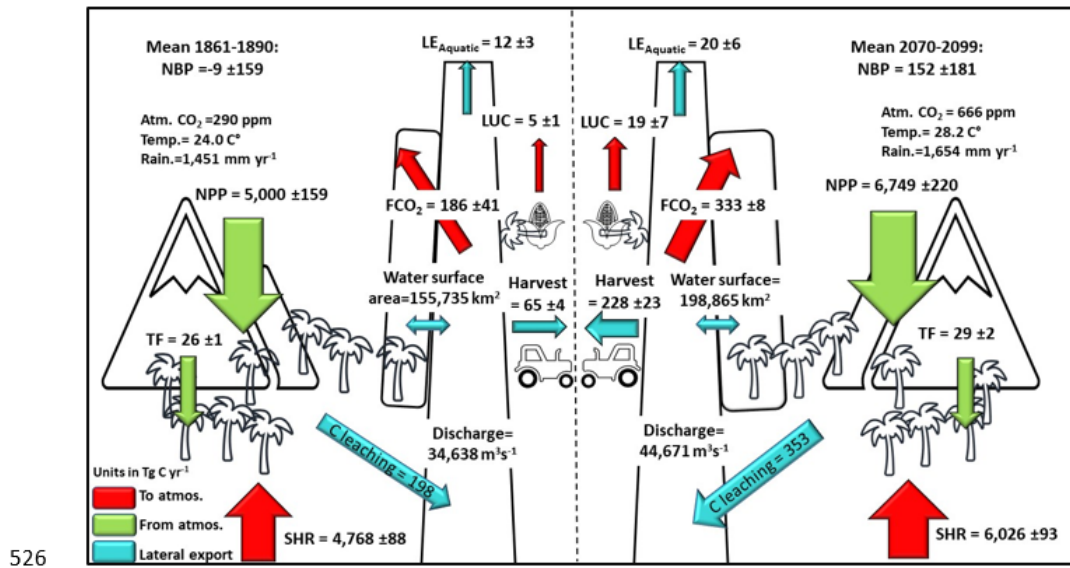
A major source of the uncertainty associated with future projections of NPP and NEP comes from our limited understanding and representation of the  $\text{CO}_2$  fertilization effect. Recent analysis of data from some of the longest-running Free-Air  $\text{CO}_2$  Enrichment (FACE) sites, consisting of early-successional temperate ecosystems, found a  $29.1 \pm 11.7\%$  stimulation of biomass over a decade (Walker et al., 2019). A meta-analysis (Liu et al., 2019) of seven temperate FACE experiments combined with process-based modelling also found substantial sensitivity ( $0.64 \pm 0.28 \text{ PgC yr}^{-1}$  per hundred ppm) of biomass accumulation to atmospheric  $\text{CO}_2$  increase, and the same study showed that ORCHIDEE model simulations were largely consistent with the experiments. However, other FACE experiments on mature temperate forests (Körner et al., 2005), as well as eucalyptus forests bring into question whether the fertilization effects observed in temperate FACE experiments can be extrapolated to other ecosystems. For example, the Swiss FACE study, a deciduous mature forest, found no significant biomass increase with enhanced  $\text{CO}_2$  (Körner et al., 2005), while a FACE experiment on a mature eucalyptus forest in Australia found that while  $\text{CO}_2$  stimulated an increase in C uptake through GPP, this did not carry to the ecosystem level, largely as a result of a concurrent increase in soil respiration (Jiang et al., 2020). Unfortunately, no results are yet available from any tropical FACE experiments, though the Amazon FACE experiment is underway and the eventual results will be crucial in developing our understanding of the  $\text{CO}_2$  fertilization effect beyond the temperate zone.”

Lines 728-732:

“There are also considerable uncertainties associated with future climate projections in the Congo basin (Haensler et al., 2013). Nutrient limitation on growth and a better representation of effect of enhanced  $\text{CO}_2$ , particularly with regards to soil respiration (Jiang et al., 2020) and tree mortality (Hubau et al., 2020), are two crucial aspects which need to be further developed.”

We have also made wording more tentative throughout (see Abstract for example and conclusion for example).

Figure 9 (now figure 10) has been simplified. As has the corresponding figure for the present day (now figure 7).



527 **Figure 10: Annual C budget (NBP) for the Congo basin for; left, the Year 1861 and right, the**  
 528 **Year 2099, simulated with ORCHILEAK. NPP is terrestrial net primary productivity, TF is**  
 529 **throughfall, SHR is soil heterotrophic respiration, FCO<sub>2</sub> is aquatic CO<sub>2</sub> evasion, LOAC is C**  
 530 **leakage to the land-ocean aquatic continuum (FCO<sub>2</sub> + LE<sub>Aquatic</sub>), LUC is flux from Land-use**  
 531 **change, and LE<sub>Aquatic</sub> is the export C flux to the coast. Range represents the standard deviation**

Discussion Section 4.1: It is not clear that CO<sub>2</sub> enrichment effects on photosynthesis results in enhancement of NPP. Though the comparisons of modeled results with regional estimates of biomass and soil C stocks seem reasonable, the empirical estimates have considerable methodological and sampling uncertainty. L500-502: That the CO<sub>2</sub> evasion from the water surfaces is sustained by leaching of dissolved CO<sub>2</sub> and DOC from soils is not established. In situ C fixation by wetlands and subsequent decomposition of this material could be a significant source of the CO<sub>2</sub> evaded as suggested by Borges, and Abril for the Amazon. Indeed, in lines 530-555, the authors discuss the likely contribution of aquatic macrophytes to the available C, and duly note the difficulty of incorporating these plants into their model. However, it is therefore odd that this possible contribution is then discounted in lines 555 to 560.

We think that the tentative language used (now lines L559-561) “Our results suggest”, in combination with the extensive discussion which you refer to appropriately reflect the limitations in our conclusions.

We would debate the conclusion that we have “discounted” the effect of macrophytes or at least that was not our intention. We fully acknowledge the important role that macrophytes are likely to play in sustaining CO<sub>2</sub> evasion from the water surface. However, we take the point that the language could be changed to make this clearer and have modified the text accordingly.

Note also, that that ORCHILEAK represents floodplains as sources of CO<sub>2</sub> to the inland water network, from the decomposition of litter and SOC, but also through root respiration of plants in that area. Hence, carbon is not only coming from upland soils, but also from wetland soils and vegetation.

Please see modified paragraph (now lines 595-625):

“The difference in our simulated riverine CO<sub>2</sub> evasion compared to the empirically derived estimate of Borges et al. (2019), could be caused by the lack of representation of aquatic plants in the ORCHILEAK model. Borges et al. (2019) used the stable isotope composition of  $\delta^{13}\text{C}$ -DIC to determine the origin of dissolved CO<sub>2</sub> in the Congo River system and found that the values were consistent with a DIC input from the degradation of organic matter, in particular from C<sub>4</sub> plants. Crucially, they further found that the  $\delta^{13}\text{C}$ -DIC values were unrelated to the contribution of *terra-firme* C<sub>4</sub> plants, rather that they were more consistent with the degradation of aquatic C<sub>4</sub> plants, namely macrophytes. ORCHILEAK does not represent aquatic plants, and the wider LSM ORCHIDEE does not have an aquatic macrophyte PFT either (though root respiration of floodplain plants for the PFTs represented, is accounted for as a C source). This could at the very least partly explain our conservative estimate of river CO<sub>2</sub> evasion, given that tropical macrophytes have relatively elevated NPPs. Rates as high as 3,500 g C m<sup>-2</sup> yr<sup>-1</sup> have been measured on floodplains in the Amazon (Silva et al., 2009). While this value is higher than the values simulated in the Cuvette Centrale by ORCHILEAK (Figure 8), they are of the same order of magnitude and so this alone cannot fully explain the discrepancy compared to the results of Borges et al. (2019). In the Amazon basin it has been shown that wetlands export approximately half of their gross primary production (GPP) to the river network compared to upland (*terra-firme*) ecosystems which only export a few percent (Abril et al. 2013). More importantly, Abril et al. (2013) found that tropical aquatic macrophytes export 80% of their GPP compared to just 36% for flooded forest. Therefore, the lack of a bespoke macrophyte PFT is indeed likely to be one reason for the discrepancy between our results and those of Borges, but largely due to their particularly high export efficiency to the river-floodplain network as opposed to differences in NPP. While being a significant limitation, creating and incorporating a macrophyte PFT would be a substantial undertaking given that the authors are unaware of any published dataset which has systematically mapped their distribution and abundance. It is important to note that while ORCHILEAK does not include the export of C from aquatic macrophytes it also neglects their NPP. Moreover, most aquatic macrophytes described in the literature have short (<1 year) life-cycles (Mitchel & Rogers, 1985). As such, while this model limitation is likely one of the causes for our relatively low estimate of riverine CO<sub>2</sub> evasion, it will only have a limited net effect on our estimate of the overall annual C balance (NBP, NEP) of the Congo basin.”

L537-539: It is not correct that strong currents limit the abundance of aquatic macrophytes in the Amazon since most of their growth occurs on floodplains where they can cover large areas.

Ok. This is taken from previous literature (Borges et al., 2015, Scientific Reports) but we have removed this.

L570-572: Both these estimates of the % of NPP per year transferred to inland waters are based on the same model. What are the estimates for the Amazon based on empirical data? L572-582: This discussion of differences between the Amazon and Congo is too simplistic and not representative of the relevant conditions in either system. It would best be deleted unless considerable more information is added. Section 4.2: As noted above, it seems a real stretch to be projecting through the 21st century. L610-625: As this section is written as a comparison with Lauerwald et al. (submitted), it does seem suitable to include until Lauerwald et al is available. Also, there are publications that project hydrological and land use changes in the Amazon.

L570-582 have been removed.

Lauerwald et al (2020) has now been accepted for publication and so we have retained the comparison of the future projections for the Amazon and the Congo.

L626-624: This paragraph does not seem necessary since these systems are quite different from the Congo and other examples could be selected. Section 4.3: Lines 636-645 re-enforce the issues raised above regarding the projections through the 21st century and the question of whether their inclusion in this paper is warranted.

Conclusion L692-696: Is it likely that an increase in DOC from 9.5 to 11.5 mg C/L will cause ecologically meaningful changes in pH?

It is unclear so we have removed these sentences.

## References

Abril, G., Martinez, J.-M., Artigas, L. F., Moreira-Turcq, P., Benedetti, M. F., Vidal, L., ... Roland, F. (2013). Amazon River carbon dioxide outgassing fuelled by wetlands. *Nature*, *505*, 395. Retrieved from <http://dx.doi.org/10.1038/nature12797>

Borges, A. V., Abril, G., Darchambeau, F., Teodoru, C. R., Deborde, J., Vidal, L. O., ... Bouillon, S. (2015)b. Divergent biophysical controls of aquatic CO<sub>2</sub> and CH<sub>4</sub> in the World's two largest rivers. *Scientific Reports*, *5*, 15614. <https://doi.org/10.1038/srep15614>

Camino-Serrano, M., Guenet, B., Luysaert, S., Ciais, P., Bastrikov, V., De Vos, B., Gielen, B., Gleixner, G., Jornet-Puig, A., Kaiser, K., Kothawala, D., Lauerwald, R., Peñuelas, J., Schrumppf, M., Vicca, S., Vuichard, N., Walmsley, D., and Janssens, I. A.: ORCHIDEE-SOM: modeling soil organic carbon (SOC) and dissolved organic carbon (DOC) dynamics along vertical soil profiles in Europe, *Geosci. Model Dev.*, *11*, 937–957, <https://doi.org/10.5194/gmd-11-937-2018>, 2018.

CBFP (Congo Basin Forest Partnership) (2009). The forests of the Congo Basin — State of the Forest 2008, Publications Office of the European Union, Luxembourg (2009), 10.2788/32259

Dos Santos, A., & Nelson, B. (2013). Leaf decomposition and fine fuels in floodplain forests of the Rio Negro in the Brazilian Amazon. *Journal of Tropical Ecology*, *29*(5), 455–458. <https://doi.org/10.1017/S0266467413000485>

Draper, F. C., Roucoux, K. H., Lawson, I. T., Mitchard, E. T. A., Coronado, E. N. H., Lähteenoja, O., ... Baker, T. R. (2014). The distribution and amount of carbon in the largest peatland complex in Amazonia. *Environmental Research Letters*, *9*(12), 124017. <https://doi.org/10.1088/1748-9326/9/12/124017>

Gumbricht, T., Roman-Cuesta, R. M., Verchot, L., Herold, M., Wittmann, F., Householder, E., Murdiyarso, D. (2017). An expert system model for mapping tropical wetlands and peatlands reveals South America as the largest contributor. *Global Change Biology*, *23*(9), 3581–3599. <https://doi.org/10.1111/gcb.13689>

Hartmann, J., R. Lauerwald, and N. Moosdorf (2014), A brief overview of the GLObal River CHEmistry Database, GLORICH, *Procedia Earth Planet. Sci.*, **10**, 23–27.

Heinimann A, Mertz O, Frolking S, Egelund Christensen A, Hurni K, Sedano F, et al. (2017) A global view of shifting cultivation: Recent, current, and future extent. *PLoS ONE* 12(9): e0184479. <https://doi.org/10.1371/journal.pone.0184479>

Hubau, W., Lewis, S.L., Phillips, O.L. *et al.* Asynchronous carbon sink saturation in African and Amazonian tropical forests. *Nature* **579**, 80–87 (2020). <https://doi.org/10.1038/s41586-020-2035-0>

Jiang, M., Medlyn, B.E., Drake, J.E. *et al.* The fate of carbon in a mature forest under carbon dioxide enrichment. *Nature* **580**, 227–231 (2020). <https://doi.org/10.1038/s41586-020-2128-9>

Korner C, Asshoff R, Bignucolo O (2005) Carbon flux and growth in mature deciduous forest trees exposed to elevated CO<sub>2</sub>. *Science*, 309, 1360–1362.

Krinner, G., Viovy, N., de Noblet-Ducoudré, N., Ogée, J., Polcher, J., Friedlingstein, P., Ciais, P., Sitch, S., and Prentice, I. C. (2005), A dynamic global vegetation model for studies of the coupled atmosphere-biosphere system, *Global Biogeochem. Cycles*, 19, GB1015, doi:[10.1029/2003GB002199](https://doi.org/10.1029/2003GB002199).

Lauerwald, R., Regnier, P., Camino-Serrano, M., Guenet, B., Guimberteau, M., Ducharne, A., ... Ciais, P. (2017). ORCHILEAK (revision 3875): a new model branch to simulate carbon transfers along the terrestrial-aquatic continuum of the Amazon basin. *Geoscientific Model Development*, 10(10), 3821–3859. <https://doi.org/10.5194/gmd-10-3821-2017>

Lauerwald, R., Regnier, P., Guenet, B., Friedlingstein, P.; Ciais, P (2020): How simulations of the land carbon sink are biased by ignoring fluvial carbon transfers – A case study for the Amazon basin. *One Earth*, 10.1016/j.oneear.2020.07.009.

Lewis, S. L., Lopez-Gonzalez, G., Sonké, B., Affum-Baffoe, K., Baker, T. R., Ojo, L. O., ... Wöll, H. (2009). Increasing carbon storage in intact African tropical forests. *Nature*, 457, 1003. Retrieved from <https://doi.org/10.1038/nature07771>

Liu, Y., Piao, S., Gasser, T., Ciais, P., Yang, H., Wang, H., ... Wang, T. (2019). Field-experiment constraints on the enhancement of the terrestrial carbon sink by CO<sub>2</sub> fertilization. *Nature Geoscience*, 12(10), 809–814. <https://doi.org/10.1038/s41561-019-0436-1>

Manzoni, S., Taylor, P., Richter, A., Porporato, A. and Ågren, G.I. (2012), Environmental and stoichiometric controls on microbial carbon-use efficiency in soils. *New Phytologist*, 196: 79-91. doi:[10.1111/j.1469-8137.2012.04225.x](https://doi.org/10.1111/j.1469-8137.2012.04225.x)

Melack, J.M., Hess, L.L., Gastil, M., Forsberg, B.R., Hamilton, S.K., Lima, I.B. and Novo, E.M. (2004), Regionalization of methane emissions in the Amazon Basin with microwave remote sensing. *Global Change Biology*, 10: 530-544. doi:[10.1111/j.1365-2486.2004.00763.x](https://doi.org/10.1111/j.1365-2486.2004.00763.x)

Potapov, P. V, Turubanova, S. A., Hansen, M. C., Adusei, B., Broich, M., Altstatt, A., ... Justice, C. O. (2012). Quantifying forest cover loss in Democratic Republic of the Congo, 2000–2010, with Landsat ETM+ data. *Remote Sensing of Environment*, 122, 106–116. <https://doi.org/10.1016/j.rse.2011.08.027>

Rasera, M. F. F. L., Krusche, A. V., Richey, J. E., Ballester, M. V. R., and Victória, R. L. (2013). Spatial and temporal variability of pCO<sub>2</sub> and CO<sub>2</sub> efflux in seven Amazonian Rivers. *Biogeochemistry*, 116(1), 241–259. <https://doi.org/10.1007/s10533-013-9854-0>

Richey, J. E., Melack, J. M., Aufdenkampe, A. K., Ballester, V. M., & Hess, L. L. (2002). Outgassing from Amazonian rivers and wetlands as a large tropical source of atmospheric CO<sub>2</sub>. *Nature*, 416, 617. Retrieved from <http://dx.doi.org/10.1038/416617a>

Rueda-Delgado G, Wantzen KM, Tolosa MB (2006) Leaf-litter decomposition in an Amazonian floodplain stream: Effects of seasonal hydrological changes. *J North Am Benthol Soc* 25:233–249. doi: 10.1899/0887-3593(2006)25[233:LDIAAF]2.0.CO;2

Tyukavina, A., Hansen, M. C., Potapov, P., Parker, D., Okpa, C., Stehman, S. V, ... Turubanova, S. (2018). Congo Basin forest loss dominated by increasing smallholder clearing. *Science Advances*, 4(11). <https://doi.org/10.1126/sciadv.aat2993>

Walker AP, De Kauwe MG, Medlyn BE, Zaehle S, Iversen CM, Asao S, Guenet B, Harper A, Hickler T, Hungate BA et al. 2019. Decadal biomass increment in early secondary succession woody ecosystems is increased by CO<sub>2</sub> enrichment. *Nature Communications* 10: 454

# 1 Historical and future contributions of inland waters to the Congo basin

## 2 carbon balance

3 Adam Hastie<sup>1,2</sup>, Ronny Lauerwald<sup>2,3,4</sup>, Philippe Ciais<sup>3</sup>, Fabrice Papa<sup>4,5,6</sup>, Pierre Regnier<sup>2</sup>

4  
5 <sup>1</sup>School of GeoSciences, University of Edinburgh, EH9 3FF, Edinburgh, Scotland, UK

6 <sup>2</sup>Biogeochemistry and Earth System Modelling, Department of Geoscience, Environment and  
7 Society, ~~Université~~ Université Libre de Bruxelles, Bruxelles, 1050, Belgium

8 <sup>3</sup>Laboratoire des Sciences du Climat et de l'Environnement (LSCE), CEA CNRS UVSQ, Gif-  
9 sur-Yvette 91191, ~~France~~ France

10 <sup>4</sup>[Université Paris-Saclay, INRAE, AgroParisTech, UMR ECOSYS, 78850, Thiverval-Grignon,](#)  
11 [France](#)

12 <sup>5,4</sup>Laboratoire d'Etudes en Géophysique et Océanographie Spatiales, Centre National de la  
13 Recherche Scientifique–Institut de recherche pour le développement–Université Toulouse Paul  
14 Sabatier–Centre national d'études spatiales, 31400 Toulouse, France

15 <sup>6,5</sup>Indo-French Cell for Water Sciences, International Joint Laboratory Institut de Recherche  
16 pour le Développement and Indian Institute of Science, Indian Institute of Science, 560012  
17 Bangalore, India

18  
19 *Correspondence to:* Adam Hastie (adam.hastie@ed.ac.uk)

20

## 21 Abstract

22 As the second largest area of contiguous tropical rainforest and second largest river basin in  
23 the world, the Congo basin has a significant role to play in the global carbon (C) cycle.

24 ~~Inventories suggest that terrestrial net primary productivity (NPP) and C storage in tree biomass~~  
25 ~~has increased in recent decades in intact forests of tropical Africa, due in large part to a~~  
26 ~~combination of increasing atmospheric CO<sub>2</sub> concentrations and climate change, while~~  
27 ~~rotational agriculture and logging have caused C losses.~~ For the present day, it has been shown

28 that a significant proportion of global terrestrial net primary productivity (NPP) is transferred  
29 laterally to the land-ocean aquatic continuum (LOAC) as dissolved CO<sub>2</sub>, dissolved organic  
30 carbon (DOC) and particulate organic carbon (POC). Whilst the importance of LOAC fluxes  
31 in the Congo basin has been demonstrated for the present day, it is not known to what extent



32 these fluxes have been perturbed historically, how they are likely to change under future  
33 climate change and land use scenarios, and in turn what impact these changes might have on  
34 the overall C cycle of the basin. Here we apply the ORCHILEAK model to the Congo basin  
35 and ~~show estimate~~ that 4% of terrestrial NPP (NPP = 5,800 ±166 Tg C yr<sup>-1</sup>) is currently  
36 exported from soils and vegetation to inland waters. Further, ~~our results suggest we found~~ that  
37 aquatic C fluxes may have undergone considerable perturbation since 1861 to the present day,  
38 with aquatic CO<sub>2</sub> evasion and C export to the coast increasing by 26% (186 ±41 Tg C yr<sup>-1</sup> to  
39 235 ±54 Tg C yr<sup>-1</sup>) and 25% (12 ±3 Tg C yr<sup>-1</sup> to 15 ±4 Tg C yr<sup>-1</sup>) respectively, largely because  
40 of rising atmospheric CO<sub>2</sub> concentrations. Moreover, under climate scenario RCP 6.0 we  
41 predict that this perturbation ~~will could~~ continue; over the full simulation period (1861-2099),  
42 we estimate that aquatic CO<sub>2</sub> evasion and C export to the coast ~~will could~~ increase by 79% and  
43 67% respectively. Finally, we show that the proportion of terrestrial NPP lost to the LOAC  
44 ~~could increase also increases~~ from approximately 3% to 5% from 1861-2099 as a result of  
45 increasing atmospheric CO<sub>2</sub> concentrations and climate change. However, our future  
46 projections of the Congo basin C fluxes in particular need to be interpreted with some caution  
47 due to model limitations. We discuss these limitations, including the wider limitations  
48 associated with applying the current generation of land surface models that ignore nutrient  
49 dynamics to make future projections of the tropical C cycle, along with potential next steps.  
50 :

## 51 **2.1. Introduction**

52 As the world's second largest area of contiguous tropical rainforest and second largest river,  
53 the Congo basin has a significant role to play in the global carbon (C) cycle. Current estimates  
54 of its C stocks and fluxes are limited by a sparsity of field data and therefore have substantial  
55 uncertainties, both quantified and unquantified (Williams et al., 2007; Lewis et al., 2009;  
56 Dargie et al., 2017). Nevertheless, it has been estimated that there is a Approximately 50 Pg C

57 ~~is~~ stored in its above ground biomass (Verhegghen et al., 2012), and up to 100 Pg C contained  
58 within its soils (Williams et al., 2007). Moreover, a recent study estimated that around 30 ~~(6.3–~~  
59 ~~46.8)~~ Pg C is stored in the peats of the Congo alone (Dargie et al., 2017). Field data suggest  
60 that storage in tree biomass increased by 0.34 ~~(0.15– 0.43)~~ Pg C yr<sup>-1</sup> in intact African tropical  
61 forests between 1968-2007 (Lewis et al., 2009) due in large part to a combination of increasing  
62 atmospheric CO<sub>2</sub> concentrations and climate change (Ciais et al., 2009; Pan et al., 2015), while  
63 satellite data indicates that terrestrial net primary productivity (NPP) has increased by an  
64 average of 10 g C m<sup>-2</sup> yr<sup>-1</sup> per year between 2001 and 2013 in tropical Africa (Yin et al., 2017).  
65 -At the same time, forest degradation, clearing for rotational agriculture and logging are causing  
66 C losses to the atmosphere (Zhuravleva et al., 2013; Tyukavina et al., 2018) while droughts  
67 have reduced vegetation greenness and water storage over the last decade (Zhou et al., 2014).  
68 A recent estimate of above ground C stocks of tropical African forests, mainly in the Congo,  
69 indicates a minor net C loss from 2010 to 2017 (Fan et al., 2019). Moreover, recent field data  
70 suggests that the above ground C sink in tropical Africa was relatively stable from 1985 to  
71 2015 (Hubau et al., 2020).  
72 There are large uncertainties associated with projecting future trends in the Congo basin  
73 terrestrial C cycle, firstly related to predicting which trajectories of future CO<sub>2</sub> levels and land  
74 use changes will occur, and secondly to our ability to fully understand and simulate these  
75 changes and in turn their impacts. Future model projections for the 21<sup>st</sup> century agree that  
76 temperature will significantly increase under both low and high emission scenarios (Haensler  
77 et al., 2013), while precipitation is only projected to substantially increase under high emission  
78 scenarios, the basin mean remaining more or less unchanged under low emission scenarios  
79 (Haensler et al., 2013). Uncertainties in future land-use change projections for Africa are  
80 among the highest for any continent (Hurt et al., 2011).

81 For the present day at [the](#) global scale, it has been estimated that between 1 and 5 Pg C yr<sup>-1</sup> is  
82 transferred laterally to the land-ocean aquatic continuum (LOAC) as dissolved CO<sub>2</sub>, dissolved  
83 organic carbon (DOC) and particulate organic carbon (POC) (Cole et al., 2007; Battin et al.,  
84 2009; Regnier et al., 2013; Drake et al., 2018; Ciais et al. [in review 2020](#)). This C can  
85 subsequently be evaded back to the atmosphere as CO<sub>2</sub>, undergo sedimentation in wetlands  
86 and inland waters, or be transported to estuaries or the coast. The tropical region is a hotspot  
87 area for inland water C cycling ([Richey et al., 2002](#); [Melack et al., 2004](#); [Abril et al., 2014](#);  
88 [Borges et al., 2015<sup>a</sup>](#); Lauerwald et al., 2015) due to high terrestrial NPP and precipitation, and  
89 a recent study used an upscaling approach based on observations to estimate present day CO<sub>2</sub>  
90 evasion from the rivers of the Congo basin at 251±46 Tg C yr<sup>-1</sup> and the lateral C (TOC +DIC)  
91 export to the coast at 15.5 (13-18) Tg C yr<sup>-1</sup> (Borges et al., 2015<sup>a</sup>; Borges et al., 2019). To put  
92 this into context, their estimate of aquatic CO<sub>2</sub> evasion represents 39% of the global value  
93 estimated by Lauerwald et al. (2015, 650 Tg C yr<sup>-1</sup>) or 14% of the global estimate of Raymond  
94 et al. (2013, 1,800 Tg C yr<sup>-1</sup>). [Note that while Lauerwald et al. \(2015\) and Raymond et al.](#)  
95 [\(2013\) relied largely on the same database of partial pressure of CO<sub>2</sub> \(pCO<sub>2</sub>\) measurements](#)  
96 [\(GloRiCh, Hartmann et al., 2014\) as the basis for their estimates, they took different, albeit](#)  
97 [both empirically led approaches. Moreover, both approaches were limited by a relative paucity](#)  
98 [of data from the tropics, which also explains the high degree of uncertainty associated with our](#)  
99 [understanding of global riverine CO<sub>2</sub> evasion.](#)

100 Whilst the importance of LOAC fluxes in the Congo basin has been demonstrated for the  
101 present day, it is not known to what extent these fluxes have been perturbed historically, how  
102 they are likely to change under future climate change and land use scenarios, and in turn what  
103 impact these changes might have on the overall C balance of the Congo. In light of these  
104 knowledge gaps, we address the following research questions:

- 105 • What is the relative contribution of LOAC fluxes (CO<sub>2</sub> evasion and C export to the  
106 coast) to the present-day C balance of the basin?
- 107 • To what extent have LOAC fluxes changed from 1860 to the present day and what are  
108 the primary drivers of this change?
- 109 • How will these fluxes change under future climate and land use change scenarios (RCP  
110 6.0 which represents the “no mitigation scenario”) and what are the implications of this  
111 change?

112

113 Understanding and quantifying these long-term changes requires a complex and integrated  
114 mass-conservation modelling approach. The ORCHILEAK model (Lauerwald et al., 2017), a  
115 new version of the land surface model ORCHIDEE (Krinner et al., 2005), is capable of  
116 simulating ~~both observed~~ terrestrial and aquatic C fluxes in a consistent manner for the present  
117 day in the Amazon (Lauerwald et al., 2017) and Lena (Bowring et al., 2019<sup>a</sup>; Bowring et al.,  
118 2019<sup>b</sup>) basins, albeit with limitations including a lack of explicit representation of POC fluxes  
119 and in-stream autotrophic production (see Lauerwald et al., 2017; Bowring et al., 2019<sup>a</sup>;  
120 Bowring et al., 2019<sup>b</sup> and Hastie et al., 2019 for further discussion). Moreover, it was recently  
121 demonstrated that this model could recreate observed seasonal and interannual variation in  
122 Amazon aquatic and terrestrial C fluxes (Hastie et al., 2019).

123 In order to accurately simulate aquatic C fluxes, it is crucial to provide a realistic representation  
124 of the hydrological dynamics of the Congo River, including its wetlands. Here, we develop  
125 new wetland forcing files for the ORCHILEAK model from the high-resolution dataset of  
126 Gumbricht et al. (2017) and apply the model to the Congo basin. After validating the model  
127 against observations of discharge, flooded area and DOC concentrations for the present day,  
128 we then use the model to understand and quantify the long- term (1861-2099) temporal trends  
129 in both the terrestrial and aquatic C fluxes of the Congo Basin.

### 130 **3.2. Methods**

131 ORCHILEAK (Lauerwald et al., 2017) is a branch of the ORCHIDEE land surface model  
132 (LSM), building on past model developments such as ORCHIDEE-SOM (Camino Serrano,  
133 2018<sup>5</sup>), and represents one of the first LSM-based approaches which fully integrates the  
134 aquatic C cycle within the terrestrial domain. ORCHILEAK simulates DOC production in the  
135 canopy and soils, the leaching of dissolved CO<sub>2</sub> and DOC to the river from the soil, the  
136 mineralization of DOC, and in turn the evasion of CO<sub>2</sub> to the atmosphere from the water  
137 surface. Moreover, it represents the transfer of C between litter, soils and water within  
138 floodplains and swamps (see section 2.2). Once within the river routing scheme, ORCHILEAK  
139 assumes that the lateral transfer of CO<sub>2</sub> and DOC are proportional to the volume of water. DOC  
140 is divided into a refractory and labile pool within the river, with half-lives of 80 and 2 days  
141 respectively. The refractory pool corresponds to the combined slow and passive DOC pools of  
142 the soil C scheme, and the labile pool corresponds to the active soil pool (see section 2.4.1).  
143 The concentration of dissolved CO<sub>2</sub> and the temperature-dependent solubility of CO<sub>2</sub> are used  
144 to calculate ~~the partial pressure of CO<sub>2</sub>~~ ( $p\text{CO}_2$ ) in the water column. In turn, CO<sub>2</sub> evasion is  
145 calculated based on  $p\text{CO}_2$ , along with a diurnally variable water surface area and a gas  
146 exchange velocity. Fixed gas exchange velocities of 3.5 m d<sup>-1</sup> and 0.65 m d<sup>-1</sup> respectively are  
147 used for rivers (including open floodplains) and forested floodplains.

148 In this study, as in previous studies (Lauerwald et al., 2017, Hastie et al. 2019, Bowring et al.,  
149 2019<sup>a,b</sup>), we run the model at a spatial resolution of 1° and use the default time step of 30 min  
150 for all vertical transfers of water, energy and C between vegetation, soil and the atmosphere,  
151 and the daily time-step for the lateral routing of water. Until now, in the Tropics, ORCHILEAK  
152 has been parameterized and calibrated only for the Amazon River basin (Lauerwald et al., 2017,  
153 Hastie et al. 2019). To adapt and apply ORCHILEAK to the specific characteristics of the  
154 Congo River basin (2.1), we had to establish new forcing files representing the maximal

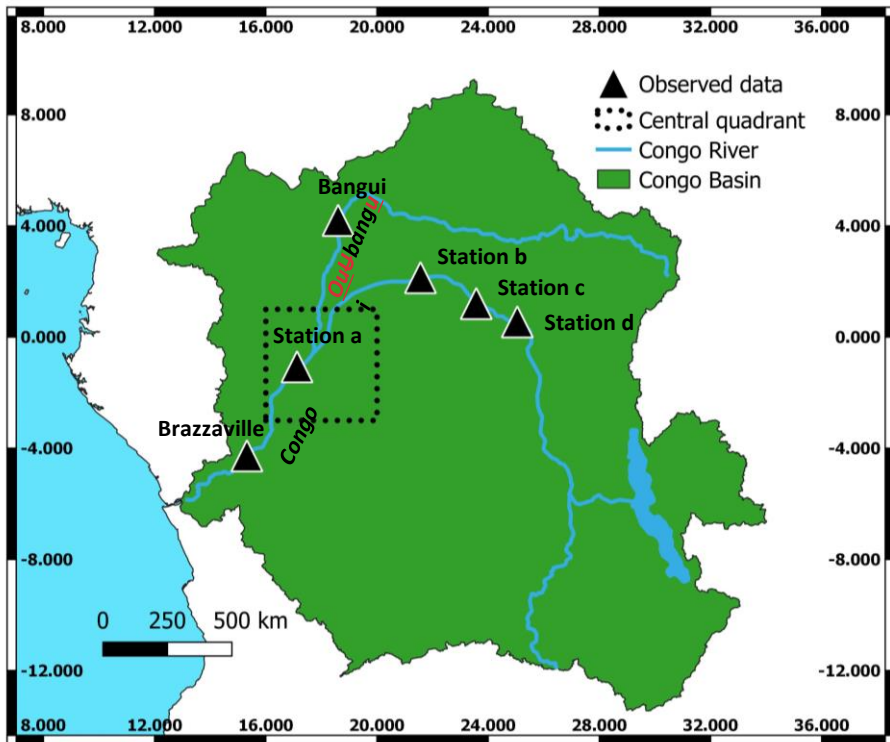
155 fraction of floodplains (MFF) and the maximal fraction of swamps (MFS) (2.2) and to  
156 recalibrate the river routing module of ORCHILEAK (2.3). All of the processes represented in  
157 ORCHILEAK remain identical to those previously represented for the Amazon ORCHILEAK  
158 (Lauerwald et al., 2017; Hastie et al., 2019). In the following methodology sections, we  
159 describe; 2.1- Congo basin description, 2.2- Development of floodplains and swamps forcing  
160 files, 2.3- Calibration of hydrology, 2.4- Simulation set-up, 2.5- Evaluation and analysis of  
161 simulated fluvial C fluxes, and 2.6- Calculating the net carbon balance of the Congo Basin. For  
162 a full description of the ORCHILEAK model please see Lauerwald et al. (2017).

### 163 **2.1 Congo basin description**

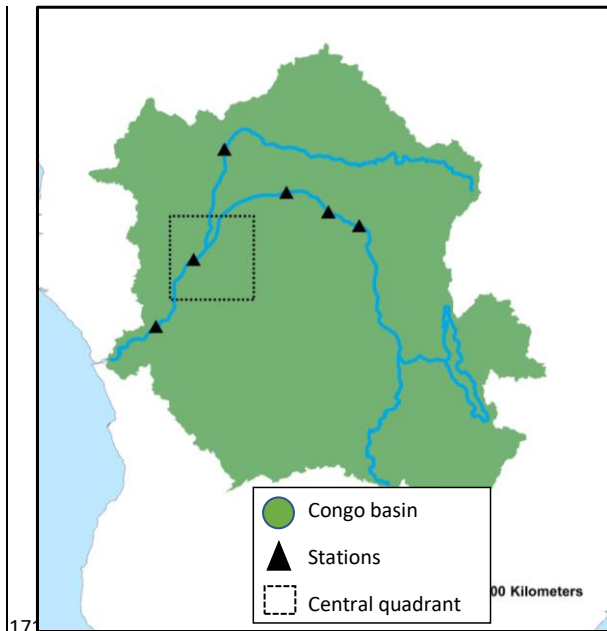
164 The Congo Basin is the world's second largest area of contiguous tropical rainforest and second  
165 largest river basin in the world (Fig. 1), covering an area of  $3.7 \times 10^6 \text{ km}^2$ , with a mean discharge  
166 of around  $42,000 \text{ m}^3 \text{ s}^{-1}$  (O'Loughlin et al., 2013) and a variation between  $24,700\text{--}75,500 \text{ m}^3$   
167  $\text{s}^{-1}$  across months (Coynel et al., 2005).

168

169



17



172 **Figure 1: Extent of the Congo Basin, central quadrant of the “Cuvette Centrale” and sampling**  
 173 **stations (for DOC and discharge) along the Congo and *Ubangi-Oubangui* Rivers (in italic).**

174

175 The major climate (ISMSIP2b, Frieler et al., 2017; Lang et al., 2017) and land-cover (LUH-

176 CMIP5) characteristics of the Congo Basin for the present day (1981-2010) are shown in Figure

177 2. The mean annual temperature is 25.2 °C but with considerable spatial variation from a low

178 of 18.4°C to a high of 27.2°C (Fig. 2 a), while mean annual rainfall is 1520mm, varying from

179 733 mm to 4087 mm (Fig. 2 b). ORCHILEAK prescribes 13 different plant functional types

180 (PFTs). Land-use is mixed with tropical broad-leaved evergreen (PFT2, Fig. 1 c), tropical

181 broad-leaved rain green (PFT3, Fig. 1 d), C<sub>3</sub> grass (PFT10, Fig. 2 e) and C<sub>4</sub> grass (PFT11, Fig.

182 2 f) covering a maximum of 26%, 35%, 8% and 25% of the basin area respectively (Table A3).

183 Most published estimates for land-cover follow national boundaries and so we can make broad

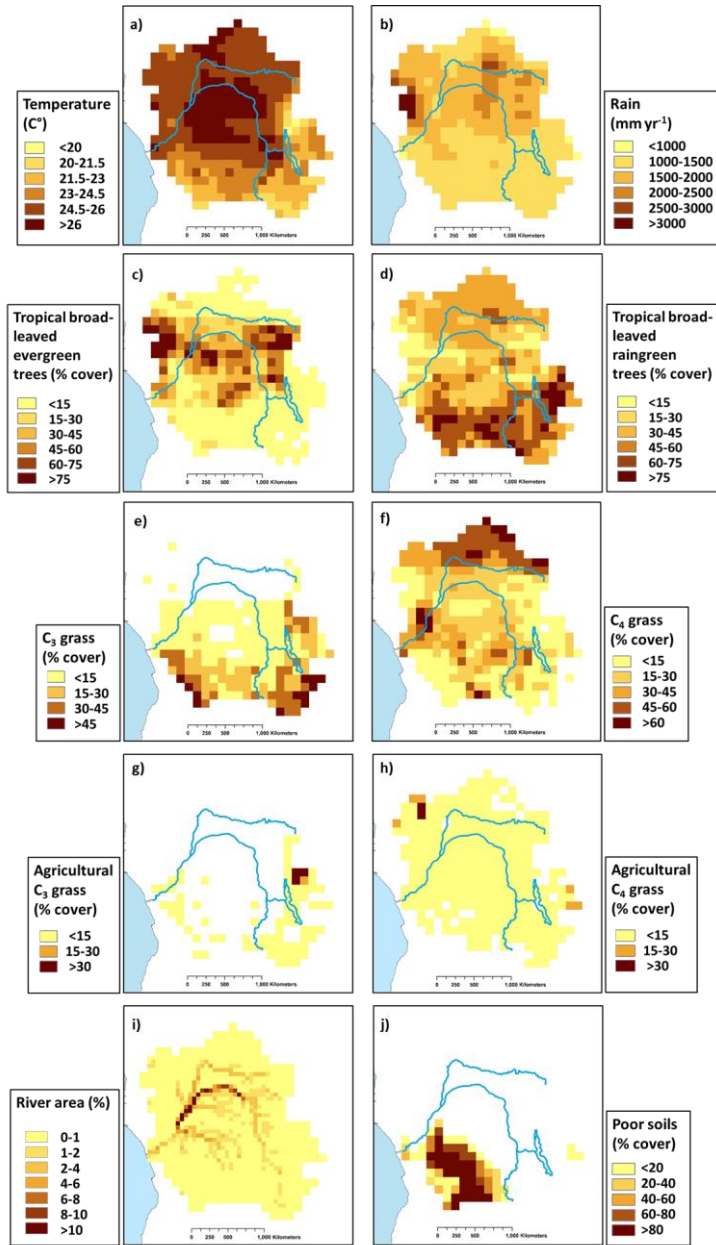
184 comparisons with published estimates for the Democratic Republic of Congo (DRC). For

185 example, our value for total forest cover for the DRC (65%), is close to the 67% and 68%

186 values estimated by the Congo Basin Forest Partnership (CBFP, 2009), and Potapov et al.



187 [\(2012\), respectively](#). Agriculture covers only a small proportion of the basin according to the  
188 LUH dataset that is based on FAO cropland area statistics, with C3 (PFT12, Fig. 2 g) and C4  
189 (PFT13, Fig. 2 h) agriculture making up a maximum basin area of 0.5 and 2% respectively  
190 ~~(Table A3)~~. In reality, a larger fraction of the basin is composed of small scale and rotational  
191 agriculture (Tyukavina et al., 2018). The ORCHILEAK model also has a “poor soils” forcing  
192 file (Fig. 2 j) which prescribes reduced decomposition rates in soils with low nutrient and pH  
193 soils such as Podzols and Arenosols (Lauerwald et al., 2017). This file is developed from the  
194 Harmonized World Soil Database (FAO/IIASA/ISRIC/ISS-CAS/JRC, 2009).



195

196 **Figure 2: Present day (1981-2010) spatial distribution of the principal climate and land-use**  
 197 **drivers used in ORCHILEAK, across the Congo Basin; a) mean annual temperature in °C, b)**  
 198 **mean annual rainfall in mm yr<sup>-1</sup>, c)-h) mean annual maximum vegetated fraction for PFTs 2,3,**

199 **10,11,12 and 13, i) river area, and j) Poor soils. All at a resolution of 1° except for river area**  
200 **(0.5°).**

## 201 **2.2 Development of floodplains and swamps forcing files**

202 In ORCHILEAK, water in the river network can be diverted to two types of wetlands,  
203 floodplains and swamps. In each grid where a floodplain exists, a temporary waterbody can be  
204 formed adjacent to the river and is fed by the river once bank-full discharge (see section 2.3)  
205 is exceeded. In grids where swamps exist, a constant proportion of river discharge is fed into  
206 the base of the soil column; ORCHILEAK does not explicitly represent a groundwater reservoir  
207 and so this imitates the hydrological coupling of swamps and rivers through the groundwater  
208 table. The maximal proportions of each grid which can be covered by floodplains and swamps  
209 are prescribed by the maximal fraction of floodplains (MFF) and the maximal fraction of  
210 swamps (MFS) forcing files respectively (Guimberteau et al., 2012). See also Lauerwald et al.  
211 (2017) and Hastie et al. (2019) for further details. We created an MFF forcing file for the Congo  
212 basin, derived from the Global Wetlands<sup>v3</sup> database; the 232 m resolution tropical wetland map  
213 of Gumbricht et al. (2017) (Fig. 3 a and b). We firstly amalgamated all the categories of wetland  
214 (which include floodplains and swamps) before aggregating them to a resolution of 0.5° (the  
215 resolution at which the floodplain/swamp forcing files are read by ORCHILEAK), assuming  
216 that this represents the maximum extent of inundation in the basin. This results in a mean MFF  
217 of ~~10.3%~~, i.e. a maximum of ~~10.3%~~ of the surface area of the Congo basin can be inundated  
218 with water. This is ~~videntical to theory similar to the~~ mean MFF value of 10% produced with  
219 the Global Lakes and Wetlands Database, GLWD (Lehner, & Döll, P.,2004; Borges et al.,  
220 2015<sup>b</sup>). We also created an MFS forcing file from the same dataset (Fig. 3 c and d), merging  
221 the ‘swamps’ and ‘fens’ wetland categories (although note that there are virtually no fens in  
222 the Congo basin) from Global Wetlands<sup>v3</sup> database (Gumbricht et al., 2017) and again  
223 aggregating them to a 0.5° resolution. Please see Table 1 of Gumbricht et al. (2017) for further  
224 details.

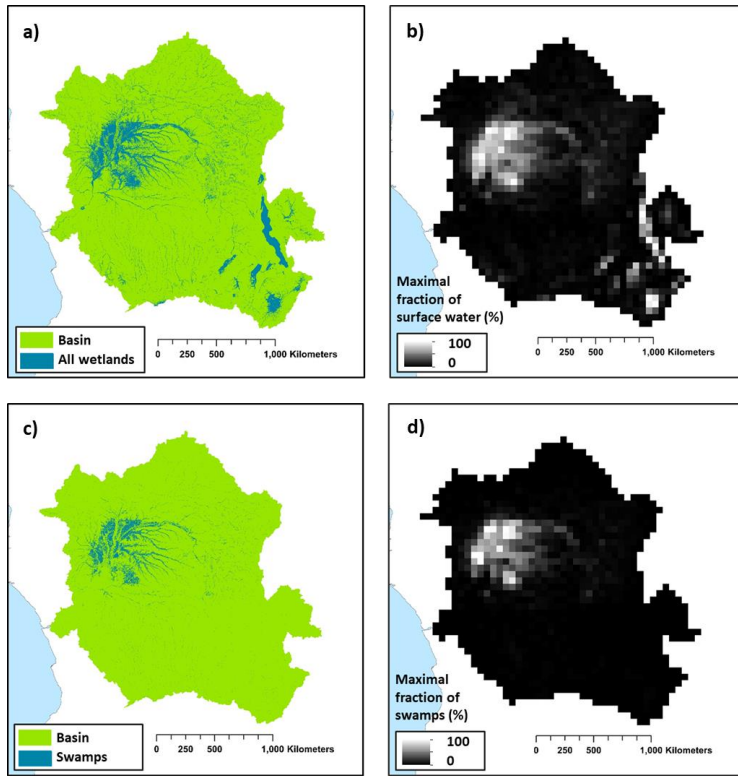


Figure 3: a) Wetland extent (from Gumbricht et al., 2017). b) The new maximal fraction of floodplain (MFF) forcing file developed from a). c) Swamps (including fens) category within Congo basin from Gumbricht et al (2017). d) the new maximal fraction of swamps (MFS) forcing file developed from c). Panels a) and b) are at the same resolution as the Gumbricht dataset (232m) while b) and d) are at a resolution of 0.5°. Note that 0.5° is the resolution of the sub unit basins in ORCHILEAK (Lauerwald et al., 2015), with each 1° grid containing four sub basins.

227

### 228 2.3 Calibration of hydrology

229 As the main driver of the export of C from the terrestrial to aquatic system, it is crucial that the  
230 model can represent present-day hydrological dynamics, at the very least on the main stem of  
231 the Congo. As this study is primarily concerned with decadal- centennial timescales our priority

232 was to ensure that the model can accurately recreate observed mean annual discharge at the  
233 most downstream gauging station Brazzaville. We also tested the model's ability to simulate  
234 observed discharge seasonality, as well as flood dynamics. Moreover, no data is available with  
235 which to directly evaluate the simulation of DOC and CO<sub>2</sub> leaching from the soil to the river  
236 network, and thus we tested the model's ability to recreate the spatial variation of observed  
237 riverine DOC ~~and pCO<sub>2</sub>~~ concentrations ~~and pCO<sub>2</sub>~~ at specific stations where measurements are  
238 available (Borges et al., 2015<sup>b</sup>; [Bouillon et al., 2012 & 2014](#), [locations](#) ~~and~~ shown in Fig. 1),  
239 river DOC ~~and CO<sub>2</sub>~~ concentration ~~and pCO<sub>2</sub>~~ being regarded as an integrator of the C transport  
240 at the terrestrial-aquatic interface.

241 We first ran the model for the present-day period, defined as from 1990 to 2005/2010  
242 depending on which climate forcing data was applied, using four climate forcing datasets;  
243 namely ISIMIP2b (Frieler et al., 2017), Princeton GPCC (Sheffield et al., 2006), GSWP3 (Kim,  
244 2017) and CRUNCEP (Viovy, 2018). We used ISIMIP2b for the historical and future  
245 simulations as it is the only climate forcing dataset to cover the full period (1861-2099).  
246 However, we compared it to other climate forcing datasets for the present day in order to gauge  
247 its ability to simulate observed discharge on the Congo River at Brazzaville (Table A1).  
248 Without calibration, the majority of the different climate forcing model runs performed poorly,  
249 unable to accurately represent the seasonality and mean monthly discharge at Brazzaville  
250 (Table A1). The best performing climate forcing dataset was ISIMIP2b followed by Princeton  
251 GPCC with root mean square errors (RMSE) of 29% and 40% and Nash Sutcliffe efficiencies  
252 (NSE) of 0.20 and -0.25, respectively. NSE is a statistical coefficient specifically used to test  
253 the predictive skill of hydrological models (Nash & Sutcliffe, 1970).

254 For ISIMIP2b we further calibrated key hydrological model parameters, namely the constants  
255 which dictate the water residence time of the groundwater (=slow reservoir), headwaters (=  
256 fast reservoir) and floodplain reservoirs in order to improve the simulation of observed

257 discharge at Brazzaville (Table 2). To do so, we tested different combinations of water  
258 residence times for the three reservoirs, eventually settling on 1, 0.5 and 0.5 (days) for the slow,  
259 fast and floodplain reservoirs respectively, all three being reduced compared to those values  
260 used in the original ORCHILEAK calibration for the Amazon (Lauerwald et al., 2017).

261 In order to calibrate the simulated discharge against observations, we first modified the flood  
262 dynamics of ORCHILEAK in the Congo Basin for the present day by adjusting bank-full  
263 discharge ( $streamr_{50th}$ , Lauerwald et al., 2017) and 95<sup>th</sup> percentile of water level heights  
264 ( $floodh_{95th}$ ). As in previous studies on the Amazon basin (Lauerwald et al. 2017, Hastie et al.,  
265 2019) we defined bank-full discharge, i.e. the threshold discharge at which floodplain  
266 inundation starts (*i.e. overtopping of banks*), as the median discharge (50<sup>th</sup> percentile i.e.  
267  $streamr_{50th}$ ) of the present-day climate forcing period (1990 to 2005). After re-running each  
268 model parametrization (different water residence times) to obtain those bank-full discharge  
269 values, we calculated  $floodh_{95th}$  over the simulation period for each grid cell (Table 1). This  
270 value is assumed to represent the water level over the river banks at which the maximum  
271 horizontal extent of floodplain inundation is reached. We then ran the model for a final time  
272 and validated the outputs against discharge data at Brazzaville (Cochoy et al., 2006, Fig.  
273 1). This procedure was repeated iteratively with the ISIMIP2b climate forcing, modifying the  
274 water residence times of each reservoir in order to find the best performing parametrization.

275 ~~We firstly Limited-observed-discharge-data is available for the Congo-basin, with the majority~~  
276 ~~concentrated on the main stem of the Congo, at Brazzaville station. After comparing~~  
277 simulated ~~versus~~ observed discharge at Brazzaville (NSE, RMSE, Table 2), ~~before~~  
278 ~~using~~ the data of Bouillon et al. (2014) to further validate discharge at Bangui (Fig. 1) on the  
279 main tributary ~~Ubangi-Oubangui~~. In addition, we compared the simulated seasonality of flooded  
280 area against the satellite derived dataset GIEMS (Prigent et al., 2007; Becker et al., 2018),  
281 within the Cuvette Centrale wetlands (Fig. 1).

## 282 **2.4 Simulation set-up**

283 A list of the main forcing files used, along with data sources, is presented in Table 1. The  
284 derivation of the floodplains and swamp (MFF & MFS) is described in section 2.2 while the  
285 calculation of “bankfull discharge” ( $\text{streamr}_{50\text{th}}$ ) and “95th percentile of water table height over  
286 flood plain” ( $\text{floodh}_{95\text{th}}$ ) (Table 1) is described in section 2.3.

### 287 **2.4.1 Soil carbon spin up**

288 ORCHILEAK includes a soil module, primarily derived from ORCHIDEE-SOM (Camino  
289 Serrano, 2018). The soil module has 3 different pools of soil DOC; the passive, slow and active  
290 pool and these are defined by their source material and residence times ( $\tau_{\text{carbon}}$ ). ORCHILEAK  
291 also differentiates between flooded and non-flooded soils; decomposition rates of DOC, SOC  
292 and litter being reduced (3 times lower) in flooded soils. In order for the soil C pools to reach  
293 steady state, we spun-up the model for around 9,000 years, with fixed land-use representative  
294 of 1861, and looping over the first 30 years of the ISMSIP2b climate forcing data (1861-1890).  
295 During the first 2,000 years of spin-up, we ran the model with an atmospheric  $\text{CO}_2$   
296 concentration of  $350 \mu\text{atm}$  and default soil C residence times ( $\tau_{\text{carbon}}$ ) halved, which allowed it  
297 to approach steady-state more rapidly. Following this, we ran the model for a further 7,000  
298 years reverting to the default  $\tau_{\text{carbon}}$  values. At the end of this process, the soil C pools had  
299 reached approximately steady state;  $<0.02\%$  change in each pool over the final century of the  
300 spin-up.

### 301 **2.4.2 Transient simulations**

302 After the spin-up, we ran a historical simulation from 1861 until the present day, 2005 in the  
303 case of the ISIMIP2b climate forcing data. We then ran a future simulation until 2099, using  
304 the final year of the historical simulation as a restart file. In both of these simulations, climate,  
305 atmospheric  $\text{CO}_2$  and land-cover change were prescribed as fully transient forcings according  
306 to the RCP6.0 scenario. For climate variables, we used the IPSL-CM5A-LR model outputs for

307 RCP 6.0, bias corrected by the ISIMIP2b procedure (Frieler et al., 2017; Lange et al., 2017),  
308 while land-use change was taken from the 5th Coupled Model Intercomparison Project  
309 (CMIP5). As our aim is to investigate long-term trends, we calculated 30-years running means  
310 of simulated C flux outputs in order to smooth interannual variations. RCP 6.0 is an emissions  
311 pathway that leads to a “stabilization of radiative forcing at 6.0 Watts per square meter ( $\text{Wm}^{-2}$ )  
312 in the year 2100 without exceeding that value in prior years” (Masui et al., 2011). It is  
313 characterised by intermediate energy intensity, substantial population growth, mid-high C  
314 emissions, increasing cropland area to 2100 and decreasing natural grassland area (van Vuuren  
315 et al., 2011). In the paper which describes the development of the future land use change  
316 scenarios under RCP 6.0 (Hurtt et al., 2011), it is shown that land use change is highly sensitive  
317 to land use model assumptions, such as whether or not shifting cultivation is included. The  
318 LUH1 reconstruction for instance indicates shifting cultivation affecting all of the tropics with  
319 a residence time of agriculture of 15 years, whereas the review from Heinimann et al. (2017)  
320 revised downwards the area of this type of agriculture, with generally low values in Congo,  
321 except in the North eEast and South East, but suggested a shorter turnover of agriculture of two  
322 years only. In view of such uncertainties, we did not include shifting agriculture in the model.  
323 ~~In our simulations, shifting cultivation is not included. Moreover, Africa is one the regions with~~  
324 ~~the largest uncertainty range, and thus,~~ there is considerable uncertainty associated with the  
325 effect of future land-use change in Africa (Hurtt et al., 2011). We chose RCP 6.0 as it represents  
326 a no mitigation (mid-high emissions) scenario, ~~and because it was the scenario applied in the~~  
327 ~~recent paper of Lauerwald et al. (submitted) to examine the long-term LOAC fluxes in the~~  
328 ~~Amazon basin. Therefore, we can directly compare our results for the Congo to those for the~~  
329 ~~Amazon.~~ Moreover, the ISIMIP2b data only provided two RCPs at the time we performed the  
330 simulations; RCP 2.6 (low emission) and RCP 6.0.



331 With the purpose of evaluating separately the effects of land-use change, climate change, and  
 332 rising atmospheric CO<sub>2</sub>, we ran a series of factorial simulations. In each simulation, one of  
 333 these factors was fixed at its 1861 level (the first year of the simulation), or in the case of fixed  
 334 climate change, we looped over the years 1861-1890. The outputs of these simulations (also  
 335 30-year running means) were then subtracted from the outputs of the main simulation (original  
 336 run with all factors varied) so that we could determine the contribution of each driver (Fig. 10,  
 337 Table 1).

<b>Variable</b>	<b>Spatial resolution</b>	<b>Temporal resolution</b>	<b>Data source</b>
Rainfall, snowfall, incoming shortwave and longwave radiation, air temperature, relative humidity and air pressure (close to surface), wind speed (10 m above surface)	1°	1 day	ISIMIP2b, IPSL-CM5A-LR model outputs for RCP6.0 (Frieler et al., 2017)
Land cover (and change)	0.5°	annual	LUH-CMIP5
Poor soils	0.5°	annual	Derived from HWSO v 1.1 (FAO/IIASA/ISRIC/ISS-CAS/JRC, 2009)
Stream flow directions	0.5°	annual	STN-30p (Vörösmarty et al., 2000)
Floodplains and swamps fraction in each grid (MFF & MFS)	0.5°	annual	derived from the wetland high resolution data of Gumbricht et al. (2017)
River surface areas	0.5°	annual	Lauerwald et al. (2015)
Bankfull discharge (stream <sub>r50th</sub> )	1°	annual	derived from calibration with ORCHILEAK (see section 2.3)
95th percentile of water table height over flood plain (floodh <sub>95th</sub> )	1°	annual	derived from calibration with ORCHILEAK (see section 2.3)

## 338 2.5 Evaluation and analysis of simulated fluvial C fluxes

339 We first evaluated DOC concentrations [and pCO<sub>2</sub>](#) at several locations along the Congo  
 340 mainstem (Fig. 1), and on the [UbangiOubangui](#) -river against the data of Borges et al. (2015<sup>b</sup>)  
 341 [and Bouillon et al. \(2012, 2014\)](#). We also compared the various simulated components of the  
 342 net C balance (e.g. NPP) of the Congo against values described in the literature (Williams et  
 343 al., 2007; Lewis et al., 2009; Verhegghen et al., 2012; Valentini et al., 2014; Yin et al., 2017).  
 344 In addition, we assessed the relationship between the interannual variation in present day

345 (1981-2010) C fluxes of the Congo basin and variation in temperature and rainfall. This was  
346 done through linear regression using STATISTICA™. We found trends in several of the fluxes  
347 over the 30-year period (1981-2010) and thus detrended the time series with the “Detrend”  
348 function, part of the “SpecsVerification” package in R (R Core Team 2013), before undertaking  
349 the statistical analysis focused on the climate drivers of inter-annual variability.

## 350 **2.6 Calculating the net carbon balance of the Congo basin**

351 We calculated Net Ecosystem Production (NEP) by summing the terrestrial and aquatic C  
352 fluxes of the Congo basin (Eq. 1), while we incorporated disturbance fluxes (Land-use change  
353 flux and harvest flux) to calculate Net Biome Production (NBP) (Eq. 2). Positive values of  
354 NBP and NEP equate to a net terrestrial C sink.

355 NEP is defined as follows:

$$356 \quad NEP = NPP + TF - SHR - FCO_2 - LE_{Aquatic} \quad (1)$$

357 Where *NPP* is terrestrial net primary production, *TF* is the throughfall flux of DOC from the  
358 canopy to the ground, *SHR* is soil heterotrophic respiration (only that evading from the *terra-*  
359 *firme* soil surface); *FCO<sub>2</sub>* is CO<sub>2</sub> evasion from the water surface and *LE<sub>Aquatic</sub>* is the lateral  
360 export flux of C (DOC + dissolved CO<sub>2</sub>) to the coast. NBP is equal to NEP except with the  
361 inclusion of the C lost (or possibly gained) via land use change (*LUC*) and crop harvest (*HAR*).  
362 Wood harvest is not included for logging and forestry practices, but during deforestation LUC,  
363 a fraction of the forest biomass is harvested and channelled to wood product pools with  
364 different decay constants. *LUC* includes land conversion fluxes and the lateral export of wood  
365 products biomass, that is, assuming that wood products from deforestation are not consumed  
366 and released as CO<sub>2</sub> over the Congo, but in other regions:

$$367 \quad NBP = NEP - (LUC + HAR) \quad (2)$$

368

## 369 **4.3. Results**

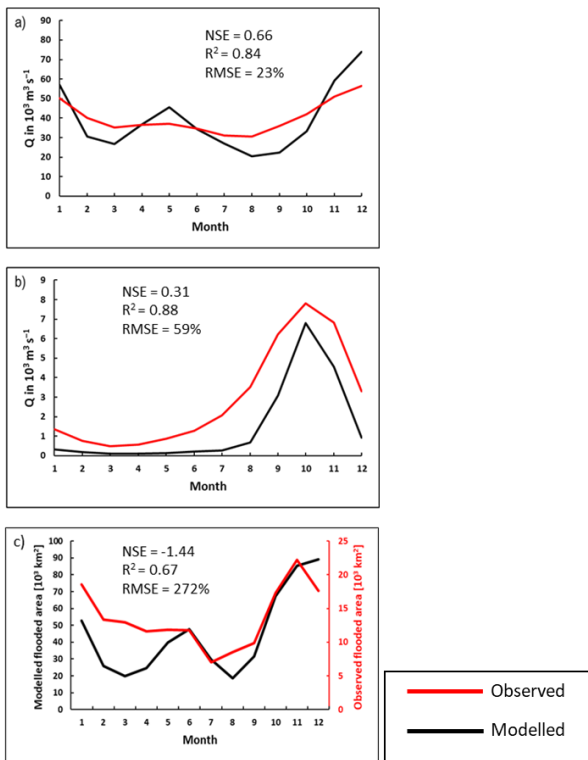
### 370 **3.1 Simulation of hydrology and aquatic carbon fluxes**

371 The final model configuration is able to closely reproduce the mean monthly discharge at  
372 Brazzaville (Fig. 4 a), Table 2) and captures the seasonality moderately well (Fig. 4 a, Table 2,  
373 RMSE =23%,  $R^2 =0.84$  versus RMSE= 29% and  $R^2 =0.23$  without calibration, Table A1). At  
374 Bangui on the UbangiOubangui-River (Fig. 1), the model is able to closely recreate observed  
375 seasonality (Fig. 4 b), RMSE =59%,  $R^2 =0.88$ ) but substantially underestimates the mean  
376 monthly discharge, our value being only 50% of the observed. We produce reasonable NSE  
377 values of 0.66 and 0.31 for Brazzaville and Bangui respectively, indicating that the model is  
378 moderately accurate in its simulation of seasonality.

379 We also evaluated the simulated seasonal change in flooded area in the central (approx.  
380 200,000 km<sup>2</sup>, Fig. 1) part of the Cuvette Centrale wetlands against the GIEMS inundation  
381 dataset (1993-2007, maximum inundation minus minimum or permanent water bodies, Prigent  
382 et al., 2007; Becker et al., 2018). While our model is able to represent the seasonality in flooded  
383 area relatively well ( $R^2 =0.75$  Fig. 4 c), it considerably overestimates the magnitude of flooded  
384 area relative to GIEMS (Fig. 4 c, Table 2). However, the dataset that we used to define the  
385 MFF and MFS forcing files (Gumbricht et al., 2017) is produced at a higher resolution than  
386 GIEMS and will capture smaller wetlands than the GIEMS dataset, and thus the greater flooded  
387 area is to be expected. GIEMS is also known to underestimate inundation under vegetated areas  
388 (Prigent et al., 2007, Papa et al., 2010) and has difficulties to capture small inundated areas  
389 (Prigent et al., 2007; Lauerwald et al., 2017). Indeed, with the GIEMS data we produce an  
390 overall flooded area for the Congo Basin of just 3%, less than one-third of that produced with  
391 the Gumbricht dataset (Gumbricht et al., 2017) or the GLWD (Lehner, & Döll, P.,2004). As  
392 such, it is to be expected that there is a large RMSE (272%, Table 2) between simulated flooded

393 area and GIEMS; more importantly, the seasonality of the two is highly correlated ( $R^2 = 0.67$ ,  
 394 Table 2). Overall, the hydrological performance of the model against those datasets is  
 395 satisfactory as the main purpose of this study is to estimate the long-term changes of aquatic C  
 396 fluxes. In particular, it can closely recreate the mean monthly/annual discharge at Brazzaville  
 397 (Table 2), the most downstream gauging station on the Congo (Fig. 1). As such, we consider  
 398 the hydrological performance to be sufficiently good for our aims.

399



400

401 **Figure 4: Seasonality of simulated versus observed discharge at a) Brazzaville on the**  
 402 **Congo (Cochoineau et al., 2006), b) Bangui on the Ubangi-Oubangui (Bouillon et al.,**  
 403 **2014) 1990-2005 monthly mean and c) flooded area in the central (approx. 200,000**  
**km<sup>2</sup>) area of the Cuvette Centrale wetlands versus GIEMS (1993-2007, Becker et al.,**  
**2018). The observed flooded area data represents the maximum minus minimum**  
**(permanent water bodies such as rivers) GIEMS inundation. See Figure 1 for locations.**

**Table 2: Performance statistics for modelled versus observed seasonality of discharge and flooded area in Cuvette Centrale**

Station	RSME	NSE	R <sup>2</sup>	Simulated mean monthly discharge (m <sup>3</sup> s <sup>-1</sup> )	Observed mean monthly discharge (m <sup>3</sup> s <sup>-1</sup> )
Brazzaville	23%	0.66	0.84	38,944	40,080
Bangui	59%	0.31	0.88	1,448	2,923
				Simulated mean monthly flooded area (10 <sup>3</sup> km <sup>2</sup> )	Observed mean monthly flooded area (10 <sup>3</sup> km <sup>2</sup> )
Flooded area (Cuvette Centrale)	272%	-1.44	0.67	44	14

405

406 In Figure 5, we compare simulated DOC concentrations at six locations (Fig. 1) along the  
 407 Congo River and Oubangui tributary, against the observations of Borges et al. (2015<sup>b</sup>). We  
 408 show that we can recreate the spatial variation in DOC concentration within the Congo basin  
 409 relatively closely with an R<sup>2</sup> of 0.74 and an RMSE of 24% (Fig. 5).

410 We are also able to simulate the broad spatial pattern of pCO<sub>2</sub> measured in Borges et al.  
 411 (2019). During high flow season (mean of 6 consecutive months of highest flow, 2009-2019)  
 412 we simulate a mean pCO<sub>2</sub> of 3,373 ppm and 5,095 ppm at Kisangani and Kinshasa  
 413 (Brazzaville) respectively, compared to the observed values of 2,424 ppm and 5,343 ppm  
 414 during high water (measured in December 2013, Borges et al., 2019) (Table 3). Similarly,  
 415 during low flow season (mean of 6 consecutive months of lowest flow, 2009-2019) we  
 416 simulate a mean pCO<sub>2</sub> of 1,563 ppm and 2,782 ppm at Kisangani and Kinshasa respectively,

417 compared to the observed values of 1,670 ppm and 2,896 ppm during falling water (June  
418 2014, Borges et al., 2019) (Table 3).

419  
420 While we are able to recreate observed spatial differences in DOC and  $p\text{CO}_2$ , as well as broad  
421 seasonal variations, we are not able to correctly predict the exact timing of the simulated  
422 highs and lows, a reflection of not fully capturing the hydrological seasonality. For example,  
423 our mean June  $p\text{CO}_2$  at Kinshasa (~~Brazzaville~~Brazzaville) is 4,470 ppm, while Borges et al  
424 measured a mean of 2,896 ppm (Table 3). However, our value for July of 2,621 ppm is much  
425 closer, and moreover our mean value for December of 5,154 ppm is relatively close to the  
426 observed value of 5,343 ppm. Similarly, we fail to predict the timing of the June falling water  
427 at KinsanganiKinsangani (Table 3).

428 In Figure 6, we compare simulated  $p\text{CO}_2$  against the observed monthly time series at Bangui  
429 on the Oubangui River (Bouillon et al., 2012 & 2014), as far as we are aware the most  
430 complete time series of  $p\text{CO}_2$  published from the Congo basin, spanning March 2010 to  
431 March 2012 (with only the single month of June 2010 missing).- Again, while the model fails  
432 to correctly predict the precise timing of the peak as with the Kinshasa and Kinsangani  
433 datasets the broad seasonal variation in  $p\text{CO}_2$  is captured, with the observed and modelled  
434 times series ranging from 227- 4040 ppm and 415- 2928 ppm, respectively (Fig. 6).

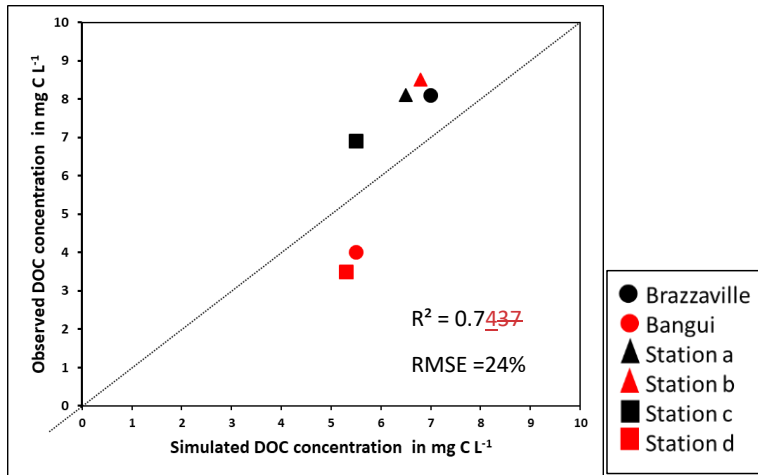
435

436

437

438

439



440

Figure 75: Observed (Borges et al., 2015<sup>a</sup>) versus simulated DOC concentrations at several sites along the Congo and Ouabangui rivers. See Fig. 1 for locations. The simulated and observed DOC concentrations represent the mean-median values across the particular sampling period at each site-location detailed in Borges et al. (2015<sup>a</sup>).

441

**Table 3: Observed (Borges et al., 2019) and modelled pCO<sub>2</sub> (in ppm) at Kinshasa (Brazzaville) and Kinsangani on the Congo river at various water levels.**

Location	Observed pCO <sub>2</sub> highwater (December 2013)	Modelled pCO <sub>2</sub> highwater (December 2019)	Modelled pCO <sub>2</sub> high flow season (mean of 6 consecutive months of highest flow 2009-2019)	Observed pCO <sub>2</sub> falling water (June 2014)	Modelled pCO <sub>2</sub> falling water (June mean 2009-2019)	Modelled pCO <sub>2</sub> low flow season (mean of 6 consecutive months of lowest flow 2009-2019)
Kinshasa (Brazzaville)	5.343	5.154	5.095	2.896	4.470	2.782

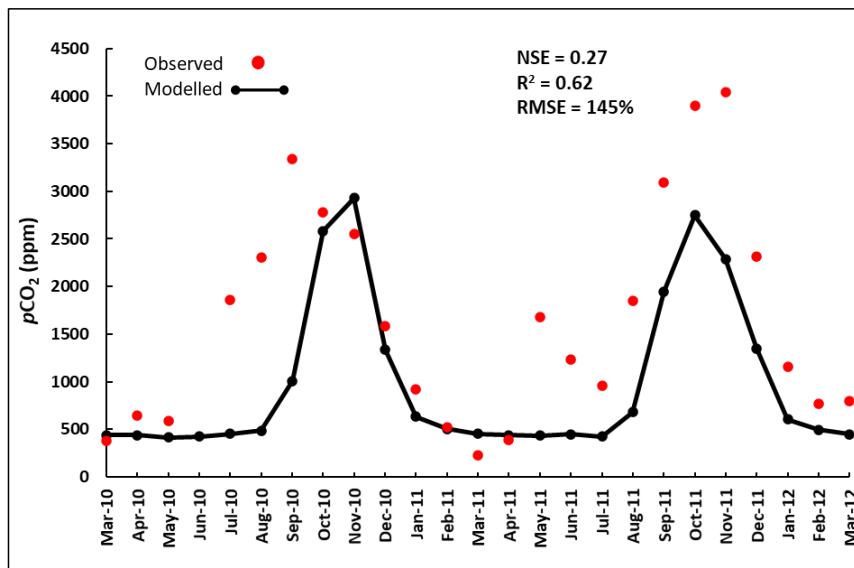
Formatted: Font: 11 pt, English (United Kingdom)

KinsanganiK	2,424	2,166	3,373	1,670	3,126	1,566
isangani						

Formatted: Font: 11 pt, English (United Kingdom)

Formatted: Centered, Space After: 0 pt

Formatted: Font: 11 pt, English (United Kingdom)



Formatted: Font: (Default) Times New Roman, 12 pt

Formatted: Keep with next

Figure 76: Time series of observed versus simulated pCO<sub>2</sub> at Bangui on the River Oubangui. Observed data is from Bouillon et al., 2012 and Bouillon et al., 2014.

Formatted: Font: Italic

Formatted: Font: Italic

Formatted: Subscript

Formatted: English (United Kingdom)

### 3.2 Carbon fluxes along the Congo basin for the present day

For the present day (1981-2010) we estimate a mean annual terrestrial net primary production (NPP) of  $5,800 \pm 166$  (standard deviation, SD) Tg C yr<sup>-1</sup> (Fig. 75), corresponding to a mean areal C fixation rate of approximately 1,500 g C m<sup>-2</sup> yr<sup>-1</sup> (Fig. 86 a). We find a significant positive correlation between the interannual variation of NPP and rainfall (detrended R<sup>2</sup>= 0.41, p<0.001, Table A2) and a negative correlation between annual NPP and temperature (detrended



453  $R^2= 0.32$ ,  $p<0.01$ , Table A2). We also see considerable spatial variation in NPP across the  
454 Congo Basin (Fig. 86 a).

455 We simulate a mean soil heterotrophic respiration (SHR) of  $5,300 \pm 99$  Tg C yr<sup>-1</sup> across the  
456 Congo basin (Fig. 75). Contrary to NPP, interannual variation in annual SHR is positively  
457 correlated with temperature (detrended  $R^2= 0.57$ ,  $p<0.0001$ , Table A2) and inversely correlated  
458 with rainfall (detrended  $R^2= 0.10$ ), though the latter relationship is not significant ( $p>0.05$ ).

459 We estimate a mean annual aquatic CO<sub>2</sub> evasion rate of  $1,363 \pm 83$  g C m<sup>-2</sup> yr<sup>-1</sup>, amounting  
460 to a total of  $235 \pm 54$  Tg C yr<sup>-1</sup> across the total water surfaces of the Congo basin (Fig. 75) and  
461 attribute 85% of this flux to flooded areas, meaning that only 32 Tg C yr<sup>-1</sup> is evaded directly  
462 from the river surface. Interannual variation in aquatic CO<sub>2</sub> evasion (1981-2010) shows a  
463 strong positive correlation with rainfall (detrended  $R^2= 0.75$ ,  $p<0.0001$ , Table A2) and a weak  
464 negative correlation with temperature (detrended  $R^2=0.09$ , not significant,  $p>0.05$ ). Aquatic  
465 CO<sub>2</sub> evasion also exhibits substantial spatial variation (Fig. 86, d), displaying a similar pattern  
466 to both terrestrial DOC leaching (DOC<sub>inp</sub>) ( $R^2= 0.81$ ,  $p<0.0001$ , Fig. 86, b) as well as terrestrial  
467 CO<sub>2</sub> leaching (CO<sub>2inp</sub>) ( $R^2= 0.96$ ,  $p<0.0001$ , Fig. 86, c) into the aquatic system, but not  
468 terrestrial NPP ( $R^2= 0.01$ ,  $p<0.05$ , Fig. 86, a). We simulate a mean annual flux of DOC  
469 throughfall from the canopy of  $27 \pm 1$  Tg C yr<sup>-1</sup> ~~and~~

470 ~~We estimate a mean annual~~ C (DOC + dissolved CO<sub>2</sub>) export flux to the coast of  $15 \pm 4$  Tg C  
471 yr<sup>-1</sup> (Fig. 75). ~~In Figure 7, we compare simulated DOC concentrations at six locations (Fig. 1)~~  
472 ~~along the Congo River and Ubangi tributary, against the observations of Borges et al. (2015<sup>b</sup>).~~  
473 ~~We show that we can recreate the spatial variation in DOC concentration within the Congo~~  
474 ~~basin relatively closely with an  $R^2$  of 0.82 and an RMSE of 19% (Fig. 7).~~

475 For the present day (1981-2010) we estimate a mean annual net ecosystem production (NEP)  
476 of  $277 \pm 137$  Tg C yr<sup>-1</sup> and a net biome production (NBP) of  $107 \pm 133$  Tg C yr<sup>-1</sup> (Fig. 75).

477 Interannually, both NEP and NBP exhibit a strong inverse correlation with temperature  
478 (detrended NEP  $R^2=0.55$ ,  $p<0.0001$ , detrended NBP  $R^2=0.54$ ,  $p<0.0001$ ) and weak positive  
479 relationship with rainfall (detrended NEP  $R^2=0.16$ ,  $p<0.05$ , detrended NBP  $R^2=0.14$ ,  $p<0.05$ ).  
480 Furthermore, we simulate a present day (1981-2010) living biomass of  $41 \pm 1$  Pg C and a total  
481 soil C stock of  $109 \pm 1$  Pg C.

482

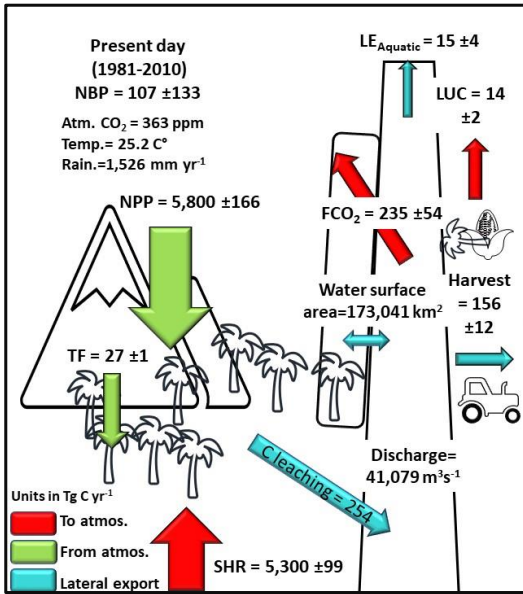
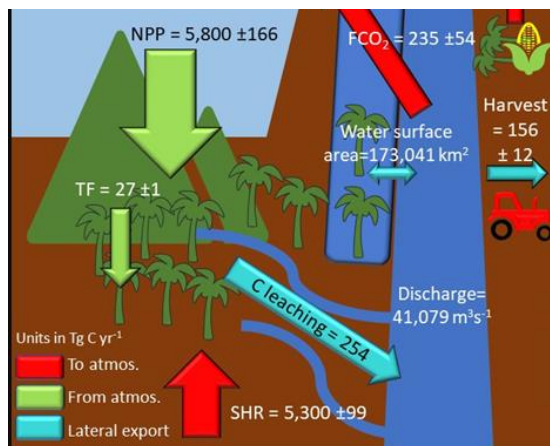


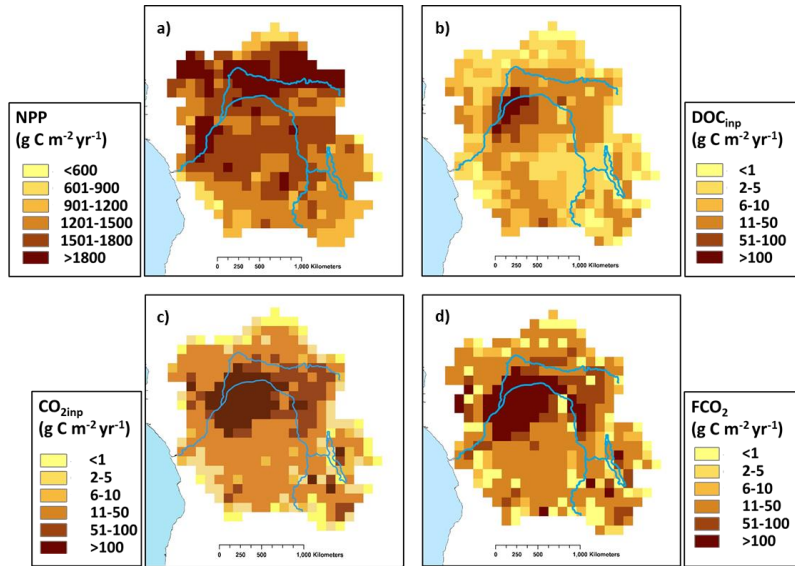
Figure 57: Annual C budget (NBP) for the Congo basin for the present day (1981-2010) simulated with ORCHILEAK, where NPP is terrestrial net primary productivity, TF is throughfall, SHR is soil heterotrophic respiration, FCO<sub>2</sub> is aquatic CO<sub>2</sub> evasion, LOAC is C leakage to the land-ocean aquatic continuum (FCO<sub>2</sub> + LE<sub>Aquatic</sub>), LUC is flux from Land-use change, and LE<sub>Aquatic</sub> is the export C flux to the coast. Range represents the standard deviation (SD) from 1981-2010.

483



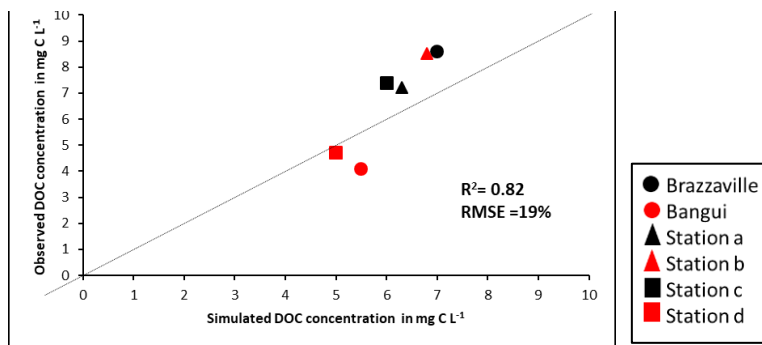
484

Formatted: Left



485

Figure 68: Present day (1981-2010) spatial distribution of a) terrestrial net primary productivity (NPP), b) dissolved organic carbon leaching-export from soils and floodplain vegetation into the aquatic system ( $DOC_{inp}$ ), c)  $CO_2$  leaching from soils and floodplain vegetation into the aquatic system ( $CO_{2inp}$ ) and d) aquatic  $CO_2$  evasion ( $FCO_2$ ). Main rivers in blue. All at a resolution of  $1^\circ$



486

### 487 3.3 Long-term temporal trends in carbon fluxes

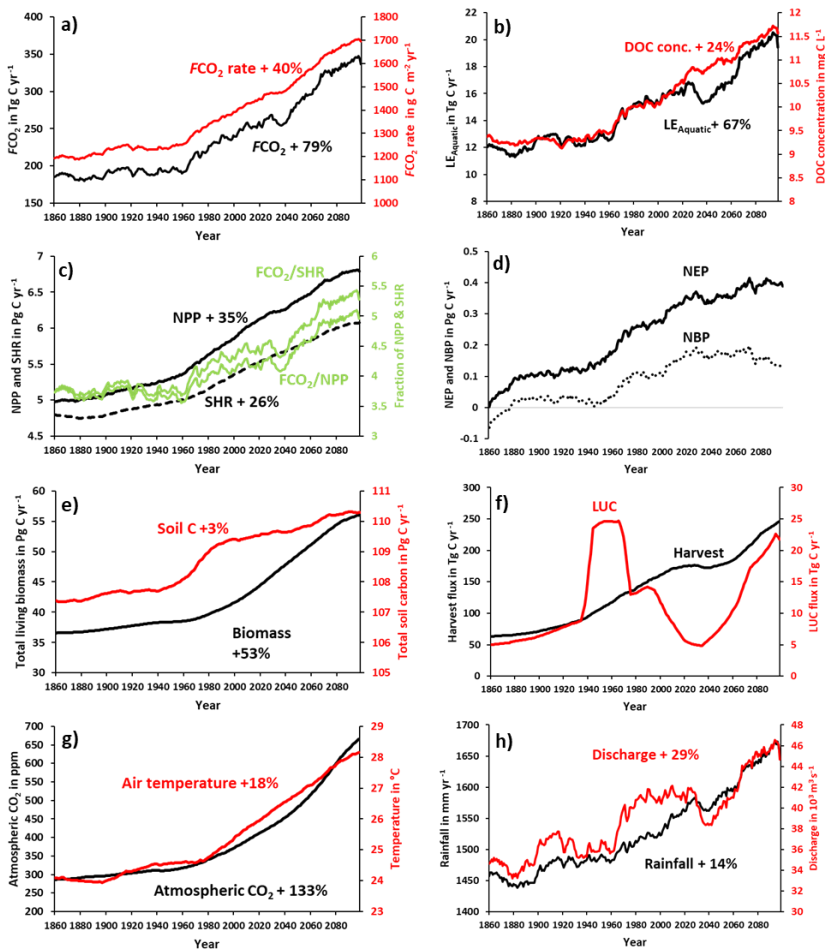
488 We find an increasing trend in aquatic  $CO_2$  evasion (Fig. 98 a) throughout the simulation  
 489 period, rising slowly at first until the 1960s when the rate of increase accelerates. In total  $CO_2$   
 490 evasion rose by 79% from 186 Tg C  $yr^{-1}$  at the start of the simulation (1861-1890 mean) (Fig.

491 [109](#)) to 333 Tg C yr<sup>-1</sup> at the end of this century (2070-2099 mean, Fig. [109](#)), while the increase  
492 until the present day (1981-2010 mean) is of +26 % (to 235 Tg C yr<sup>-1</sup>), though these trends are  
493 not uniform across the basin (Fig A1). The lateral export flux of C to the coast ( $LE_{\text{Aquatic}}$ )  
494 follows a similar relative change (Fig. [98b](#)), rising by 67% in total, from 12 Tg C yr<sup>-1</sup> (Fig. [109](#))  
495 to 15 Tg C yr<sup>-1</sup> for the present day, and finally to 20 Tg C yr<sup>-1</sup> (2070-2099 mean, Fig. [109](#)).  
496 This is greater than the equivalent increase in DOC concentration (24%, Fig. [98b](#)) due to the  
497 concurrent rise in rainfall (by 14%, Fig [98h](#)) and in turn discharge (by 29%, Fig. [98h](#)).

498 Terrestrial NPP and SHR also exhibit substantial increases of 35% and 26% respectively across  
499 the simulation period and similarly rise rapidly after 1960 (Fig. [98-c](#)). NEP, NBP (Fig. [98-d](#))  
500 and living biomass (Fig. [98 e](#)) follow roughly the same trend as NPP, but NEP and NBP begin  
501 to slow down or even level-off around 2030 and in the case of NBP, we actually simulate a  
502 decreasing trend over approximately the final 50 years. Interestingly, the proportion of NPP  
503 lost to the LOAC also increases from approximately 3% to 5% (Fig. [98c](#)). We also find that  
504 living biomass stock increases by a total of 53% from 1861 to 2099. Total soil C also increases  
505 over the simulation but only by 3% from 107 to 110 Pg C yr<sup>-1</sup> (Fig. [98-e](#)). Emissions from land-  
506 use change (LUC) show considerable decadal fluctuation increasing rapidly in the second half  
507 of the 20<sup>th</sup> century and decreasing in the mid-21<sup>st</sup> century before rising again towards the end  
508 of the simulation (Fig. [98-f](#)). The harvest flux (Fig. [98-f](#)) rises throughout the simulation with  
509 the exception of a period in the mid-21<sup>st</sup> century during which it stalls for several decades. This  
510 is reflected in the change in land-use areas from 1861- 2099 (Fig. A2, Table A3) during which  
511 the natural forest and grassland PFTs marginally decrease while both C<sub>3</sub> and C<sub>4</sub> agricultural  
512 grassland PFTs increase.

513

514



516 **Figure 89:** Simulation results for various C fluxes and stocks from 1861-2099, using IPSL-  
 517 CM5A-LR model outputs for RCP 6.0 (Frierler et al., 2017). All panels except for atmospheric  
 518 CO<sub>2</sub>, biomass and soil C correspond to 30-year running means of simulation outputs. This  
 519 was done in order to suppress interannual variation, as we are interested in longer-term  
 520 trends.

520

### 521 3.4 Drivers of simulated trends in carbon fluxes

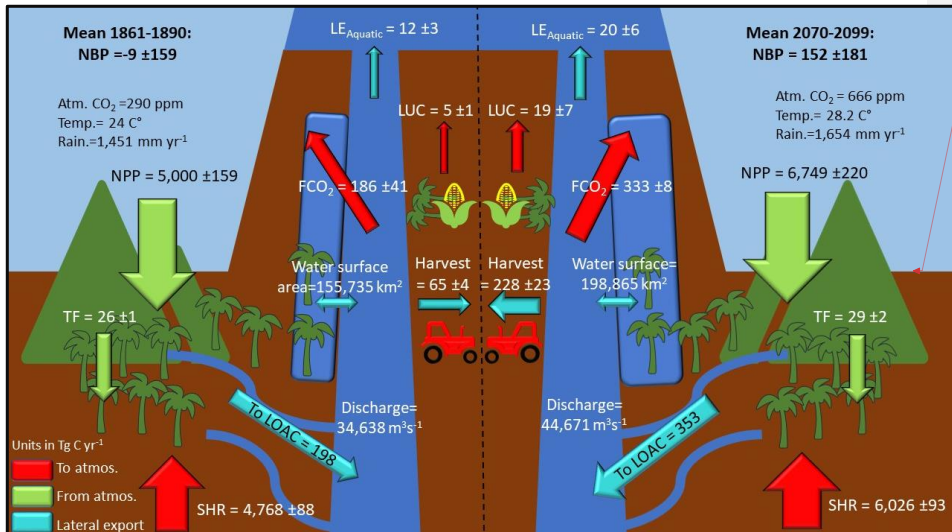
522 The dramatic increase in the concentration of atmospheric CO<sub>2</sub> (Fig. 98 g) and subsequent  
 523 fertilization effect on terrestrial NPP has the greatest overall impact on all of the fluxes across

524 the simulation period (Fig. 110). It is responsible for the vast majority of the growth in NPP,  
525 SHR, aquatic CO<sub>2</sub> evasion and flux of C to the coast (Fig. 110 a, b, c & d). The effect of LUC  
526 on these four fluxes is more or less neutral, while the impact of climate change is more varied.  
527 The aquatic fluxes (Fig. 110 c, d) respond positively to an acceleration in the increase of both  
528 rainfall (and in turn discharge, Fig. 98 h) and temperature (Fig. 98 g) starting around 1970.  
529 From around 2020, the impact of climate change on the lateral flux of C to the coast (Fig 110  
530 d) reverts to being effectively neutral, likely a response to a slowdown in the rise of rainfall  
531 and indeed a decrease in discharge (Fig 98 h), as well as perhaps the effect of temperature  
532 crossing a threshold. The response of the overall loss of terrestrial C to the LOAC (i.e. the ratio  
533 of LOAC/NPP, Fig. 110 e) is relatively similar to the response of the individual aquatic fluxes  
534 but crucially, climate change exerts a much greater impact, contributing substantially to an  
535 increase in the loss of terrestrial NPP to the LOAC in the 1960s, and again in the second half  
536 of the 21<sup>st</sup> century. These changes closely coincide with the pattern of rainfall and in particular  
537 with changes in discharge (Fig. 98 h).

538 Overall temperature and rainfall increase by 18% and 14% from 24°C to 28°C and 1457mm to  
539 1654mm respectively, but in Fig. A2 one can see that this increase is non-uniform across the  
540 basin. Generally speaking, the greatest increase in temperature occurs in the south of the basin  
541 while it is the east that sees the largest rise in rainfall (Fig. A2). Land-use changes are similarly  
542 non-uniform (Fig. A2).

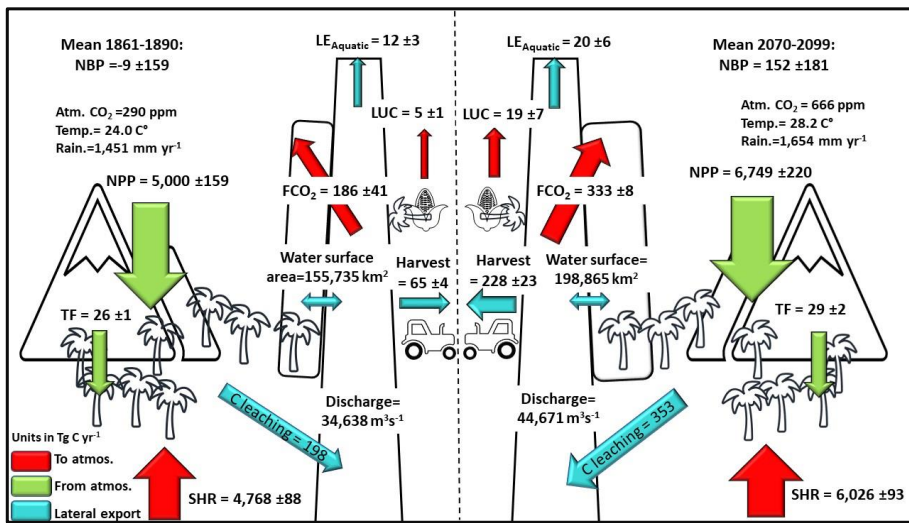
543 The response of NBP and in NEP (Fig. 110 f, g) to anthropogenic drivers is more complex. The  
544 simulated decrease in NBP towards the end of the run is influenced by a variety of factors;  
545 LUC and climate begin to have a negative effect on NBP (contributing to a decrease in NBP)  
546 at a similar time while the positive impact (contributing to an increase in NBP) of atmospheric  
547 CO<sub>2</sub> begins to slow down and eventually level-off (Fig. 110 g). LUC continues to have a  
548 positive effect on NEP (Fig. 110 f) due to the fact that the expanding C<sub>4</sub> crops have a higher

549 NPP than forests, while it has an overall negative effect on NBP at the end of the simulation  
 550 due to the inclusion of emissions from crop harvest.



Formatted: Left

551



552

553 **Figure 910:** Annual C budget (NBP) for the Congo basin for; left, the Year 1861 and right, the  
 554 Year 2099, simulated with ORCHILEAK. NPP is terrestrial net primary productivity, TF is  
 555 throughfall, SHR is soil heterotrophic respiration, FCO<sub>2</sub> is aquatic CO<sub>2</sub> evasion, LOAC is C  
 556 leakage to the land-ocean aquatic continuum (FCO<sub>2</sub> + LE<sub>Aquatic</sub>), LUC is flux from Land-use



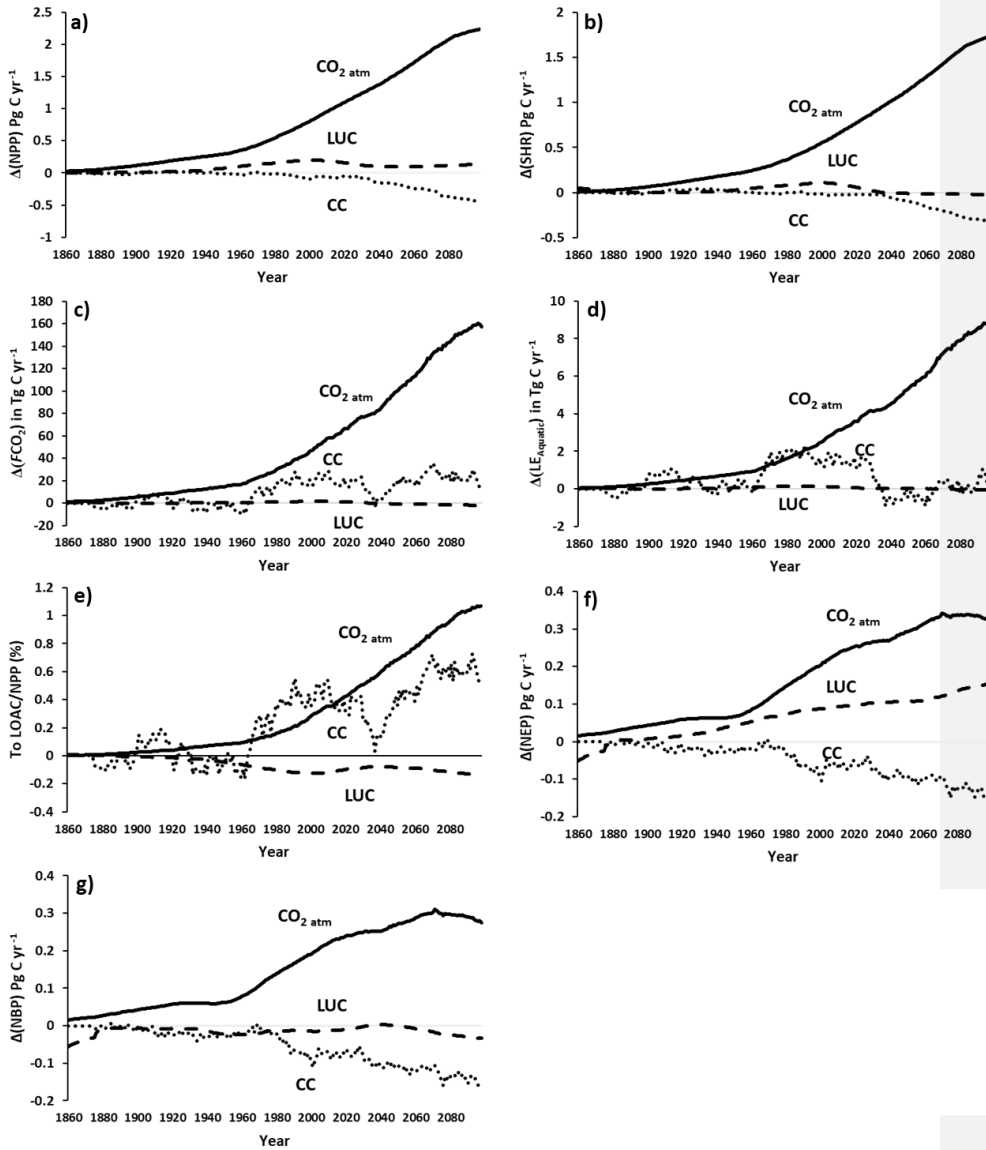
557 change, and  $LE_{Aquatic}$  is the export C flux to the coast. Range represents the standard deviation  
558 (SD).

559

560

561

562



564 **Figure 1011:** Contribution of anthropogenic drivers; atmospheric CO<sub>2</sub> concentration (CO<sub>2 atm</sub>), climate change (CC) and land use change (LUC) to changes in the various carbon fluxes  
 565 along the Congo Basin, under IPSL-CM5A-LR model outputs for RCP 6.0 (Frieler et al., 2017).

## 566 **5.4. Discussion**

### 567 **4.1 Congo basin carbon balance**

568 We simulate a mean present-day terrestrial NPP of approximately  $1,500 \text{ g C m}^{-2} \text{ yr}^{-1}$  (Fig. 6),  
569 substantially larger than the MODIS derived value of around  $1,000 \text{ g C m}^{-2} \text{ yr}^{-1}$  from Yin et al.  
570 (2017) across central Africa, though it is important to note that satellite derived estimates of  
571 NPP can underestimate the impact of  $\text{CO}_2$  fertilization, namely its positive effect on  
572 photosynthesis (De Kauwe et al., 2016; Smith et al., 2019). Our stock of the present-day living  
573 biomass of 41.1 Pg C is relatively close to the total Congo vegetation biomass of 49.3 Pg C  
574 estimated by Verhegghen et al. (2012) based on the analysis of MERIS satellite data. Moreover,  
575 our simulated Congo Basin soil C stock of  $109 \pm 1.1 \text{ Pg C}$  is consistent with the approximately  
576 120-130 Pg C across Africa between the latitudes  $10^\circ\text{S}$  to  $10^\circ\text{N}$  in the review of Williams et  
577 al. (2007), between which the Congo represents roughly 70% of the land area. Therefore, their  
578 estimate of soil C stocks across the Congo only would likely be marginally smaller than ours.  
579 It is also important to note that neither estimate of soil C stocks explicitly take into account the  
580 newly discovered peat store of 30 Pg C (Dargie et al., 2017) and therefore both are likely to  
581 represent conservative values. In addition, Williams et al. (2007) estimate the combined fluxes  
582 from conversion to agriculture and cultivation to be around  $100 \text{ Tg C yr}^{-1}$  in tropical Africa  
583 (largely synonymous with the Congo Basin), which is relatively close to our present day  
584 estimate of harvesting + land-use change flux of  $170 \text{ Tg C yr}^{-1}$ .

585 Our results suggest that  $\text{CO}_2$  evasion from the water surfaces of the Congo is sustained by  
586 ~~leaching-the transfer~~ of dissolved  $\text{CO}_2$  and DOC with 226 Tg C and 73 Tg C, respectively, from  
587 ~~wetland~~ soils ~~and vegetation~~ to the aquatic system each year (1980-2010, Fig. 86). Moreover,  
588 we find that a disproportionate amount of this transfer occurs ~~(Fig. 6)~~ within the Cuvette  
589 Centrale wetland (Fig. 1, Fig. 86) in the centre of the basin, in agreement with a recent study  
590 by Borges et al. (2019). In our study, this is due to the large areal proportion of inundated land,

591 facilitating the exchange between soils and aquatic systems. Borges et al. (2019) conducted  
592 ~~extensive~~ measurements of DOC and  $p\text{CO}_2$ , amongst other chemical variables, along the  
593 Congo mainstem and its tributaries from Kinshasa in the West of the basin (beside Brazzaville,  
594 Fig. 1) through the Cuvette Centrale to Kisangani in the East (close to station d in Fig. 1). They  
595 found that both DOC and  $p\text{CO}_2$  approximately doubled from Kisangani downstream to  
596 Kinshasa (Table 3), and demonstrated that this variation is overwhelmingly driven by fluvial-  
597 wetland connectivity, highlighting the importance of the vast Cuvette Centrale wetland in the  
598 aquatic C budget of the Congo basin.

599 Our estimate of the integrated present-day aquatic  $\text{CO}_2$  evasion from the river surface of the  
600 Congo basin ( $32 \text{ Tg C yr}^{-1}$ ) is the same as that estimated by Raymond et al. (2013) (also  $32 \text{ Tg}$   
601  $\text{C yr}^{-1}$ ), downscaled over the same basin area, but smaller than the  $59.7 \text{ Tg C yr}^{-1}$  calculated by  
602 Lauerwald et al. (2015) and far smaller than that of Borges et al. (2015<sup>a</sup>),  $133\text{-}177 \text{ Tg C yr}^{-1}$  or  
603 Borges et al. (2019),  $251\pm 46 \text{ Tg C yr}^{-1}$ . ~~The recent study of Borges et al. (2019) is based on by~~  
604 ~~far and away the most extensive dataset of Congo basin  $p\text{CO}_2$  measurements to date and thus~~  
605 ~~suggests that we substantially underestimate total riverine  $\text{CO}_2$  evasion.~~ As previously  
606 discussed, we simulate the ~~broad spatial and temporal~~ variation in ~~observed~~ DOC  
607 ~~concentrations and  $p\text{CO}_2$  measured by Borges et al. (2015<sup>a, b</sup>, Fig. 5, Table 37)~~ relatively  
608 ~~well~~ and our mean riverine gas exchange velocity  $k$  of  $3.5 \text{ m d}^{-1}$  is similar to the ~~2.9 m~~  
609  ~~$\text{d}^{-1}$  used by Borges et al. (2015<sup>a</sup>).~~ It is therefore somewhat surprising that our ~~basin-wide~~  
610 estimate of riverine  $\text{CO}_2$  evasion is so different, ~~and likely to be related to ORCHILEAK~~  
611 ~~underestimating dissolved  $\text{CO}_2$  inputs into the river network.~~ Below we discuss some possible  
612 explanations for this discrepancy related to methodological ~~differences and~~ limitations.

613 ~~One potential cause for the differences could be the river gas exchange velocity  $k$ . However,~~  
614 ~~we used~~ applied a mean riverine gas exchange velocity  $k$  of  $3.5 \text{ m d}^{-1}$  which is similar to the ~~2.9~~  
615  ~~$\text{m d}^{-1}$  used by Borges et al. (2015<sup>a</sup>).~~ Moreover, a sensitivity analysis was performed in

616 Lauerwald et al. (2017) which showed that in the physical approach of ORCHILEAK, CO<sub>2</sub>  
617 evasion is not very sensitive to the  $k$  value, unlike data-driven models. Namely, Lauerwald et  
618 al (2017) showed that an increase or decrease of  $k$  for rivers and swamps of 50% only led  
619 to 1% and -4% change in total CO<sub>2</sub> evasion, respectively. Therefore, we can discount  $k$  as a  
620 major source of the discrepancy.

621 Another potential reason for our smaller riverine CO<sub>2</sub> evasion could be river surface area. We  
622 simulate a mean present day (1980-2010) total river surface area of 25,900 km<sup>2</sup>, compared to  
623 the value of 23,670 km<sup>2</sup> used in Borges et al (2019, supplementary information) and so  
624 similarly we think that this can be discounted as a major causesource of discrepancy.

625 The difference in our simulated riverine CO<sub>2</sub> evasion compared to the empirically derived  
626 estimate of Borges et al. (2019), could be caused by the lack of representation of aquatic plants  
627 in the ORCHILEAK model. Borges et al. (2019) used the stable isotope composition of  $\delta^{13}\text{C}$ -  
628 DIC to determine the origin of dissolved CO<sub>2</sub> in the Congo River system and found that the  
629 values were consistent with a DIC input from the degradation of organic matter, in particular  
630 from C<sub>4</sub> plants. Crucially, they further found that the  $\delta^{13}\text{C}$ -DIC values were unrelated to the  
631 contribution of *terra-firme* C<sub>4</sub> plants, rather that they were more consistent with the degradation  
632 of aquatic C<sub>4</sub> plants, namely macrophytes. The ORCHILEAK model does not represent aquatic  
633 plants, and the wider LSM ORCHIDEE does not have an aquatic macrophyte PFT either  
634 (though root respiration of floodplain plants for the PFTs represented, is accounted for as a C  
635 source). This could at the very least partly explain our conservative estimate of river CO<sub>2</sub>  
636 evasion, given that tropical macrophytes have relatively elevated NPPs. Rates as high as 3,500  
637 g C m<sup>-2</sup> yr<sup>-1</sup> have been measured on floodplains in the Amazon (Silva et al., 2009). While this  
638 value is higher than the values represented in simulated in the Cuvette Centrale by  
639 ORCHILEAK (Figure 8), they are of the same order of magnitude and so this alone cannot  
640 fully explain the discrepancy compared to the results of Borges et al. (2019). In the Amazon

641 basin it has been shown that wetlands export approximately half of their gross primary  
642 production (GPP) to the river network compared to upland (*terra-firme*) ecosystems which  
643 only export a few percent (Abril et al. 2013). More importantly, Abril et al. (2013) found that  
644 tropical aquatic macrophytes exported 80% of their GPP compared to just 36% for flooded  
645 forest. Therefore, the lack of a bespoke macrophyte PFT is indeed likely to be one reason for  
646 the discrepancy between our results and those of Borges, but largely due to their particularly  
647 high export efficiency to the river-floodplain network as opposed to differences in NPP. While  
648 being a significant limitation, creating and incorporating a macrophyte PFT would be a  
649 substantial undertaking given that the authors are unaware of any published dataset which has  
650 systematically mapped their distribution and abundance. It is important to note that while  
651 ORCHILEAK does not include the export of C from aquatic macrophytes it also neglects their  
652 NPP. Moreover, most aquatic macrophytes described in the literature have short (<1 year) life-  
653 cycles (Mitchel & Rogers, 1985). As such, while this model limitation is likely one of the  
654 causes for our relatively low estimate of riverine CO<sub>2</sub> evasion, it will only have a limited net  
655 effect on our estimate of the overall annual C balance (NBP, NEP) of the Congo basin.

656 Finally, another cause~~One reason~~ for the difference in riverine CO<sub>2</sub> evasion could be that the  
657 resolution of ORCHILEAK (0.5 degree river network and 1° for C fluxes) is not sufficient to  
658 fully capture the dynamics of the smallest streams of the Congo Basin which have been shown  
659 to have the highest DOC and CO<sub>2</sub> concentrations (Borges et al., 2019). Indeed, ORCHILEAK  
660 typically doesn't not simulate the highest observed pCO<sub>2</sub> measurements of the smallest  
661 tributaries (i.e. > 16,000 ppm). This is partly because for the fast reservoir (headwaters) in  
662 ORCHILEAK we assume full pCO<sub>2</sub> equilibrium with the atmosphere over one full day, which  
663 prevents very high pCO<sub>2</sub> values from building in the water column.

664 However~~Despite these limitations~~, it is important to note that in our simulations, the evasion  
665 flux from rivers only contributes 15% of total aquatic CO<sub>2</sub> evasion, and including the flux from

666 wetlands/floodplains, we produce a total of 235 Tg C yr<sup>-1</sup>. Moreover, the majority of this  
667 flux evasion comes from occurs in the Cuvette Centrale (Fig. 8) which suggests that while  
668 ORHILEAK fails to attribute the majority a large portion of this flux to small rivers (owing to  
669 the coarse resolution of the river network) we nonetheless do capture the source of carbon. In  
670 other words, in ORCHILEAK the majority of this carbon evades directly from the floodplain  
671 and wetlands of the Cuvette Centrale as opposed to the small rivers.

672

673 ~~Another limitation of the ORCHILEAK model is the lack of representation of aquatic plants.~~  
674 ~~Borges et al. (2019) used the stable isotope composition of  $\delta^{13}\text{C}$ -DIC to determine the origin~~  
675 ~~of dissolved CO<sub>2</sub> in the Congo River system and found that the values were consistent with the~~  
676 ~~degradation of organic matter, in particular from C<sub>4</sub> plants. Crucially, they further found that~~  
677 ~~the  $\delta^{13}\text{C}$ -DIC values were unrelated to the contribution of *terra firme* C<sub>4</sub> plants, rather that they~~  
678 ~~were more consistent with the degradation of aquatic C<sub>4</sub> plants, namely macrophytes. This also~~  
679 ~~concurs with the wider conclusions of a previous paper comparing the Congo and the Amazon~~  
680 ~~(Borges et al., 2015<sup>b</sup>), which highlighted that aquatic macrophytes are more prevalent in the~~  
681 ~~Congo river and its tributaries compared to the Amazon where strong water currents limit their~~  
682 ~~abundance. The ORCHILEAK model does not represent aquatic plants, and the wider LSM~~  
683 ~~ORCHIDEE does not have an aquatic macrophyte PFT either. This could at least partly explain~~  
684 ~~our conservative estimate of river CO<sub>2</sub> evasion, given that tropical macrophytes have relatively~~  
685 ~~NPP. Rates as high as 3,500 g C m<sup>-2</sup> yr<sup>-1</sup> have been measured on floodplains in the Amazon~~  
686 ~~(Silva et al., 2009). While this value is higher than the values represented in the Cuvette~~  
687 ~~Centrale by ORCHILEAK (Figure 6), they are of the same order of magnitude and so this~~  
688 ~~cannot fully explain the discrepancy compared to the results of Borges et al. (2019). In the~~  
689 ~~Amazon basin it has been shown that wetlands export approximately half of their gross primary~~  
690 ~~production (GPP) to the river network compared to upland (*terra firme*) ecosystems which~~

691 ~~only export a few percent (Abril et al. 2013). More importantly, Abril et al. (2013) found that~~  
692 ~~tropical aquatic macrophytes exported 80% of their GPP compared to just 36% for flooded~~  
693 ~~forest. Therefore, the lack of a bespoke macrophyte PFT may indeed be one reason for the~~  
694 ~~discrepancy between our results and those of Borges, but largely due to their particularly high~~  
695 ~~export efficiency to the river floodplain network as opposed to differences in NPP. While being~~  
696 ~~a significant limitation, creating and incorporating a macrophyte PFT would be a substantial~~  
697 ~~undertaking given that the authors are unaware of any published dataset which has~~  
698 ~~systematically mapped their distribution and abundance. It is important to that while~~  
699 ~~ORCHLEAK does not include the export of C from aquatic macrophytes it also neglects their~~  
700 ~~NPP. Moreover, most aquatic macrophytes described in the literature have short (<1 year) life-~~  
701 ~~cycles (Mitchel & Rogers., 1985). As such, this model limitation will only have a very limited~~  
702 ~~net effect on our estimate of the overall annual C balance (NBP, NEP) of the Congo basin, and~~  
703 ~~indeed the other components of NBP.~~

704 Our simulated export of C to the coast of 15 (15.3) Tg C yr<sup>-1</sup> is virtually identical to the  
705 TOC+DIC export estimated by Borges et al. (2015<sup>a</sup>) of 15.5 Tg C yr<sup>-1</sup>, which is consistent with  
706 the fact that we simulate a similar spatial variation of DOC concentrations (Fig. 87 and Fig. 1  
707 for locations). It is also relatively similar to the 19 Tg C yr<sup>-1</sup> (DOC + DIC) estimated by  
708 Valentini et al. (2014) in their synthesis of the African carbon budget. Valentini et al. (2014)  
709 used the largely empirical based Global Nutrient Export from WaterSheds (NEWS) model  
710 framework and they point out that Africa was underrepresented in the training data used to  
711 develop the regression relationships which underpin the model, and thus this could explain the  
712 small disagreement.

713 Of the total 15 Tg C yr<sup>-1</sup> exported to the coast, we simulate a 2.4 Tg C yr<sup>-1</sup> component of  
714 dissolved CO<sub>2</sub>, which is relatively similar to the empirically derived estimate of the total DIC  
715 export of 3.3 Tg C yr<sup>-1</sup> calculated in Wang et al. (2013). According to Wang et al., dissolved



716 CO<sub>2</sub> accounts for the majority (1.9 Tg C yr<sup>-1</sup>) with the rest being the weathering derived flux  
717 of HCO<sub>3</sub><sup>-</sup>. Thus, the discrepancy between the two estimates is likely to be largely caused by  
718 our lack of accounting for the weathering derived flux (HCO<sub>3</sub><sup>-</sup>) which they estimate at 1.4 Tg  
719 C yr<sup>-1</sup>. In summary, despite this model limitation the results of Wang et al., (2013) suggest that  
720 we still capture the majority of the DIC flux.

721  
722 ~~Our estimate of 4% of NPP per year being transferred to inland waters is substantially lower~~  
723 ~~than that estimated for the Amazon, where around 12% of NPP is lost to the aquatic system~~  
724 ~~each year (Hastie et al., 2019). There are a number of differences between the drivers in the~~  
725 ~~two basins, which could explain this. Mean annual rainfall is 44% greater in the Amazon, and~~  
726 ~~mean annual discharge is 4 times higher, while a maximum of approximately 14% of the~~  
727 ~~surface of the Amazon Basin is covered by water compared to 10% of the Congo (Borges et~~  
728 ~~al., 2015<sup>b</sup>; Hastie et al., 2019). Moreover, upland runoff is the main source of water in the~~  
729 ~~wetlands of the Congo as opposed to the Amazon where exchanges between the river and~~  
730 ~~floodplain dominate (Lee et al., 2011; Borges et al., 2015<sup>b</sup>). Indeed, the water levels of wetlands~~  
731 ~~in the Congo have been shown to be consistently higher than adjacent river levels (Lee et al.,~~  
732 ~~2011). This also partly explains why for the Congo we find that only 15% of aquatic CO<sub>2</sub>~~  
733 ~~evasion comes from the river water surface compared to 25% for the Amazon (Hastie et al.,~~  
734 ~~2019).~~

#### 736 4.2 Trends in terrestrial and aquatic carbon fluxes

737 There is relatively sparse observed data available on the long-term trends of terrestrial C fluxes  
738 in the Congo. Yin et al. (2017) used MODIS data to estimate NPP between 2001 and 2013  
739 across central Africa. They found that NPP increased on average by 10 g C m<sup>-2</sup> per year, while

740 we simulate an average annual increase of  $4 \text{ g C m}^{-2} \text{ yr}^{-1}$  over the same period across the Congo  
741 Basin. The two values are not directly comparable as they do not cover precisely the same  
742 geographic area but it is encouraging that our simulations exhibit a similar trend to remote  
743 sensing data. As previously noted, MODIS derived estimates of NPP do not fully include the  
744 effect of  $\text{CO}_2$  fertilization (de Kauwe et al., 2016) whereas ORCHILEAK does. Thus, the  
745 MODIS NPP product may underestimate the increasing trend in NPP, which would bring our  
746 modeled trend further away from this dataset. On the other hand, forest degradation effects and  
747 recent droughts have been associated with a decrease of greenness (Zhou et al., 2014) and  
748 above ground biomass loss (Qie et al., 2019) in tropical forests.

749 Up to a point, our results also concur with estimates based on the upscaling of biomass  
750 observations (Lewis et al., 2009; Hubau et al., 2019). Lewis et al. (2009) up-scaled forest plot  
751 measurements to calculate that intact tropical African forests represented a net uptake of  
752 approximately  $300 \text{ Tg C yr}^{-1}$  between 1968 and 2007 and this is consistent with our NEP  
753 estimate of  $275 \text{ Tg C yr}^{-1}$  over the same period. However, more recently an analysis based on  
754 an extension of the same dataset found that the above ground carbon sink in tropical Africa  
755 was relatively stable from 1985 to 2015 (Hubau et al., 2020).

756 A major source of the uncertainty associated with future projections of NPP and NEP comes  
757 from our limited understanding and representation of the  $\text{CO}_2$  fertilization effect. Recent  
758 analysis of data from some of the longest-running Free-Air  $\text{CO}_2$  Enrichment (FACE) sites,  
759 consisting of early-successional temperate ecosystems, found a  $29.1 \pm 11.7\%$  stimulation of  
760 biomass over a decade (Walker et al., 2019). A meta-analysis (Liu et al., 2019) of seven  
761 temperate FACE experiments combined with process-based modelling also found substantial  
762 sensitivity ( $0.64 \pm 0.28 \text{ PgC yr}^{-1}$  per hundred ppm) of biomass accumulation to atmospheric  
763  $\text{CO}_2$  increase, and moreover the same study showed that ORCHIDEE model simulations  
764 were largely consistent with the experiments. However, other FACE experiments on mature

765 temperate forests (Körner et al., 2005), as well as eucalyptus forests bring into question whether  
766 the fertilization effects observed in temperate FACE experiments can be extrapolated to other  
767 ecosystems. For example, the Swiss FACE study, a deciduous mature forest, found no  
768 significant biomass increase with enhanced CO<sub>2</sub> (Körner et al., 2005), while a FACE  
769 experiment on a mature eucalyptus forest in Australia found that while CO<sub>2</sub> stimulated an  
770 increase in C uptake through GPP, this did not carry to the ecosystem level, largely as a result  
771 of a concurrent increase in soil respiration (Jiang et al., 2020). Unfortunately, no results are yet  
772 available from any tropical FACE experiments, though the Amazon FACE experiment is  
773 underway and the eventual results will be crucial in developing our understanding of the CO<sub>2</sub>  
774 fertilization effect beyond the temperate zone.

775 ~~With these limitations in our understanding of tropical forest ecosystems in mind, Our results~~  
776 ~~of the historic trend in NEP (not including LUC and harvest fluxes) also generally concur with~~  
777 ~~other modelling studies of tropical Africa (Fisher et al., 2013). Fisher et al. (2013) used nine~~  
778 ~~different land surface models to show that the African tropical biome already represented a~~  
779 ~~natural (i.e. no disturbance, but also neglecting LOAC fluxes) net uptake of around 50 Tg C~~  
780 ~~yr<sup>-1</sup> in 1901 and that this uptake more than doubled by 2010. We find a similar trend though~~  
781 ~~we simulate higher absolute NEP. Indeed, one of the models used in Fisher was ORCHIDEE~~  
782 ~~and using this model alone, they calculate a virtually identical estimate of net uptake of 277 Tg~~  
783 ~~C yr<sup>-1</sup> for the present day, though this estimate neglects the transfers of C along the LOAC and~~  
784 ~~would therefore be reduced with their inclusion. Our results also generally concur with~~  
785 ~~estimates based on the upscaling of biomass observations (Lewis et al., 2009). Lewis et al.~~  
786 ~~(2009) up-scaled forest plot measurements to calculate that intact tropical African forests~~  
787 ~~represented a net uptake of approximately 300 Tg C yr<sup>-1</sup> between 1968 and 2007 and this is~~  
788 ~~consistent with our NEP estimate 275 Tg C yr<sup>-1</sup> over the same period.~~

789 ~~o~~ver the entire simulation period (1861-2099), we estimate that aquatic CO<sub>2</sub> evasion will  
790 increase by 79% and the export of C to the coast by 67%. This increase is considerably higher  
791 than the ~~235%~~ and ~~2730%~~ rise in outgassing and export predicted for the Amazon basin  
792 (Lauerwald et al., [submitted2020](#)), over the same period and under the same scenario. This is  
793 largely due to the fact climate change is predicted to have a substantial negative impact on the  
794 aquatic C fluxes in the Amazon, something that we do not find for the Congo where rainfall is  
795 projected to substantially increase over the 21<sup>st</sup> century (RCP 6.0). In the Amazon, Lauerwald  
796 et al. ([submitted2020](#)) show that while there are decadal fluctuations in precipitation and  
797 discharge, total values across the basin remain unchanged in 2099 compared to 1861. However,  
798 changes in the spatial distribution of precipitation mean that the total water surface area actually  
799 decreases in the Amazon. Indeed, while we find an increase in the ratio of C exports to the  
800 LOAC/NPP from 3 to 5%, Lauerwald et al. ([submitted2020](#)) find a comparative decrease. ~~The~~  
801 ~~increase in the proportion of NPP lost to the aquatic system (Fig. 8, 9) as well as in the~~  
802 ~~concentration of DOC (by 24% at Brazzaville) that we find in the Congo, could have important~~  
803 ~~secondary effects, not least the potential for greater DOC concentrations to cause a reduction~~  
804 ~~in pH levels (Laudon & Buffam, 2008) with implications for the wider ecology (Weiss et al.,~~  
805 ~~2018).~~

806 Our simulated increase in DOC export to the coast up to the present day is smaller than findings  
807 recently published for the Mississippi River using the Dynamic Land Ecosystem Model  
808 (DLEM, Ren et al., 2016). In addition, the Mississippi study identified LUC including land  
809 management practices (e.g. irrigation and fertilization), followed by change in atmospheric  
810 CO<sub>2</sub>, as the biggest factors in the 40% increase in DOC export to the Gulf of Mexico (Ren et  
811 al., 2016). Another recent study (Tian et al., 2015), found an increase in DIC export from  
812 eastern North America to the Atlantic Ocean from 1901-2008 but no significant trend in DOC.

813 They demonstrated that climate change and increasing atmospheric CO<sub>2</sub> had a significant  
814 positive effect on long-term C export while land-use change had a substantial negative impact.

#### 815 4.3 Limitations and further model developments

816 It is important to note that we can have greater confidence in the historic trend (until present-  
817 day), as the future changes are more reliant on the skill of Earth System model predictions and

818 of course on the accuracy of the RCP 6.0 scenario. ~~There are for example, large uncertainties~~  
819 ~~associated with the future CO<sub>2</sub> fertilization effect (Schimel et al., 2015)As discussed above,~~

820 ~~our understanding and representation of CO<sub>2</sub> fertilization, especially in the tropics, is a major~~  
821 ~~limitation. Moreover, ~~and~~ the majority of land surface models, ORCHILEAK included in its~~

822 current iteration, do not represent the effect of nutrient limitation on plant growth meaning that  
823 estimates of land C uptake may be too large (Goll et al., 2017). There are also considerable

824 uncertainties associated with future climate projections in the Congo basin (Haensler et al.,  
825 2013). ~~Nutrient limitation on growth and a better representation of effect of enhanced CO<sub>2</sub>,~~

826 ~~particularly with regards to soil respiration (Jiang et al., 2020) and tree mortality (Hubau et al.,~~  
827 ~~2020), are two crucial aspects which need to be further developed. However, in most cases the~~

828 ~~future trends that we find are more or less continuations of the historic trends, which already~~  
829 ~~represent substantial changes to the magnitude of many fluxes.~~

830 ~~Moreover~~Additionally, we do not account for methane fluxes from Congo wetlands, estimated  
831 at 1.6 to 3.2 Tg (CH<sub>4</sub>) per year (Tathy et al., 1992), and instead assume that all C is evaded in

832 the form of CO<sub>2</sub>. Another limitation is the lack of accounting for bespoke peatland dynamics  
833 in the ORCHILEAK model. ORCHILEAK is able to represent the general reduction in C

834 decomposition in water-logged soils and indeed Hastie et al. (2019) demonstrated that  
835 increasing the maximum floodplain extent in the Amazon Basin led to an increase in NEP

836 despite fueling aquatic CO<sub>2</sub> evasion because of the effect of reducing soil heterotrophic

Formatted: Subscript

Formatted: Subscript

837 respiration. Furthermore, ORCHILEAK uses a “poor soils” mask forcing file (Fig. 2 j) based  
838 on the Harmonized World Soil Database (FAO/IIASA/ISRIC/ISS-CAS/JRC, 2009), which  
839 prescribes reduced decomposition rates in low nutrient and pH soils (e.g. Podzols and  
840 Arenosols). The effect of the “poor soils” forcing can clearly be seen in the spatial distribution  
841 of the soil C stock in Fig. A3, where the highest C storage coincides with the highest proportion  
842 of poor soils. Interestingly, this does not include the Cuvette Centrale wetlands (Fig. 1), an area  
843 which was recently identified as containing the world’s largest intact tropical peatland and a  
844 stock of around 30 Pg C (Dargie et al., 2017). One potential improvement that could be made  
845 to ORCHILEAK would be the development of a new tailored “poor soils” forcing file for the  
846 Congo Basin which explicitly includes Histosols, perhaps informed by the Soil Grids database  
847 (Hengl et al., 2014), to better represent the Cuvette Centrale. This could in turn, be validated  
848 and/or calibrated against the observations of Dargie et al. (2017). A more long-term aim could  
849 be the integration/ coupling of the ORCHIDEE-PEAT module with ORCHILEAK.  
850 ORCHIDEE-PEAT (Qiu et al., 2019) represents peat as an independent sub-grid hydrological  
851 soil unit in which peatland soils are characterized by peat-specific hydrological properties and  
852 multi-layered transport of C and water. Thus far, it has only been applied to northern peatlands,  
853 and calibrating it to tropical peatlands, along with integrating it within ORCHILEAK would  
854 require considerable further model development, but would certainly be a valuable longer-term  
855 aspiration. This could also be applied across the tropical region and would allow us to  
856 comprehensively explore the implications of climate change and land-use change for tropical  
857 peatlands.- In addition, ORCHILEAK does not simulate the erosion and subsequent burial of  
858 POC within river and floodplain sediments. Although it does not represent the lateral transfer  
859 of POC, it does incorporate the decomposition of inundated litter as an important source of  
860 DOC and dissolved CO<sub>2</sub> to the aquatic system; i.e. it is assumed that POC from submerged  
861 litter decomposes locally in ORCHILEAK. Moreover, previous studies have found that DOC

862 as opposed to POC (Spencer et al., 2016; Bouillon et al., 2012) overwhelmingly dominates the  
863 total load of C in the Congo.  
864 ~~As previously noted,~~ the representation of the rapid C loop of aquatic macrophytes should  
865 also be made a priority in terms of improving models such as ORCHILEAK, particularly in the  
866 tropics. ~~As previously discussed,~~ ORCHILEAK also fails to account for the weathering derived  
867 ~~flux ( $\text{HCO}_3^-$ ).~~ Finally, ~~as discussed earlier~~ the issue of shifting cultivation demands further  
868 ~~attention; at least for the present day a shifting cultivation forcing file could be developed based~~  
869 ~~on remote sensing data (Tyukavina et al., 2018).~~ For ~~further additional~~ discussion of  
870 the limitations of ORCHILEAK, please also see Lauerwald et al. (2017) and Hastie et al.  
871 (2019).

## 872 **6.5. Conclusions**

873 For the present day, we show that aquatic C fluxes, and in particular  $\text{CO}_2$  evasion, are important  
874 components of the Congo Basin C balance, larger than for example the combined fluxes from  
875 LUC and harvesting, with around 4% of terrestrial NPP being exported to the aquatic system  
876 each year. ~~Our simulations show~~We find that these fluxes ~~may~~ have undergone considerable  
877 perturbation since 1861 to the present day, and that under RCP 6.0 this perturbation ~~will~~ could  
878 continue; over the entire simulation period (1861-2099), we estimate that aquatic  $\text{CO}_2$  evasion  
879 will increase by 79% and the export of C to the coast by 67%. We further find that the ratio of  
880 C exports to the LOAC/NPP ~~increases~~ could increase from 3 to 5%, driven by both rising  
881 atmospheric  $\text{CO}_2$  concentrations and climate change. ~~The increase in the proportion of NPP~~  
882 ~~transferred to the aquatic system (Fig. 8, 9), as well as in the concentration of DOC (by 24% at~~  
883 ~~Brazzaville), could also have important secondary effects, not least the potential for greater~~  
884 ~~DOC concentrations to cause a reduction in pH levels (Laudon & Buffam, 2008) with~~  
885 ~~implications for the wider ecology (Weiss et al., 2018).~~ This calls for long-term monitoring of

Formatted: Subscript

Formatted: Superscript

886 C levels and fluxes in the rivers of the Congo basin, and further investigation of the potential  
887 impacts of such change. Our results also highlight the limitations of the current generation of  
888 land surface models and call for investment into further model development, including  
889 additional model developments.

890

891 *Code availability.* A description of the general ORCHIDEE code can be found here:  
892 [http://forge.ipsl.jussieu.fr/orchidee/browser#tags/ORCHIDEE\\_1\\_9\\_6/ORCHIDEE](http://forge.ipsl.jussieu.fr/orchidee/browser#tags/ORCHIDEE_1_9_6/ORCHIDEE).

893 The main part of the ORCHIDEE code was written by Krinner et al. (2005). See d'Orgeval et  
894 al. (2008) for a general description of the river routing scheme. For the updated soil C module  
895 please see Camino Serrano (2015). For the source code of ORCHILEAK see Lauerwald et al.  
896 (2017)- <https://doi.org/10.5194/gmd-10-3821-2017-supplement>

897 For details on how to install ORCHIDEE and its various branches, please see the user guide:  
898 <http://forge.ipsl.jussieu.fr/orchidee/wiki/Documentation/UserGuide>

899 *Author contribution.* AH, RL, PR and PC all contributed to the conceptualization of the study.  
900 RL developed the model code, AH developed the novel forcing files for Congo, and AH  
901 performed the simulations. FP provided the GIEMS dataset for model validation. AH prepared  
902 the manuscript with contributions from all co-authors. RL and PR provided supervision and  
903 guidance to AH throughout the research. PR acquired the primary financial support that  
904 supported this research.

905 *Competing interests.* The authors declare that they have no conflict of interest.

906 *Financial support.* Financial support was received from the European Union's Horizon 2020  
907 research and innovation programme under the Marie Skłodowska- Curie grant agreement No.  
908 643052 (C-CASCADES project). PR acknowledges funding from the European Union's



909 Horizon 2020 research and innovation programme under Grant Agreement 776810 (project  
910 VERIFY). RL acknowledges funding from the ANR ISIPEDIA ERA4CS project.

911

## 912 References

- 913 Abril, G., Martinez, J.-M., Artigas, L. F., Moreira-Turcq, P., Benedetti, M. F., Vidal, L., ...  
914 Roland, F. (2013). Amazon River carbon dioxide outgassing fuelled by wetlands. *Nature*,  
915 505, 395. Retrieved from <http://dx.doi.org/10.1038/nature12797>
- 916 Battin, T. J., Luysaert, S., Kaplan, L. A., Aufdenkampe, A. K., Richter, A., & Tranvik, L. J.  
917 (2009). The boundless carbon cycle. *Nature Geoscience*, 2, 598. Retrieved from  
918 <https://doi.org/10.1038/ngeo618>
- 919 Becker, M.; Papa, F.; Frappart, F.; Alsdorf, D.; Calmant, S.; Da Silva, J.S.; Prigent, C.;  
920 Seyler, F. Satellite-based estimates of surface water dynamics in the Congo River Basin. *Int.*  
921 *J. Appl. Earth Obs. Geoinf.* 2018, 196–209
- 922 Borges, A. V., Darchambeau, F., Teodoru, C. R., Marwick, T. R., Tamooh, F., Geeraert, N.,  
923 ... Bouillon, S. (2015)<sup>a</sup>. Globally significant greenhouse-gas emissions from African inland  
924 waters. *Nature Geoscience*, 8, 637. Retrieved from <https://doi.org/10.1038/ngeo2486>
- 925 Borges, A. V., Abril, G., Darchambeau, F., Teodoru, C. R., Deborde, J., Vidal, L. O., ...  
926 Bouillon, S. (2015)<sup>b</sup>. Divergent biophysical controls of aquatic CO<sub>2</sub> and CH<sub>4</sub> in the World's  
927 two largest rivers. *Scientific Reports*, 5, 15614. <https://doi.org/10.1038/srep15614>
- 928 Borges, A. V., Darchambeau, F., Lambert, T., Morana, C., Allen, G. H., Tambwe, E.,  
929 Toengaho Sembaito, A., Mambo, T., Nlandu Wabakhangazi, J., Descy, J.-P., Teodoru, C. R.,  
930 and Bouillon, S (2019): Variations in dissolved greenhouse gases (CO<sub>2</sub>, CH<sub>4</sub>, N<sub>2</sub>O) in the  
931 Congo River network overwhelmingly driven by fluvial-wetland connectivity,  
932 *Biogeosciences*, 16, 3801–3834, <https://doi.org/10.5194/bg-16-3801-2019>.
- 933 Bouillon, S., Yambélé, A., Spencer, R. G. M., Gillikin, D. P., Hernes, P. J., Six, J., Merckx,  
934 R., and Borges, A. V.: Organic matter sources, fluxes and greenhouse gas exchange in the  
935 Oubangui River (Congo River basin), *Biogeosciences*, 9, 2045–2062,  
936 <https://doi.org/10.5194/bg-9-2045-2012>, 2012.
- 937 Bouillon, S., Yambélé, A., Gillikin, D. P., Teodoru, C., Darchambeau, F., Lambert, T., &  
938 Borges, A. V. (2014). Contrasting biogeochemical characteristics of the Oubangui River and  
939 tributaries (Congo River basin). *Scientific Reports*, 4, 5402. Retrieved from  
940 <https://doi.org/10.1038/srep05402>
- 941 Bowring, S. P. K., Lauerwald, R., Guenet, B., Zhu, D., Guimberteau, M., Tootchi, A.,  
942 Ducharne, A., and Ciais, P (2019)<sup>a</sup>: ORCHIDEE MICT-LEAK (r5459), a global model for  
943 the production, transport, and transformation of dissolved organic carbon from Arctic  
944 permafrost regions – Part 1: Rationale, model description, and simulation protocol, *Geosci.*  
945 *Model Dev.*, 12, 3503–3521, <https://doi.org/10.5194/gmd-12-3503-2019>, 2019.

946 Bowring, S. P. K., Lauerwald, R., Guenet, B., Zhu, D., Guimberteau, M., Regnier, P.,  
947 Tootchi, A., Ducharne, A., and Ciais, P (2019)<sup>b</sup>: ORCHIDEE MICT-LEAK (r5459), a global  
948 model for the production, transport and transformation of dissolved organic carbon from  
949 Arctic permafrost regions, Part 2: Model evaluation over the Lena River basin, *Geosci.*  
950 *Model Dev. Discuss.*, <https://doi.org/10.5194/gmd-2018-322>, in review, 2019.

951 [Camino-Serrano, M., Guenet, B., Luyssaert, S., Ciais, P., Bastrikov, V., De Vos, B., Gielen,](#)  
952 [B., Gleixner, G., Jornet-Puig, A., Kaiser, K., Kothawala, D., Lauerwald, R., Peñuelas, J.,](#)  
953 [Schrumpf, M., Vicca, S., Vuichard, N., Walmsley, D., and Janssens, I. A.: ORCHIDEE-](#)  
954 [SOM: modeling soil organic carbon \(SOC\) and dissolved organic carbon \(DOC\) dynamics](#)  
955 [along vertical soil profiles in Europe, \*Geosci. Model Dev.\*, 11, 937–957,](#)  
956 <https://doi.org/10.5194/gmd-11-937-2018>, 2018  
957 [Camino-Serrano, M., Guenet, B., Luyssaert,](#)  
958 [S., & Janssens, I. A. \(2018\). ORCHIDEE-SOM: modeling soil organic carbon \(SOC\) and](#)  
959 [dissolved organic carbon \(DOC\) dynamics along vertical soil profiles in](#)  
960 [Europe. \*Geoscientific Model Development\*, 11, 937–957. \[https://doi.org/10.5194/gmd-11-\]\(https://doi.org/10.5194/gmd-11-937-2018\)](#)

961

962 [CBFP \(Congo Basin Forest Partnership\) \(2009\). The forests of the Congo Basin — State of](#)  
963 [the Forest 2008, Publications Office of the European](#)  
964 [Union, Luxembourg \(2009\), \[10.2788/32259\]\(https://doi.org/10.2788/32259\),](#)

965 Ciais, P., Piao, S.-L., Cadule, P., Friedlingstein, P., & Chédin, A. (2009). Variability and  
966 recent trends in the African terrestrial carbon balance. *Biogeosciences*, 6(9), 1935–1948.  
967 <https://doi.org/10.5194/bg-6-1935-2009>

968 [Ciais, P., Yao, Y., Gasser, T., Baccini, A., Wang, Y., Lauerwald, R., ... Zhu, D. \(2020\).](#)  
969 [Empirical estimates of regional carbon budgets imply reduced global soil heterotrophic](#)  
970 [respiration. \*National Science Review\*. <https://doi.org/10.1093/nsr/nwaa145>](#)

971 [Ciais, P., Gasser, T., Lauerwald, R., Peng, S., Raymond, P. A., Wang, Y., Zhu, D. \(2017\):](#)  
972 [Observed regional carbon budgets imply reduced soil heterotrophic respiration. \*Nature\*, in](#)  
973 [review.](#)

974 Cochonneau, G., Sondag, F., Guyot, J.-L., Geraldo, B., Filizola, N., Fraizy, P., Laraque, A.,  
975 Magat, P., Martinez, J.-M., Noriega, L., Oliveira, E., Ordonez, J., Pombosa, R., Seyler, F.,  
976 Sidgwick, J., and Vauchel, P.: The environmental observation and research project, ORE  
977 HYBAM, and the rivers of the Amazon basin, in: *Climate Variability and Change –*  
978 *Hydrological Impacts*, IAHS Publ. 308, edited by: Demuth, S., Gustard, A., Planos, E.,  
979 Scatena, F., and Servat, E., IAHS Press, UK, 44–50, 2006

980 Coynel, A., P. Seyler, H. Etcheber, M. Meybeck, and D. Orange (2005), Spatial and seasonal  
981 dynamics of total suspended sediment and organic carbon species in the Congo River, *Global*  
982 *Biogeochem. Cycles*, 19, GB4019, doi: [10.1029/2004GB002335](https://doi.org/10.1029/2004GB002335).

983 Creese, A., Washington, R., & Jones, R. (2019). Climate change in the Congo Basin:  
984 processes related to wetting in the December–February dry season. *Climate Dynamics*, 53(5),  
985 3583–3602. <https://doi.org/10.1007/s00382-019-04728-x>

Field Code Changed

Formatted: No underline, Font color: Auto

Formatted: No underline, Font color: Auto

Formatted: English (United Kingdom)

Field Code Changed

986 Dargie, G. C., Lewis, S. L., Lawson, I. T., Mitchard, E. T. A., Page, S. E., Bocko, Y. E., &  
 987 Ifo, S. A. (2017). Age, extent and carbon storage of the central Congo Basin peatland  
 988 complex. *Nature*, 542, 86. Retrieved from <https://doi.org/10.1038/nature21048>

989 De Kauwe, M. G., Keenan, T. F., Medlyn, B. E., Prentice, I. C. and Terrer, C. (2016) Satellite  
 990 based estimates underestimate the effect of CO<sub>2</sub> fertilisation on net primary  
 991 productivity. *Nature Climate Change*, 6, 892-893

992 d'Orgeval, T., Polcher, J., & de Rosnay, P. (2008). Sensitivity of the West African  
 993 hydrological cycle in ORCHIDEE to infiltration processes. *Hydrology and Earth System  
 994 Sciences*, 12, 1387– 1401. <https://doi.org/10.5194/hess-12-1387-2008>

995 Drake, T. W., Raymond, P. A., & Spencer, R. G. M. (2018). Terrestrial carbon inputs to  
 996 inland waters: A current synthesis of estimates and uncertainty. *Limnology and  
 997 Oceanography Letters*, 3(3), 132–142. <http://doi.org/10.1002/lol2.10055>

998 Fan, L., Wigneron, J.-P., Ciais, P., Chave, J., Brandt, M., Fensholt, R., ... Peñuelas, J. (2019).  
 999 Satellite-observed pantropical carbon dynamics. *Nature Plants*, 5(9), 944–951.  
 1000 <https://doi.org/10.1038/s41477-019-0478-9>

1001 FAO/IIASA/ISRIC/ISS-CAS/JRC: Harmonized World Soil Database (version 1.1), FAO,  
 1002 Rome, 2009.

1003 Fisher JB, Sikka M, Sitch S, Ciais P, Poulter B, Galbraith D, Lee J-E, Huntingford C, Viovy  
 1004 N, Zeng N, Ahlstrom A, Lomas MR, Levy PE, Frankenberg C, Saatchi S, Malhi Y. 2013  
 1005 African tropical rainforest net carbon dioxide fluxes in the twentieth century. *Phil Trans R  
 1006 Soc B* 368: 20120376. <http://dx.doi.org/10.1098/rstb.2012.0376>

1007 Frieler, K., Lange, S., Piontek, F., Reyer, C. P. O., Schewe, J., Warszawski, L., ... Yamagata,  
 1008 Y. (2017). Assessing the impacts of 1.5 °C global warming – simulation protocol of the Inter-  
 1009 Sectoral Impact Model Intercomparison Project (ISIMIP2b). *Geosci. Model Dev.*, 10(12),  
 1010 4321–4345. <https://doi.org/10.5194/gmd-10-4321-2017>

1011 Goll, D. S., Vuichard, N., Maignan, F., Jornet-Puig, A., Sardans, J., Violette, A., Peng, S.,  
 1012 Sun, Y., Kvakic, M., Guimberteau, M., Guenet, B., Zaehle, S., Penuelas, J., Janssens, I., and  
 1013 Ciais, P.: A representation of the phosphorus cycle for ORCHIDEE (revision 4520), *Geosci.  
 1014 Model Dev.*, 10, 3745-3770, <https://doi.org/10.5194/gmd-10-3745-2017>, 2017.

1015 Guimberteau, M., Drapeau, G., Ronchail, J., Sultan, B., Polcher, J., Martinez, J.-M., Prigent,  
 1016 C., Guyot, J.-L., Cochonneau, G., Espinoza, J. C., Filizola, N., Fraizy, P., Lavado, W., De  
 1017 Oliveira, E., Pombosa, R., Noriega, L., and Vauchel, P.: Discharge simulation in the sub-  
 1018 basins of the Amazon using ORCHIDEE forced by new datasets, *Hydrol. Earth Syst. Sci.*, 16,  
 1019 911–935, <https://doi.org/10.5194/hess-16-911-2012>, 2012.

1020 Gumbricht, T., Roman-Cuesta, R. M., Verchot, L., Herold, M., Wittmann, F., Householder,  
 1021 E., Murdiyarso, D. (2017). An expert system model for mapping tropical wetlands and  
 1022 peatlands reveals South America as the largest contributor. *Global Change Biology*, 23(9),  
 1023 3581–3599. <https://doi.org/10.1111/gcb.13689>

1024 Haensler, A., Saeed, F. and Jacob, D. (2013): Assessment of projected climate change signals  
 1025 over central Africa based on a multitude of global and regional climate projections. In:

Formatted: French (France)

1026 Climate Change Scenarios for the Congo Basin. [Haensler A., Jacob D., Kabat P., Ludwig F.  
1027 (eds.)]. Climate Service Centre Report No. 11, Hamburg, Germany, ISSN: 2192-4058

1028 Hastie, A., Lauerwald, R., Ciais, P., Regnier, P (2019). Aquatic carbon fluxes dampen the  
1029 overall variation of net ecosystem productivity in the Amazon basin: An analysis of the  
1030 interannual variability in the boundless carbon cycle. *Global Change*  
1031 *Biology*, 25: 2094– 2111. <https://doi.org/10.1111/gcb.14620>

1032 [Hartmann, J., R. Lauerwald, and N. Moosdorf \(2014\), A brief overview of the GLObal RIver](#)  
1033 [CHEmistry Database. GLOrICH. Procedia Earth Planet. Sci., 10, 23–27.](#)

1034 [Heinimann A, Mertz O, Froelking S, Egelund Christensen A, Hurni K, Sedano F, et al. \(2017\)](#)  
1035 [A global view of shifting cultivation: Recent, current, and future extent. PLoS ONE 12\(9\):](#)  
1036 [e0184479. https://doi.org/10.1371/journal.pone.0184479](#)

1037 Hengl, T., de Jesus, J. M., MacMillan, R. A., Batjes, N. H., Heuvelink, G. B. M., Ribeiro, E.,  
1038 ... Ruiperez Gonzalez, M. (2014). SoilGrids1km-global soil information based on automated  
1039 mapping. PLoS One, 9, e105992. <https://doi.org/10.1371/journal.pone.0105992>

1040 [Hubau, W.; Lewis, S.L.; Phillips, O.L.; Affum-Baffoe, K.; Beeckman, H.; Cuní-Sánchez, A.;](#)  
1041 [Daniels, A.K.; Ewango, C.E.N.; Fauset, S.; Mukinzi, J.M.; et al. Asynchronous carbon sink](#)  
1042 [saturation in African and Amazonian tropical forests. Nature 2020, 579, 80–87.](#)

1043 Hurtt, G. C., Chini, L. P., Froelking, S., Betts, R. A., Feddema, J., Fischer, G., ... Wang, Y. P.  
1044 (2011). Harmonization of land-use scenarios for the period 1500–2100: 600 years of global  
1045 gridded annual land-use transitions, wood harvest, and resulting secondary lands. *Climatic*  
1046 *Change*, 109(1), 117. <https://doi.org/10.1007/s10584-011-0153-2>

1047 [Jiang, M., Medlyn, B.E., Drake, J.E. et al. The fate of carbon in a mature forest under carbon](#)  
1048 [dioxide enrichment. Nature 580, 227–231 \(2020\). https://doi.org/10.1038/s41586-020-2128-9](#)

1049 Kim, H. (2017). *Global Soil Wetness Project Phase 3 Atmospheric Boundary Conditions*  
1050 *(Experiment 1)* [Data set]. Data Integration and Analysis System (DIAS).  
1051 <https://doi.org/10.20783/DIAS.501>

1052 [Korner C, Asshoff R, Bignucolo O \(2005\) Carbon flux and growth in mature deciduous forest](#)  
1053 [trees exposed to elevated CO2. Science, 309, 1360–1362.](#)

1054 Lange., S (2017). "ISIMIP2b Bias-Correction Code," *Zenodo*, doi: [10.5281/zenodo.1069050](https://doi.org/10.5281/zenodo.1069050)

1055 Laudon, H., and I. Buffam (2008), Impact of changing DOC concentrations on the potential  
1056 distribution of acid sensitive biota in a boreal stream network, *Hydrol. Earth Syst.*  
1057 *Sci.*, 12(2), 425–435.

1058 Lauerwald, R., Laruelle, G. G., Hartmann, J., Ciais, P., & Regnier, P. A. G. (2015). Spatial  
1059 patterns in CO2 evasion from the global river network. *Global Biogeochemical Cycles*, 29(5),  
1060 534–554. <https://doi.org/10.1002/2014GB004941>

1061 Lauerwald, R., Regnier, P., Camino-Serrano, M., Guenet, B., Guimberteau, M., Ducharne,  
1062 A., ... Ciais, P. (2017). ORCHILEAK (revision 3875): a new model branch to simulate  
1063 carbon transfers along the terrestrial–aquatic continuum of the Amazon basin. *Geoscientific*  
1064 *Model Development*, 10(10), 3821–3859. <https://doi.org/10.5194/gmd-10-3In821-2017>

Formatted: English (United Kingdom)

Formatted: English (United Kingdom)

Formatted: English (United Kingdom)

Formatted: Font: Not Italic

Formatted: Font: Not Italic, English (United Kingdom)

Formatted: English (United Kingdom)

1065 Lauerwald, R., Regnier, P., Guenet, B., Friedlingstein, P; Ciais, P (2020): How simulations of  
1066 the land carbon sink are biased by ignoring fluvial carbon transfers – A case study for the  
1067 Amazon basin. ~~submitted to~~ *One Earth*, [10.1016/j.oneear.2020.07.009](https://doi.org/10.1016/j.oneear.2020.07.009).

1068 Lee, H., Beighley, R. E., Alsdorf, D., Jung, H. C., Shum, C. K., Duan, J., ... Andreadis, K.  
1069 (2011). Characterization of terrestrial water dynamics in the Congo Basin using GRACE and  
1070 satellite radar altimetry. *Remote Sensing of Environment*, 115(12), 3530–3538.  
1071 <https://doi.org/https://doi.org/10.1016/j.rse.2011.08.015>

1072 Lehner, B., & Döll, P. (2004). Development and validation of a global database of lakes,  
1073 reservoirs and wetlands. *Journal of Hydrology*, 296(1–4), 1–22.  
1074 <https://doi.org/https://doi.org/10.1016/j.jhydrol.2004.03.028>

1075 Lewis, S. L., Lopez-Gonzalez, G., Sonké, B., Affum-Baffoe, K., Baker, T. R., Ojo, L. O., ...  
1076 Wöll, H. (2009). Increasing carbon storage in intact African tropical forests. *Nature*, 457,  
1077 1003. Retrieved from <https://doi.org/10.1038/nature07771>

1078 [Liu, Y., Piao, S., Gasser, T., Ciais, P., Yang, H., Wang, H., ... Wang, T. \(2019\). Field-](https://doi.org/10.1038/s41561-019-0436-1)  
1079 [experiment constraints on the enhancement of the terrestrial carbon sink by CO2 fertilization.](https://doi.org/10.1038/s41561-019-0436-1)  
1080 [Nature Geoscience](https://doi.org/10.1038/s41561-019-0436-1), 12(10), 809–814. <https://doi.org/10.1038/s41561-019-0436-1>

1081 Masui, T., Matsumoto, K., Hijioaka, Y., Kinoshita, T., Nozawa, T., Ishiwatari, S., Kato, E.,  
1082 Shukla, P.R., Yamagata, Y., Kainuma, M., 2011. A emission pathway to stabilize at 6 W/m2  
1083 of radiative forcing. *Climatic Change*, doi:10.1007/s10584-011-0150-5. Morgan, M.G.,  
1084 Adams, P., Keith, D.W., 2006. Elicitation of expert judgments of aerosol forcing. *Climatic*  
1085 *Change* 75, 195–214

1086 [Melack, J.M., Hess, L.L., Gastil, M., Forsberg, B.R., Hamilton, S.K., Lima, I.B. and Novo,](https://doi.org/10.1111/j.1365-2486.2004.00763.x)  
1087 [E.M. \(2004\). Regionalization of methane emissions in the Amazon Basin with microwave](https://doi.org/10.1111/j.1365-2486.2004.00763.x)  
1088 [remote sensing. \*Global Change Biology\*, 10: 530-544. doi:10.1111/j.1365-2486.2004.00763.x](https://doi.org/10.1111/j.1365-2486.2004.00763.x)

1089 Mitchell D.S., Rogers K.H. (1985) Seasonality/aseasonality of aquatic macrophytes in  
1090 Southern Hemisphere inland water. In: Davies B.R., Walmsley R.D. (eds) Perspectives in  
1091 Southern Hemisphere Limnology. Developments in Hydrobiology, vol 28. Springer,  
1092 Dordrecht

1093 Nash, J. E., and J. V. Sutcliffe. 1970. River flow forecasting through conceptual models: Part  
1094 1. A discussion of principles. *J. Hydrology* 10(3): 282-290

1095 O'Loughlin, F., M. A. Trigg, G. J.-P. Schumann, and P. D. Bates (2013), Hydraulic  
1096 characterization of the middle reach of the Congo River, *Water Resour. Res.*, 49, 5059–5070,  
1097 doi:[10.1002/wrcr.20398](https://doi.org/10.1002/wrcr.20398).

1098 Pan, S., Dangal, S. R. S., Tao, B., Yang, J., & Tian, H. (2015). Recent patterns of terrestrial  
1099 net primary production in Africa influenced by multiple environmental changes. *Ecosystem*  
1100 *Health and Sustainability*, 1(5), 1–15. <https://doi.org/10.1890/EHS14-0027.1>

1101 Papa, F., Prigent, C., Aires, F., Jimenez, C., Rossow, W. B., and Matthews,  
1102 E. (2010), Interannual variability of surface water extent at the global scale, 1993–2004, *J.*  
1103 *Geophys. Res.*, 115, D12111, doi:[10.1029/2009JD012674](https://doi.org/10.1029/2009JD012674).

Formatted: Font: Not Italic

Field Code Changed

- 1104 [Potapov, P. V., Turubanova, S. A., Hansen, M. C., Adusei, B., Broich, M., Altstatt, A., ...](#)  
1105 [Justice, C. O. \(2012\). Quantifying forest cover loss in Democratic Republic of the Congo,](#)  
1106 [2000–2010, with Landsat ETM+ data. \*Remote Sensing of Environment\*, 122, 106–116.](#)  
1107 <https://doi.org/https://doi.org/10.1016/j.rse.2011.08.027>
- 1108 Potter, C., Klooster, S., & Genovese, V. (2012). Net primary production of terrestrial  
1109 ecosystems from 2000 to 2009. *Climatic Change*, 115(2), 365–378.  
1110 <https://doi.org/10.1007/s10584-012-0460-2>
- 1111 Prigent, C., Papa, F., Aires, F., Rossow, W. B., and Matthews, E.: Global inundation  
1112 dynamics inferred from multiple satellite observations, 1993–2000, *J. Geophys. Res.*, 112,  
1113 D12107, <https://doi.org/10.1029/2006jd007847>, 2007.
- 1114 Qie, L., Telford, E. M., Massam, M. R., Tangki, H., Nilus, R., Hector, A., & Ewers, R. M.  
1115 (2019). Drought cuts back regeneration in logged tropical forests. *Environmental Research*  
1116 *Letters*, 14(4), 45012. <https://doi.org/10.1088/1748-9326/ab0783>
- 1117 Qiu, C., Zhu, D., Ciais, P., Guenet, B., Peng, S., Krinner, G., Tootchi, A., Ducharne, A., and  
1118 Hastie, A.: Modelling northern peatland area and carbon dynamics since the Holocene with  
1119 the ORCHIDEE-PEAT land surface model (SVN r5488), *Geosci. Model Dev.*, 12, 2961–  
1120 2982, <https://doi.org/10.5194/gmd-12-2961-2019>, 2019.
- 1121 R Core Team. (2013). R: A language and environment for statistical computing. [Available at  
1122 <http://www.r-project.org>.]
- 1123 Raymond, P. A., Hartmann, J., Lauerwald, R., Sobek, S., McDonald, C., Hoover, M., ...  
1124 Guth, P. (2013). Global carbon dioxide emissions from inland waters. *Nature*, 503(7476),  
1125 355–359. Retrieved from <https://doi.org/10.1038/nature12760>
- 1126 Regnier, P., Friedlingstein, P., Ciais, P., Mackenzie, F. T., Gruber, N., Janssens, I. A., ...  
1127 Thullner, M. (2013). Anthropogenic perturbation of the carbon fluxes from land to ocean.  
1128 *Nature Geosci*, 6(8), 597–607. Retrieved from <http://dx.doi.org/10.1038/ngeo1830>
- 1129 Ren, W., H. Tian, W.-J. Cai, S. E. Lohrenz, C. S. Hopkinson, W.-J. Huang, J. Yang, B. Tao,  
1130 S. Pan, and R. He (2016). Century long increasing trend and variability of dissolved organic  
1131 carbon export from the Mississippi River basin driven by natural and anthropogenic forcing,  
1132 *Global Biogeochem. Cycles*, 30, 1288–1299, doi:10.1002/2016GB005395.
- 1133 Reynolds, C., Jackson, T. & Rawls, W. Estimating available water content by linking 424 the  
1134 FAO soil map of the world with global soil profile databases and pedo-transfer 425 functions.  
1135 *Am. Geophys. Union Fall Meet. EOS Trans. Spring Meet. Suppl.* 80, S132 426 (1999).
- 1136 [Richey, J. E., Melack, J. M., Aufdenkampe, A. K., Ballester, V. M., & Hess, L. L. \(2002\).](#)  
1137 [Outgassing from Amazonian rivers and wetlands as a large tropical source of atmospheric](#)  
1138 [CO<sub>2</sub>](#)
- 1139 Schimel D, Stephens BB, Fisher JB. 2015. Effect of increasing CO<sub>2</sub> on the terrestrial carbon  
1140 cycle. *Proceedings of the National Academy of Sciences, USA* 112: 436–441
- 1141 Sheffield, J., Goteti, G., & Wood, E. F. (2006). Development of a 50-Year High-Resolution  
1142 Global Dataset of Meteorological Forcings for Land Surface Modeling. *Journal of Climate*,  
1143 19(13), 3088–3111. <https://doi.org/10.1175/JCLI3790.1>

Formatted: English (United Kingdom)

Formatted: Subscript

1144 Silva, T.S.F., Costa, M.P.F. & Melack, J.M. Annual net primary production of macrophytes  
 1145 in the eastern Amazon floodplain. *Wetlands* (2009) 29: 747. <https://doi.org/10.1672/08-107.1>

1146 Smith, W.K., Fox, A.M., MacBean, N., Moore, D.J.P. and Parazoo, N.C. (2020),  
 1147 Constraining estimates of terrestrial carbon uptake: new opportunities using long-term  
 1148 satellite observations and data assimilation. *New Phytol*, 225: 105-112.  
 1149 doi:10.1111/nph.16055

1150 Spencer, R. G. M., P. J. Hernes, B. Dinga, J. N. Wabakanghanzi, T. W. Drake, and J. Six  
 1151 (2016), Origins, seasonality, and fluxes of organic matter in the Congo River. *Global*  
 1152 *Biogeochem. Cycles*, 30, 1105–1121, doi: 10.1002/2016GB005427.

1153 Sullivan, M. J. P., Talbot, J., Lewis, S. L., Phillips, O. L., Qie, L., Begne, S. K., ... Zemagho,  
 1154 L. (2017). Diversity and carbon storage across the tropical forest biome. *Scientific Reports*, 7,  
 1155 39102. Retrieved from <https://doi.org/10.1038/srep39102>

1156 Tathy, J. P., B. Cros, R. A. Delmas, A. Marengo, J. Servant, and M. Labat (1992), Methane  
 1157 emission from flooded forest in central Africa, *J. Geophys. Res.*, 97(D6), 6159–6168,  
 1158 doi:10.1029/90JD02555.

1159 Tian, H., Q. Yang, R. G. Najjar, W. Ren, M. A. M. Friedrichs, C. S. Hopkinson, and S. Pan  
 1160 (2015), Anthropogenic and climatic influences on carbon fluxes from eastern North America  
 1161 to the Atlantic Ocean: A process-based modeling study, *J. Geophys. Res. Biogeosci.*, 120,  
 1162 752–772, doi:10.1002/2014JG002760.

1163 Tyukavina, A., Hansen, M. C., Potapov, P., Parker, D., Okpa, C., Stehman, S. V., ...  
 1164 Turubanova, S. (2018). Congo Basin forest loss dominated by increasing smallholder  
 1165 clearing. *Science Advances*, 4(11). <https://doi.org/10.1126/sciadv.aat2993>

1166 Valentini, R., Arneeth, A., Bombelli, A., Castaldi, S., Cazzolla Gatti, R., Chevallier, F., Ciaia,  
 1167 P., Grieco, E., Hartmann, J., Henry, M., Houghton, R. A., Jung, M., Kutsch, W. L., Malhi, Y.,  
 1168 Mayorga, E., Merbold, L., Murray-Tortarolo, G., Papale, D., Peylin, P., Poulter, B.,  
 1169 Raymond, P. A., Santini, M., Sitch, S., Vaglio Laurin, G., van der Werf, G. R., Williams, C.  
 1170 A., and Scholes, R. J.: A full greenhouse gases budget of Africa: synthesis, uncertainties, and  
 1171 vulnerabilities, *Biogeosciences*, 11, 381–407, doi:10.5194/bg11-381-2014, 2014

1172 Verhegghen, A., Mayaux, P., de Wasseige, C., & Defourny, P. (2012). Mapping Congo Basin  
 1173 vegetation types from 300 m and 1 km multi-sensor time series for carbon stocks and forest  
 1174 areas estimation. *Biogeosciences*, 9(12), 5061–5079. <https://doi.org/10.5194/bg-9-5061-2012>

1175 Viovy, N.. (2018). *CRUNCEP Version 7 - Atmospheric Forcing Data for the Community*  
 1176 *Land Model*. Research Data Archive at the National Center for Atmospheric Research,  
 1177 Computational and Information Systems Laboratory. <http://rda.ucar.edu/datasets/ds314.3/>.

1178 [Walker AP, De Kauwe MG, Medlyn BE, Zaehle S, Iversen CM, Asao S, Guenet B, Harper](#)  
 1179 [A, Hickler T, Hungate BA et al. 2019. Decadal biomass increment in early secondary](#)  
 1180 [succession woody ecosystems is increased by CO2 enrichment. Nature Communications](#)  
 1181 [10:454.](#)

1182 [Weiss, L. C., Pötter, L., Steiger, A., Kruppert, S., Frost, U., & Tollrian, R. \(2018\). Rising](#)  
 1183 [pCO2 in Freshwater Ecosystems Has the Potential to Negatively Affect Predator-Induced](#)

Formatted: English (United Kingdom)

Formatted: English (United Kingdom)

Formatted: No underline, Font color: Auto

Formatted: No underline, Font color: Auto, English (United Kingdom)

Formatted: English (United Kingdom)

1184 Defenses in *Daphnia*. *Current Biology*, 28(2), 327–332.e3.  
1185 <https://doi.org/https://doi.org/10.1016/j.cub.2017.12.022>

1186 Williams, C. A., Hanan, N. P., Neff, J. C., Scholes, R. J., Berry, J. A., Denning, A. S., and  
1187 Baker, D. A.: Africa and the global carbon cycle, *Carbon Balance and Management*, 2(3),  
1188 doi:10.1186/1750-0680-2-3, 2007.

1189 Yin, S., Li, X., & Wu, W. (2017). Comparative analysis of NPP changes in global tropical  
1190 forests from 2001 to 2013. *IOP Conference Series: Earth and Environmental Science*, 57(1),  
1191 12009. Retrieved from <http://stacks.iop.org/1755-1315/57/i=1/a=012009>

1192 Zhou, L., Tian, Y., Myneni, R. B., Ciais, P., Saatchi, S., Liu, Y. Y., ... Hwang, T. (2014).  
1193 Widespread decline of Congo rainforest greenness in the past decade. *Nature*, 509(7498), 86–  
1194 90. <https://doi.org/10.1038/nature13265>

1195 Zhuravleva, I., Turubanova, S., Potapov, P., Hansen, M., Tyukavina, A., Minnemeyer, S., ...  
1196 Thies, C. (2013). Satellite-based primary forest degradation assessment in the Democratic  
1197 Republic of the Congo, 2000–2010. *Environmental Research Letters*, 8(2), 24034.  
1198 <https://doi.org/10.1088/1748-9326/8/2/024034>

1199

1200

1201

1202



1203 *Appendix A*

1204

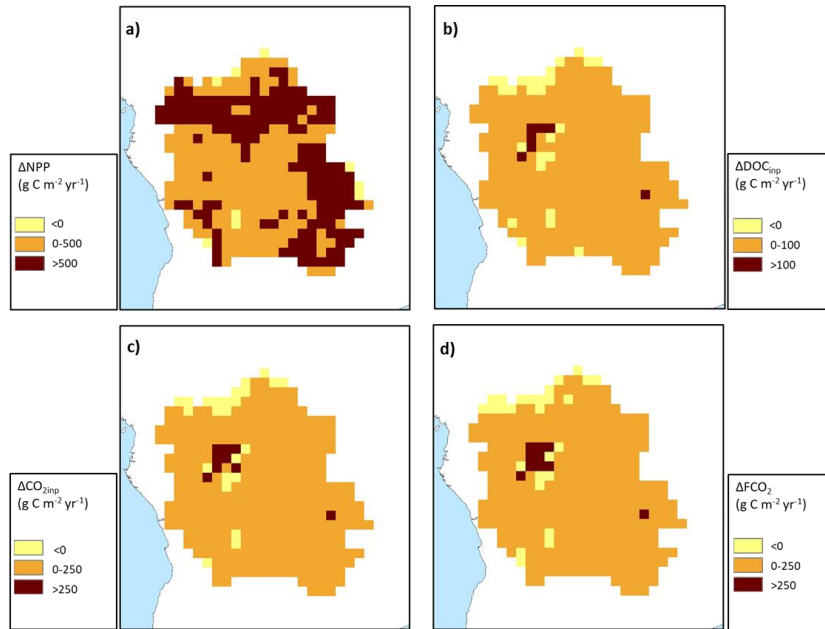
**Table A 1: Performance statistics for modelled versus observed seasonality of discharge on the Congo at Brazzaville**

Climate forcing	RSME	NSE	R <sup>2</sup>	Mean monthly discharge (m <sup>3</sup> s <sup>-1</sup> )
ISIMIP	29%	0.20	0.23	38,944
Princeton GPCC	40%	-0.25	0.20	49,784
GSWP3	46%	-4.13	0.04	24,880
CRUNCEP	65%	-15.94	0.01	16,394
Observed (HYBAM)				40,080

1205

**Table A 2: Pearson correlation coefficient (r) between detrended carbon fluxes and detrended climate variables**

	SHR	Aquatic CO <sub>2</sub> evasion	Lateral C	NEP	Rain	Temp.	MEI
NPP	-0.48	0.68	0.72	0.90	0.64	-0.57	-0.09
SHR		-0.41	-0.48	-0.71	-0.32	0.76	0.04
Aquatic CO <sub>2</sub> evasion			0.92	0.41	0.87	-0.30	-0.21
Lateral C				0.52	0.81	-0.38	-0.15
NEP					0.40	-0.74	-0.01
Rain						-0.31	-0.26
Temp.							0.03



1206

Figure A 1: Change ( $\Delta$ , 2099 minus 1861) in the spatial distribution of a) terrestrial NPP, b) DOC leaching into the aquatic system, c)  $CO_2$  leaching into the aquatic system and d) aquatic  $CO_2$  evasion. All at a resolution of  $1^\circ$

1207

1208

1209

1210

1211

1212

1213

1214

1215

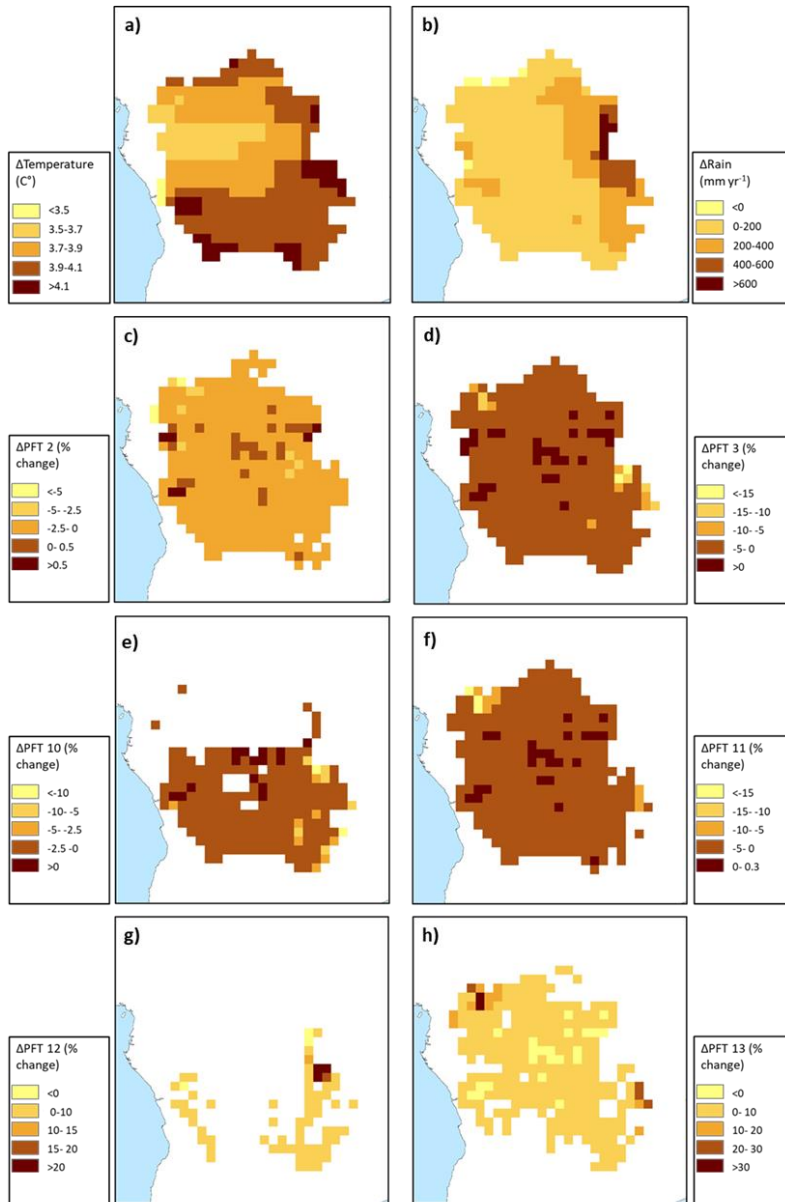
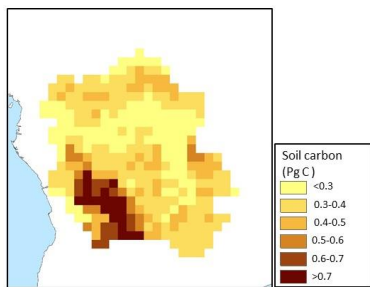


Figure A 2: Change ( $\Delta$ , 2099 minus 1861) in the spatial distribution of the principal climate and land-use drivers across the Congo Basin; a) mean annual temperature in  $^{\circ}\text{C}$ , b) mean annual rainfall in  $\text{mm yr}^{-1}$ , c)-h) mean annual maximum vegetated fraction for PFTs 2,3, 10,11,12 and 13. All at a resolution of  $1^{\circ}$ .

1217

1218

Period	Temp.	Rain.	PFT2	PFT3	PFT10	PFT11	PFT12	PFT13
1861-1890	24.0	1451	0.263	0.375	0.154	0.254	0.015	0.014
1981-2010	25.2	1526	0.255	0.359	0.154	0.255	0.038	0.030
2070-2099	28.2	1654	0.258	0.362	0.147	0.245	0.039	0.037



**Figure A 3: Spatial distribution of simulated total carbon stored in soils for the present day (1981-2020).**

1219

1220

1221